EXTREME EVENTS AND THE IMPACT OF CLIMATE CHANGE ON VICTORIA'S COASTLINE

Report to EPA and Melbourne Water

Environment Protection Authority
State Government of Victoria

June 1996

EXTREME EVENTS AND THE IMPACT OF CLIMATE CHANGE ON VICTORIA'S COASTLINE

Report to EPA and Melbourne Water

Authors:
Kathleen L McInnes – CSIRO Division of Atmospheric Research
Graeme D Hubbert – Global Environmental Modelling Services

Environment Protection Authority
Olderfleet Buildings
477 Collins Street
Melbourne Victoria 3000
Australia

Printed on recycled paper

Publictation 488

ISBN 0 7306 7505 X

Foreword

Coastal zones around the world are likely to be particularly vulnerable to climate change resulting from global warming. Sea level rise could potentially have wide-ranging impacts on natural and social systems, physical infrastructure, and regional economies. The frequency and severity of storms is critically important to assessing the potential risk of coastal damage.

This report examines the possible impacts of storm surge events in Port Phillip Bay under a climate change scenario of higher sea levels and stronger winds, a feasible outcome by the end of the next century.

Two recent meteorological events which occurred in 1994 have been simulated for present-day and enhanced greenhouse conditions. Sea level heights were modelled and coastal areas potentially inundated by these events were identified.

In order to identify potential changes in the frequency and severity of westerly winds, which are responsible for the majority of storm surges along southern Australia, an analysis of results from global climate models was undertaken.

While this study outlines the likely impact of a climate change scenario which may be rather extreme, the results provide an indication of the relative sensitivity of different areas along the Port Phillip Bay coastline. The report provides a basis for further investigations as climate change scenarios become more precise, and will be of assistance to coastal planners and managers looking ahead to the next century.

The contribution of $20,000 by the Department of the Environment, Sport and Territories towards this study is gratefully acknowledged.

BRIAN ROBINSON

CHAIRMAN

Contents

Glossary

1×CO_2	Describes present-day (or sometimes pre- industrial) climate as simulated by a global climate model. Also referred to as the control climate.
2×CO_2	Describes conditions simulated by a climate model in which the atmospheric concentration of carbon dioxide is instantaneously doubled from the equivalent of a present-day (or sometimes pre-industrial) concentration, and the atmosphere has been allowed to reach equilibrium after responding to the increase in carbon dioxide.
AHD	Australian Height Datum. The datum for the Australian Map Grid. This is approximately equal to mean sea level.
AMG	Australian Map Grid. The co-ordinate system used by surveyors and engineers. Units are in metres to the east or north of the map origin (ie. eastings and northings).
AOGCM	Atmosphere-Ocean General Circulation Model. A GCM model of the atmosphere which has been coupled to a global ocean model to enable realistic ocean circulations to be modelled.
ECMWF	European Centre for Medium Range Weather Forecasting.
GCM	Global Climate Model.
LAM	Limited Area Model. Model of either the atmosphere or ocean which is run over a limited domain, usually at much higher resolution than GCMs.
MSLP	Mean Sea Level Pressure.
RASP	Regional ASsimilation-Prognosis system.
seiche	A wave that oscillates in a bay or gulf from a few minutes to a few hours as a result of seismic or atmospheric disturbances.
slab ocean	The approximation to the ocean used in GCMs which are not coupled to dynamic ocean models. The ocean is treated as a slab of water, typically 50 m deep, and ocean circulations are not modelled.
SST	Sea Surface Temperature.
tidal constituents	The spectral components which contribute to the total tidal signal. The main tidal constituent is the lunar semi-diurnal (half

daily) or M_2 tide which has a period of 12.42 hours. Other lunar semidiurnal constituents are the N_2, S_2 and K_2 with periods of 12.60, 12.00 and 11.97 hours respectively. The diurnal constituents, O_1, P_1 and K_1 have periods of 25.82, 24.07 and 23.93 hours respectively. Each of these constituents contributes amplitudes of at least 0.05 m in Bass Strait.

Acknowledgments

The authors wish to express their gratitude to a number of people who contributed to various aspects of this study. Rhonda Boyle from EPA was extremely helpful throughout the course of this study and in particular with the presentation of the report. From CSIRO Division of Atmospheric Research, Dr Barrie Pittock and Dr Peter Whetton provided valuable comments on the manuscript. The authors are also grateful to Malcolm Haylock for his significant contribution to the analysis of the GCM output.

Topographic and bathymetric data for the high resolution grids were obtained from Paul Doherty (MITS), Dennis Hearn (EPA), and Peter Newton and Gerardo Trinidad (CSIRO Division of Building Construction and Engineering). Geoff Crapper and Martin Dunkley (Melbourne Water), and Robert Molloy of the CSIRO project team of the Port Phillip Bay study provided useful advice in obtaining the topographic data.

Regional analyses from the Bureau of Meteorology were kindly made available by Paul Stewart. Sea level data for verification of the storm surge models were obtained from various sources. The authors wish to thank Bill Mitchell and Marion Tate from the National Tidal Facility for providing sea level residuals at Thevenard, Portland, Lorne, Stony Point and Williamstown, as well as Figures 2.2 and 2.3. Geoff Crapper provided storm surge and wind verification data for St Kilda for the two events, as well as river flow rate information and Keith Bonaface provided levee information on the Mordialloc domain.

Executive Summary

The coastal zone is particularly vulnerable to climatic changes as a result of the enhanced greenhouse effect, because of the projected mean sea level rise resulting from thermal expansion of the oceans. However, temporary fluctuations in sea level, which occur as a result of storm surges, are potentially more destructive to the coastal zone. These are driven by severe atmospheric disturbances and different coastal regions are affected by different types of severe weather events. The intensity and frequency of severe atmospheric storms is important when determining the risk of coastal damage through storm surge occurrence. This provides an added uncertainty when assessing the impact of climatic change on storm surge generation in coastal regions, since possible changes to the frequency and intensity of the atmospheric storms which generate the surges must first be determined.

This study outlines a methodology for assessing the impact of climate change on Victoria's coastline. It examines and combines both the projected mean changes in climate, such as mean sea level rise, with the possible changes in extreme weather events. High resolution limited area modelling using atmospheric and storm surge models is employed to model actual extreme storm surge events and GCM simulations are analyzed to determine the possible impact of climate change on storm surge forcing.

An analysis of storm surges along the southern coastline of Australia over recent years indicates that in the majority of cases they are caused by the westerly winds associated with cold fronts and tend to occur during the colder months of the year. There is a strong relationship between sea levels recorded in Bass Strait and those recorded in Port Phillip Bay, which indicates that areas such as Port Phillip Bay cannot be considered in isolation, particularly when conducting modelling studies.

The rainfall produced by the fronts is usually not sufficient to produce flooding, so the risk of inundation through the combined effects of storm surge and flood is minimal. However, other types of meteorological conditions are identified which could lead to more extreme inundation. For example, lows which intensify in Bass Strait can produce both flooding and storm surges. Combinations of conditions consisting of heavy rainfall events over Victoria followed by strong westerlies could also lead to flooding situations which coincide with storm surges.

Several GCM simulations were analyzed to determine if any changes could be identified in the frequency and severity of westerly wind days between the $1\times CO_2$ and $2\times CO_2$ simulations. Daily data and seasonally averaged winds from two GCM experiments were analyzed, as well as the seasonally averaged winds from a coupled AOGCM. Results over the region of interest were inconclusive, due to a lack of agreement between the different model simulations as to whether westerly wind days would become more or less frequent or severe under a doubling of CO_2. Examination of the seasonally averaged differences between the $2\times CO_2$ and $1\times CO_2$ daily data over southern Australia, suggested that changes of $\pm 10\%$ in the frequency and intensity of

severe westerly wind days were possible. However, a reduction in the frequency and intensity of strong westerlies was more often indicated in the $2\times CO_2$ simulations.

To enable an investigation of the possible impacts of atmospheric forcing on storm surges, a worst case scenario was devised to incorporate into sensitivity experiments conducted using a high resolution storm surge model. The most extreme event was taken to be a 10% increase in the strength of the winds of a present day extreme event. The worst case scenario for mean sea level rise for the year 2070 (a rise of 80 cm) was chosen to incorporate into sensitivity experiments. It should be noted that a best case scenario, with a 10% reduction in wind strength and a mean sea level rise of only 10 cm by 2070, would produce less dramatic increases in storm surge inundation over present day conditions.

Two storm surge events were chosen for modelling on a domain encompassing most of the southern coastline with a grid resolution of 12 km. The events occurred in May and November 1994 and the model captured the main features of the two events extremely well. Sensitivity experiments in which the wind speeds were varied by differing amounts were conducted, using the storm surge model to determine the relationship between wind speed changes and storm surge heights. It was found that, for wind speeds ranging from a 10% reduction to a 20% increase, the storm surge response was approximately twice that of the wind speed change on the open coastline

A set of storm surge simulations was also conducted over Port Phillip Bay at 500 m grid resolution. On this grid, tidal forcing was applied so that areas of inundation could be studied. A set of three experiments was conducted for the two cases; a control simulation; a simulation in which mean sea level was increased by 80 cm; and a simulation which incorporated the sea level rise, along with a 10% increase in the surface wind speed. In the control simulations of the two cases, the total sea level heights at St Kilda verified well against observations. The second sensitivity experiment produced sea levels which were approximately 80 cm higher at each location. In the third experiment, the stronger winds produced peak surges which were over 20 cm higher again. Slightly higher increases in sea level were seen on the eastern side of the Bay in this experiment relative to the western side.

Three sections of the coastline were then modelled on higher resolution grids, to identify areas most vulnerable to inundation. The sensitivity experiments were performed to provide an estimation of the worst possible inundation which could be expected under maximum mean sea level increases and storm intensities, even though it is unlikely that this set of circumstances would arise by 2070. Overtopping of the levee banks occurred on both the north and south side of the Mordialloc Creek in these simulations and the area inundated was sensitive to both the wind strength and to the slight differences in the prevailing wind directions between the two cases studied. No overtopping of the Patterson River occurred. The importance of the levee banks was illustrated in the worst case scenario simulations which were conducted without levee banks. The flooding then extended from the Mordialloc Creek to the Patterson River on the eastern side of the railway and was consistent with that which occurred during the 1934 flood event.

Hobsons Bay exhibited similar relative increases in inundation to Mordialloc under the two sensitivity experiments although differences in relation to the different storm forcing were apparent. The Werribee region, located on the northwest of the Bay, showed more sensitivity to the imposed mean sea level rise than to increases in wind strength. These results highlight the site-specific and storm-specific nature of this type of problem and the need to model different regions separately, under a variety of storm conditions.

It should be noted that the purpose of this study was to outline a methodology for assessing the potential impact of climate change at the regional scale. To this end, the inundation simulations have been carried out to demonstrate the relative sensitivity of different regions to different storm forcings and scenarios of climate change. The resolution of the inundation model and hence the topographic features resolved in the model is not of sufficient accuracy for detailed planning decisions to be made and hence the results should be used to provide qualitative guidance only.

CHAPTER 1: Introduction

1.1 Rationale

Accelerated sea level rise in the event of global climate change induced by the enhanced greenhouse effect is considered a major policy concern at all levels of government. However, mean sea level rise is only one of a number of climatic factors which may impact on coastal areas as illustrated in Figure 1.1.

Temporary and localized sea level increases produced by storm surges are potentially more hazardous and destructive to coastal regions than mean sea level rise as they can cause flooding of low lying coastal areas. In addition to this, the higher sea levels caused by the surge expose more elevated and potentially vulnerable regions of the coastline to the damaging effects of wind generated surface waves.

Storm surges are caused by severe weather systems impacting on the ocean surface, producing sea level elevations which are independent of the normal tidal variations. The oceanic response to severe storms is a function of both the strength of the atmospheric disturbance and the structure of the coastal zone. For this reason, the potential impact of sea level rise is site specific and requires consideration of both the local coastal geomorphology and the meteorology of the region. An area of considerable uncertainty, in relation to global climatic change induced by the enhanced greenhouse effect, is how daily weather patterns and, severe storms in particular, will be affected by climatic change.

Flooding from extreme rainfall may also be caused by the same atmospheric storms which are responsible for storm surge generation. In such circumstances, worsened coastal flooding could result from flooded river systems which are unable to drain normally in the presence of elevated sea levels from the storm surge.

This study focuses on the meteorology relevant to Victorian coastal areas and its relationship to storm surge generation. The likely impact of the enhanced greenhouse effect on the meteorology of the region is assessed in terms of possible changes to storm surge frequency and severity. Particular emphasis is given to Port Phillip Bay.

1.2 Background

A number of previous studies have investigated the impact of sea level rise on Victoria's coastline. Black et al. (1990) examined the extreme sea levels attainable in Port Phillip Bay through mean sea level rise. Their study investigated the effects of a mean sea level rise on tidal variation in Port Phillip Bay and tidal amplitudes were found to increase for increasing mean sea level. This is due to less frictional attenuation

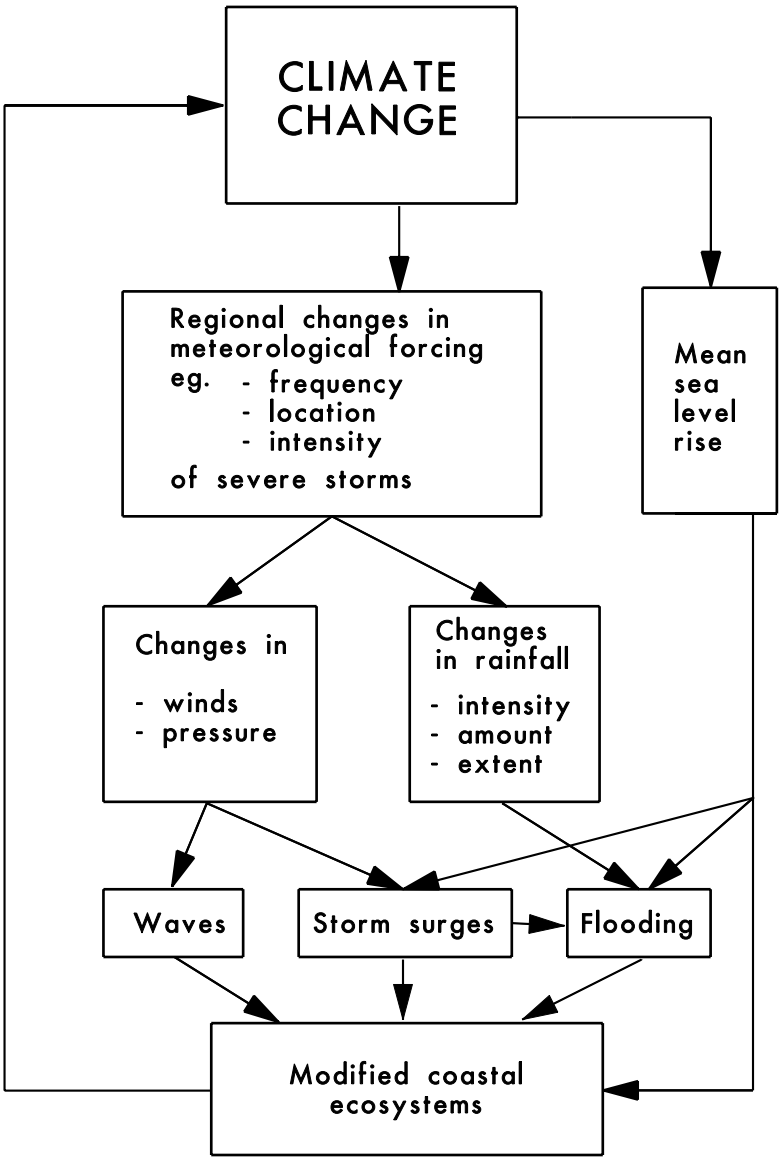

Figure 1.1: Schematic illustrating the interactions of various processes which may act to modify the coastal zone under climatic change.

occurring over the entrance region to Port Phillip Bay. The atmospheric conditions which contribute most to extreme sea levels in the Bay were identified to be consist of a combination of westerly winds and low barometric pressures. Sudden changes in wind direction were also found to cause seiches in the Bay which could further contribute to temporary sea level rise. When the optimal set of background conditions contributing to extreme sea levels was applied to a background state containing the projected mean sea level rise, smaller extreme sea level heights were obtained relative to the prevailing mean sea level conditions. In that study, the possible changes to atmospheric forcing, resulting from the enhanced greenhouse effect, were not considered.

The Coastal Investigations Unit (1992) produced an extensive study of the vulnerability of Victoria's coastline to a mean sea level rise. Their study considered factors such as the coastal topography, geology and sediment type, and employed model re-

sults to estimate the likely impact of different mean sea level rises. Possible variations in climatic conditions, such as winds and changes in storm movements, were not taken into consideration.

1.3 Methodology

Existing studies into the potential impacts of greenhouse warming on the Victorian coastline have not examined the relationship between the atmospheric forcing and storm surge activity. No studies to date have attempted to assess the likely impact of greenhouse warming on the significant weather systems that are responsible for storm surge generation. The effects of greenhouse warming on weather systems may include changes in storm movement, intensity and frequency which are factors relevant to storm surge generation.

Storm surges alone can cause inundation of low lying coastal regions. However, the situation can be greatly exacerbated in circumstances where the storm surge coincides with increased river flow rates associated with flood waters. The likely effect of greenhouse warming on the rainfall amounts produced by severe storms is therefore also an important consideration.

In this study, the meteorology associated with storm surge generation in the Victorian region is identified and described. The impact of climate change, in terms of mean sea level and surface temperature, is discussed. Model output from the CSIRO9 Mark I and Mark II General Circulation Model (GCM) experiments and the coupled Atmosphere-Ocean GCM (AOGCM) experiment is used to determine if changes to the meteorological forcing in the Victorian region are likely under enhanced greenhouse warming.

The sensitivities of storm surges to climate change along the southern coastline and in Port Phillip Bay are investigated through high resolution atmospheric and oceanic modelling of two observed storm surge events. Atmospheric model simulations are carried out under control conditions and conditions consistent with enhanced greenhouse warming. Sensitivity experiments are performed with the storm surge model to determine the impact of different wind strengths on the peak storm surge height at various locations along the southern coast.

Finally, a high resolution inundation model is run over Port Phillip Bay and three sub-regions centred on Hobsons Bay, Werribee and Mordialloc. Experiments with elevated mean sea level and increased wind speed are also conducted to illustrate the extent of coastal inundation which could occur under a worst case scenario for climatic change.

CHAPTER 2: Extreme Sea Levels in Victoria

2.1 Storm Surges

2.1.1 Causes

Storm surges are temporary elevations or depressions in sea surface height, driven by surface winds and changes in atmospheric pressure. Their severity depends on the strength and duration of the atmospheric disturbance and the structure of the coastal terrain. Severe storm surges can cause inundation of low lying coastal plains and flooding of river systems. Combined with wind generated wave action, storm surges can contribute to coastal and estuarine erosion.

Although temperature and density variations within the ocean (baroclinic effects) have a significant influence on deep ocean circulation over long timescales, the main short-term variations in ocean circulation, particularly on a continental shelf, are due to surface wind stress and surface pressure. Consequently, baroclinic effects can generally be ignored for the purpose of predicting the direct ocean response to a severe weather system. The response of the ocean surface to changes in atmospheric pressure (the inverse barometer effect) amounts to a 1 cm rise in sea level per hPa drop in surface pressure.

Surface winds exert a stress on the ocean surface which induces a current in the direction of the wind. The earth's rotation then deflects the current to the left (right) in the southern (northern) hemisphere. When a coastal barrier blocks the deflected flow, elevated sea levels are produced at the coast. This effect is known as surface wind drift (Vecchio, 1980) or coastal current setup (Black et al. 1990). Along the southern coastline, elevation of sea level would be induced by winds with a large westerly component. Wind setup, an additional effect produced by the wind, is produced when a wind blowing over the sea surface maintains a slope on the water surface in the direction of the wind. This effect is most pronounced in wide enclosed shallow bays where the onshore flow is steady over a period of time. Black et al. (1990) estimate that for Bass Strait - with an average width of 240 km, depth of 70 m and a southerly wind of 10 m s^{-1} - sea levels would be elevated by 5 cm along the southern coastline.

Storm surges can also be generated remotely and propagate as coastally trapped waves. In the southern hemisphere, coastally trapped waves travel in an anticlockwise sense around the coastline.

2.1.2 Coastal Inundation

Although surges occur independently of the natural tidal variation, they will obviously have more impact if they coincide with the maximum tidal amplitude. Low lying coastal terrain is most vulnerable to flooding by storm surges.

Existing flooding situations can also be prolonged or worsened by storm surges. This can happen in situations when the atmospheric storm responsible for the storm surge also produces extreme rainfall or if a storm surge generating system occurs soon after a severe rainfall event. In either circumstance, the storm surge can elevate sea levels in the vicinity of river outflows, thereby reducing the drainage rates and contributing to flooding of river systems.

2.1.3 Storm Surges in Victoria

As part of the Baseline Sea Level Monitoring Station Project, the National Tidal Facility (NTF) of Flinders University of South Australia, with the support of the Department of Environment, Sports and Territories, has been monitoring sea level heights at designated stations around Australia (Figure 2.1) using sophisticated and accurate Seaframe gauges. These data have been collected since June 1993 and provide valuable information on the nature and frequency of sea level fluctuations along the southern coastline.

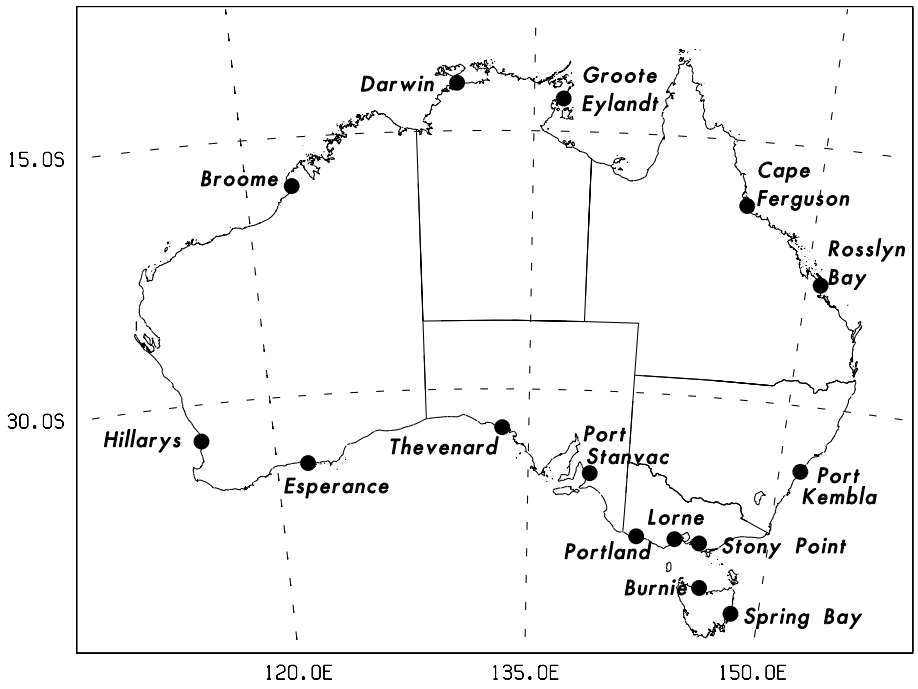

Figure 2.1: Locations of Australian Baseline sea level monitoring stations.

A feature commonly observed along the south coast is a surge recorded as far west as Esperence or Hillarys which propagates around the southern coastline to Bass Strait. Once reaching the Bass Strait gauges of Lorne, Stony Point and Burnie, the signal exhibits a resonating characteristic with a frequency of 12 hours, which may occur in response to the dramatic change in bathymetry at the western edge of Bass Strait (Figure 2.2). An example of this is seen in Figure 2.3 which shows a time series of the sea level height residuals at the stations shown in Figure 2.1 for May 1994. These data are produced by subtracting the predicted tide heights at the given stations from

the observed sea levels. Three episodes of elevated sea levels were recorded in Bass Strait during May 1994, on the 17th, 21st and 27th (these events were identified on the basis of sea level residuals 0.4 m or greater occurring at either Lorne or Stony Point). The last event was the most severe and is the subject of model simulations which are presented in chapter 4.

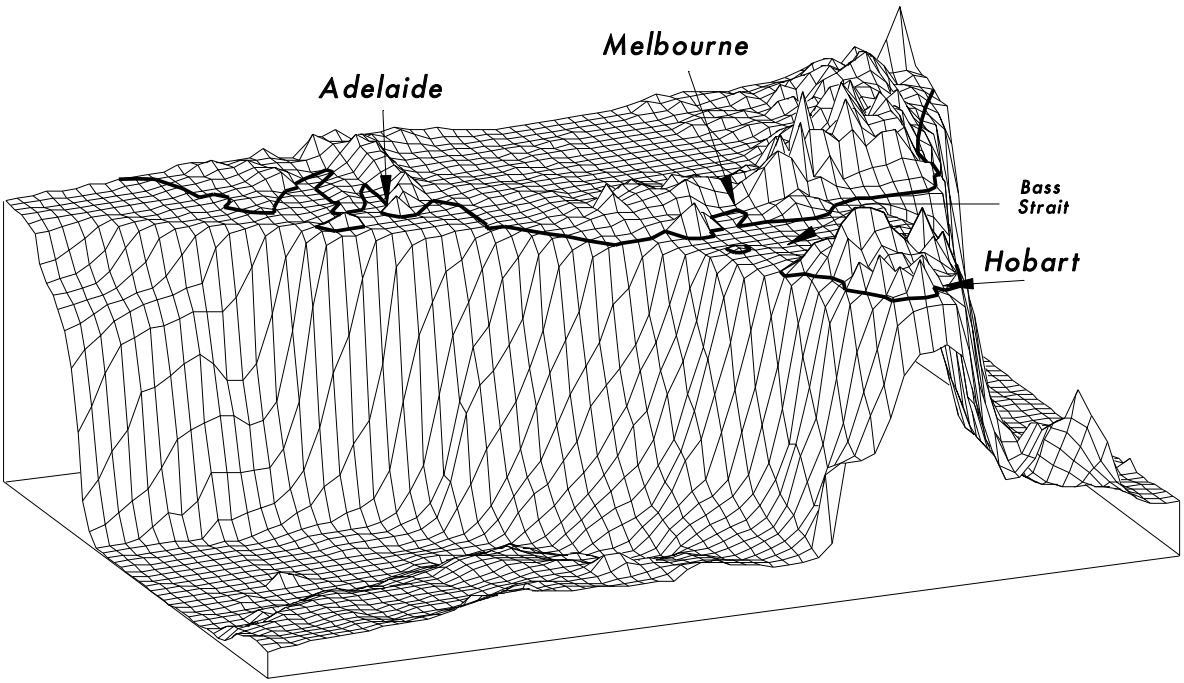

Figure 2.2: A three-dimensional representation of the southeastern Australian coastline showing the sudden change in depth at the eastern and western edges of Bass Strait.

A second example, also modelled in the present study, is shown in Figure 2.4 for November 1994. During this month a particularly severe storm surge occurred in Bass Strait on the 6th and 7th, with peak residuals at Stony Point reaching one metre in height. Unlike the three events recorded in May which affected the coastline at least as far west as Esperence, this particular event shows only a weak signal at Thevenard and builds in amplitude at the stations further east.

All incidences of residual sea levels higher than 0.4 m at either Lorne or Stony Point between June 1993 and May 1995, were counted. A total of 23 events occurred and are represented in a frequency histogram (Figure 2.5). These data suggest that elevated sea level events are more pronounced from mid-autumn to mid-spring, with the lowest incidence occurring in the warmer months.

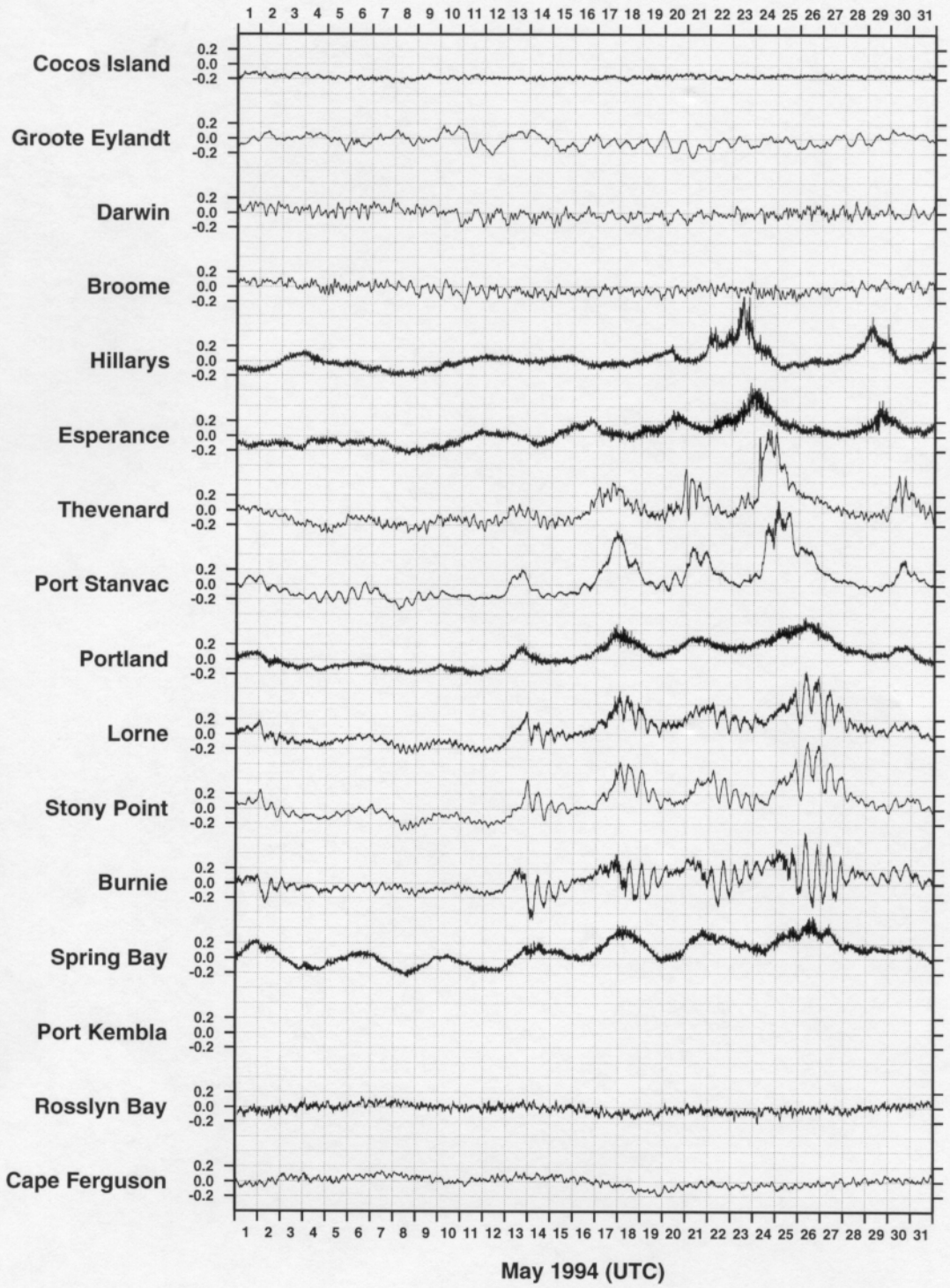

Figure 2.3: Residual sea-level heights for May 1994 at the stations indicated in Fig. 2.1.

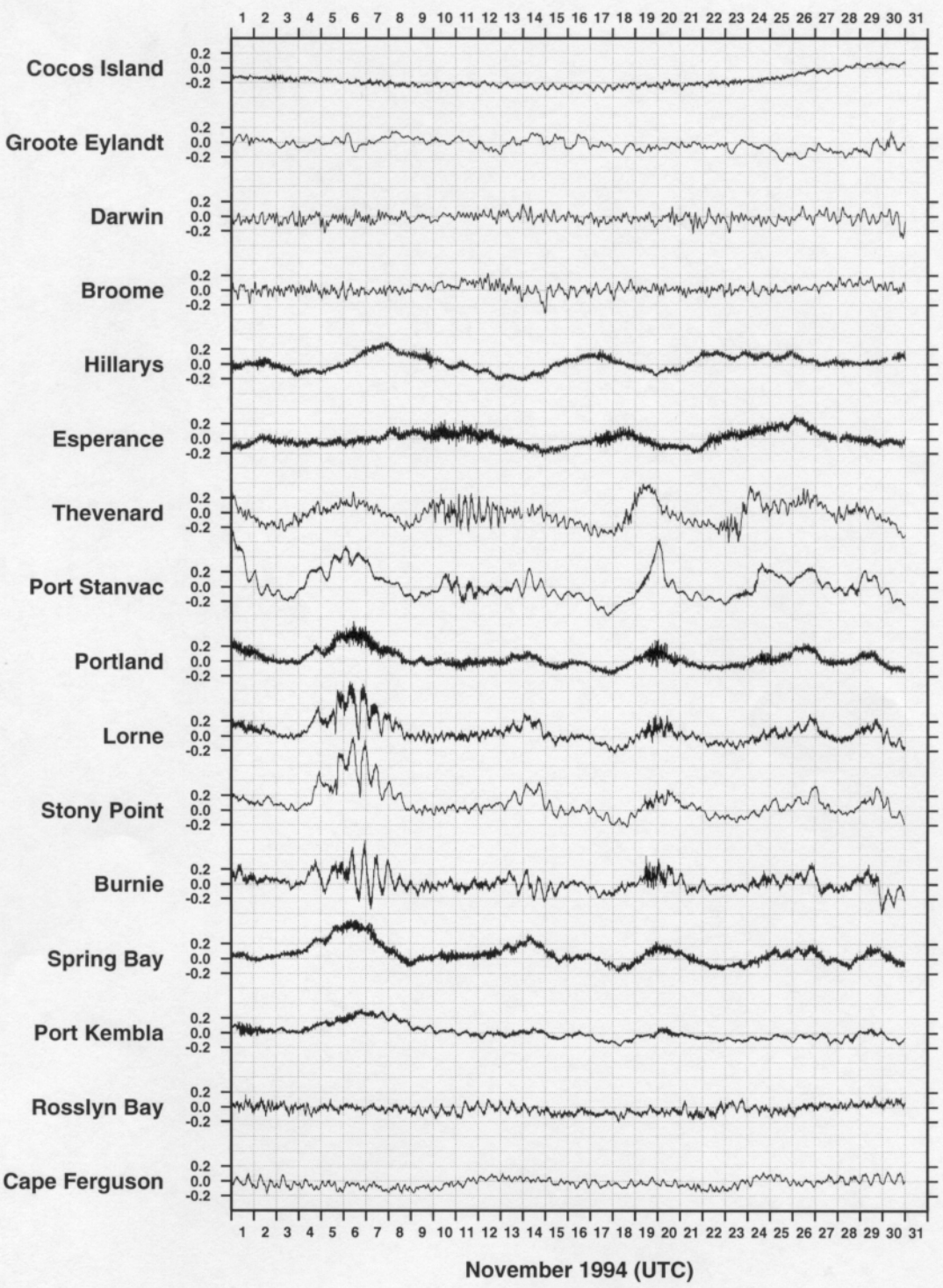

Figure 2.4: Residual sea-level heights for November 1994 at the stations indicated in Fig. 2.1.

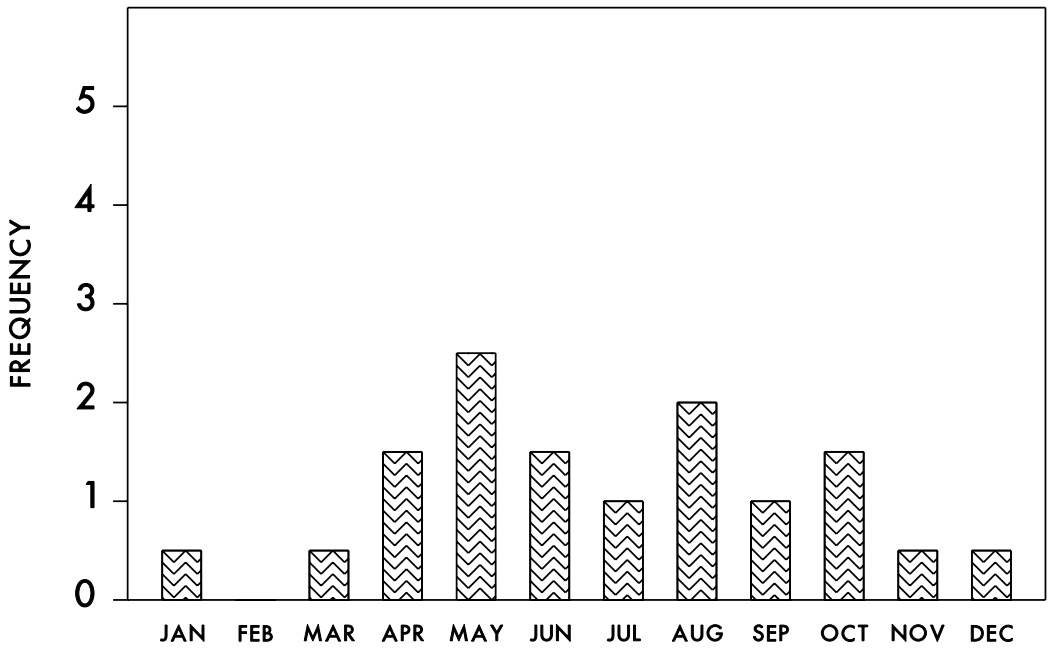

Figure 2.5: Frequency histogram showing the incidence of elevated sea levels at Lorne and Stony Point, based on NTF data from June 1993 to March 1995.

2.1.4 Storm Surges in Port Phillip Bay

To determine to what extent elevated sea levels in Port Phillip Bay are forced locally or remotely, it is important to understand the relationship between storm surge activity occurring in the Bay and that occurring in Bass Strait. An understanding of the underlying causes of storm surges in Port Phillip Bay is needed to determine the possible impacts of the enhanced greenhouse effect. To address this question, sea level residuals at Williamstown at the northern end of Port Phillip Bay for the period June 1993 to December 1994 have been examined and compared to those recorded at Lorne and Stony Point. Of the 23 events recorded at the Bass Strait gauges during this interval, 16 also registered sea levels of at least 0.4 m at Williamstown.

The residual sea levels at Williamstown were generally slightly lower than the average of the levels recorded at Lorne and Stony Point, although in two of the 23 cases, the Williamstown residuals were higher. There were also two cases (December 1993 and January 1994) where sea level residuals of 0.4 m and above were recorded at Williamstown while those at Lorne and Stony Point were less than 0.4 m. The December case coincided with a low pressure system located in Bass Strait, whereas the January case appears to have been associated with the passage of a cold front.

The relationship between residual sea levels in Port Phillip Bay and Bass Strait during May and November 1994 is illustrated in Figure 2.6. The sea level changes at the Bass Strait locations are clearly reflected in the Williamstown data. The only notable difference is that the resonance present at Lorne and Stony Point, particularly during the periods of higher sea levels, is not apparent at Williamstown.

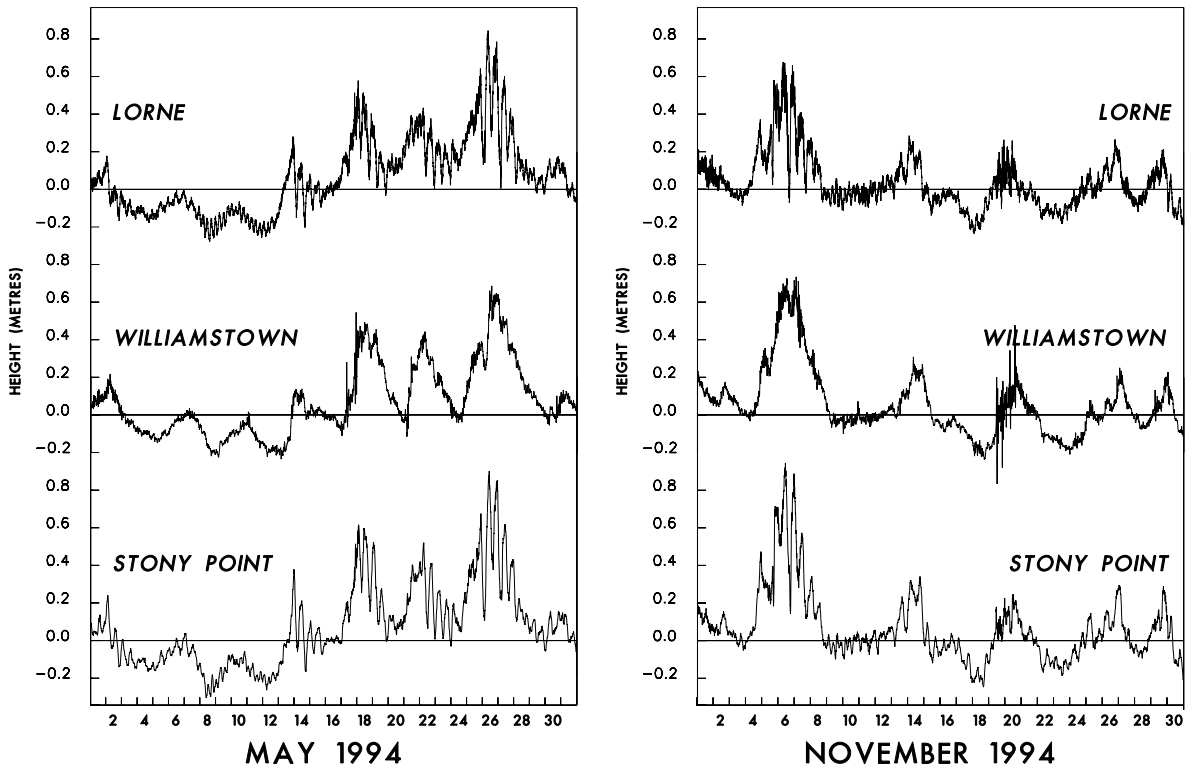

Figure 2.6: Example of the relationship between the residual sea level signals at Lorne and Stony Point in Bass Strait and Williamstown in Port Phillip Bay during May and November 1994.

2.1.5 Return Periods for Port Phillip Bay

The one in one hundred year return period sea levels have been calculated by Mitchell and Tawn (Private Communication) at a number of locations around Australia. At Williamstown and Mordialloc in Port Phillip Bay, the values based on their analysis are 1.02 and 1.09 m AHD respectively. However, this is contrary to Adams (1987) who calculated a 1% probability tide level of 1.3 m AHD for Williamstown.

An explanation of this discrepancy is beyond the scope of the present study. The observed maximum sea level heights at Williamstown for the May and November cases which are modelled in the present study were 1.046 and 1.074 m AHD respectively. According to Adams (1987), these events have return periods at Williamstown of between two and five years.

2.2 Meteorology affecting storm surge generation

2.2.1 Cold Fronts

An examination of the prevailing meteorological conditions during each of the 23 storm surge events identified in the previous section reveals that in all cases the southern coastline is under the influence of winds from a predominantly westerly di-

rection - both in the lead up and during the event. The westerlies usually occur in conjunction with the passage of cold fronts. While cold fronts affect the southern coastline throughout the year, they are likely to have their greatest impact during the winter months when the subtropical ridge has moved northwards and is located over the continent. During this time the southern coastal regions are generally under the influence of a more sustained westerly wind regime.

In storm surges along the southern coast the major component of the surge height is due to the effect of the surface wind. The low pressure systems associated with frontal passage are usually located well to the south of the continent, so that the contribution to the storm surge due to the inverse barometer effect is relatively minor. There is, however, the possibility of low pressure systems moving northward into Bass Strait and generating storm surges. One such event occurred in November 1934 and will be discussed separately in the following section.

In the summer months, cold fronts along the southern coastline are often the shallow, northern extents of deeper frontal systems which pass well to the south of the continent (McInnes et al. 1994 and Reeder et al. 1991). They tend to be preceeded by northerly or northwesterly winds and following their passage is usually a ridge of high pressure which brings lighter winds to the coastal regions. The incidence of sustained westerlies over a period of several days is therefore less common during the summer months.

The cold moist westerly or southwesterly airstream following the passage of a front usually results in significant rainfall over mountain and coastal areas. Rainfall intensities however, are not generally high enough to cause flooding of the major rivers flowing into Port Phillip Bay. The likelihood of surge events coinciding with flooding events in this region due to cold fronts is therefore relatively minor.

Storm surges which are initiated at a particular location along the coastline are capable of propagating as a coastally trapped wave to regions well removed from the initial forcing. In the southern hemisphere, such waves travel with the coast to their left. Their speed of propagation is a function of the depth of the continental shelf and, along the southern coastline, is of the order of 10 m s^{-1}. Since the typical propagation speed of frontal systems along the southern coast is also of the order of 10 m s^{-1}, a question arises as to whether the resulting surges are behaving as a free or a forced response to the atmospheric disturbance. In other words, are the sustained westerlies important for maintaining the surge height as it moves eastward or will the surge, once initiated, propagate independently of any further atmospheric forcing? The fact that surge events appear to be generated during sustained periods of westerly winds along the south coast and are often detected as far west as Esperance, suggests that the surges are possibly a forced response to the atmospheric forcing. Further investigation is required to properly answer this question.

2.2.2 The 1934 Flood

In late November and early December of 1934 one of the most damaging floods in recorded history occurred on the Yarra River. About 144 mm of rain fell at Melbourne between 1900 local time on November 29 and 0230 local time on 1 December, 1934. All tributaries of the Yarra River were flooded and extensive inundation occurred in low lying suburbs around Melbourne including Heidleberg, Kew, Collingwood, Toorak, Richmond and South Melbourne. Many footbridges and boatsheds along the Yarra were washed away and the Burke Road Bridge was under water.

In addition to floods along the Yarra River, the Mordialloc Creek and Patterson River breached their banks, flooding houses on the eastern side of the railway line to about 2 metres in depth. More than 2,500 people were rendered homeless following flooding at Mordialloc, Aspendale, Edithvale, Chelsea and Carrum.

The storm responsible for the floods also caused the highest recorded tide level at Williamstown, which has been estimated by Adams (1987) to be 1.33 m AHD at 2100 local time on 30 November. South to southwesterly gales persisted from 1300 hours and reached a peak of 28 m s^{-1} at 1700 hours local time on 30 November.

The destruction caused by the 1934 storm was not confined to Port Phillip Bay - extensive areas in eastern Victoria were also affected by flooding. The Latrobe River burst its banks and flooded the Yallourn open cut mine. The entire township of Kooweerup was inundated and 4,000 residents were evacuated. Wonthaggi reported its worst storm damage in 41 years and residents of Tarwin and Tarwin Lower were isolated by floodwaters. The main roads between Warburton and Healesville were closed due to landslides.

The death toll due to the floods was at least 14 people and the storm damage for Victoria estimated at around £1,000,000. In addition, a steamship (the Coramba) was lost in severe seas in Bass Strait, resulting in the death of all 17 crew members. The steamship was en route to Melbourne from Warrnambool on 29 November. It is believed that on reaching Port Phillip Heads the following morning, storm conditions were too severe for it to risk entering the Bay and it proceeded to Western Port. It was wrecked off Phillip Island at approximately 2230 local time November 30, around the time peak gale conditions were reported at this location.

The synoptic conditions surrounding this event are summarized in Figure 2.7. In the 24 hours from 0900 local time on 29 November, a low pressure system moved into Bass Strait from the southwest and intensified, bringing strong southerly to southwesterly winds and rainfall to the eastern part of the state. It is likely that some further intensification of the low took place during the following 12 hours, as it is during this time that the strongest gales were reported with an average speed of 22 m s^{-1}. In the 12 hours from 1800 local time on 30 November, the gales were reported, to moderate before increasing again to around 16 m s^{-1} by 0900 local time on 1 December.

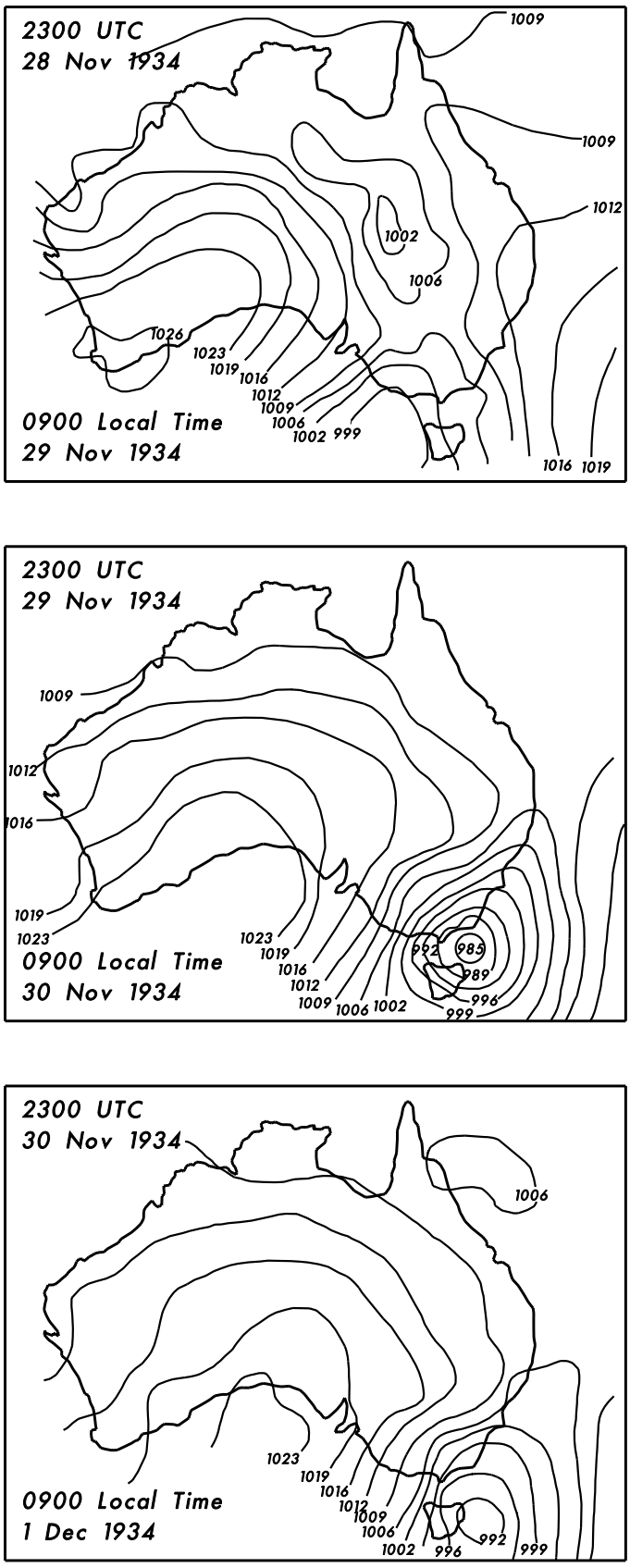

Figure 2.7: Analyses of mean sea level pressure for the 1934 flood event.

2.2.3 East Coast Lows

Low pressure systems which form off the east coast of Australia, known as east coast lows (eg. Holland et al. 1987) or cut-off lows (McInnes et al. 1992), have been shown to generate storm surges on the east coast of Australia (McInnes and Hubbert 1993). This is due to the southerly air stream which becomes established when the centre of the low is located offshore. These lows can produce intense rainfall, creating the potential for coastal flooding from the combined effects of rainfall and storm surge. Elevated sea levels at already flooded river outflows can reduce the drainage rate still further and exacerbate or prolong the flooding upstream.

Much of the Victorian coastline is too far south to be affected by storm surges generated by this type of system. However, their rain bearing capacity can result in flooding particularly in eastern Victoria. The combination of such an event, followed by a storm surge through Bass Strait generated by a separate weather system (such as the passage of a cold front) has the potential to cause the same combined flooding situation over the low lying coastal regions along Victoria's coast.

2.2.4 Summary

Three types of meteorological situations have been identified as causing elevated sea levels and inundation along Victoria's coast. These are summarized below.

1 **Westerly Wind Events** Westerly winds associated with the movement of cold fronts produce elevated sea levels along large stretches of the southern coastline. Such disturbances also affect Port Phillip Bay and most commonly occur from autumn through spring. Storm surges are caused more by westerly winds rather than the inverse barometer effect, as the associated low pressure system is usually located well to the south of the continent. Rainfall is usually widespread but not generally severe enough to cause major flooding.

2 **Bass Strait Depressions** The 1934 flood is an extreme example of such an event. A low pressure system moves into Bass Strait and possibly undergoes further intensification. Storm surges are likely to be caused by a combination of inverse barometer effect as well as wind setup on the northern parts of Bass Strait and Port Phillip Bay under the influence of strong southerly to southwesterly winds, which occur once the centre of the low has moved further east. Extreme rainfall is likely to occur with this type of system.

3 **Combined Rainfall/Surge Events** Severe coastal inundation is possible if flooding occurs in coastal areas as a result of extreme rainfall, followed by a storm surge. The types of systems which could produce extreme rainfall include east coast lows, which are most likely to affect eastern Victoria, or other depressions which can affect coastal and inland regions throughout the state. The weather conditions which are then most likely to produce a storm surge to follow are a westerly wind event.

In the present study, the two cases chosen for detailed modelling fall into the first class of event. Extreme examples of storm surges occurring as a result of the second and third class of events have not occurred in Port Phillip Bay over recent years to provide accurate observational data against which detailed modelling could be tested.

CHAPTER 3: Impact of Climate Change

3.1 Mean Sea Surface Temperature Increase

Scenarios of future global warming which include the range of possible climatic sensitivities and future greenhouse gas emissions have been produced by Wigley and Raper (1992) using a simple model which accounts for heat absorption by the oceans. Based on their results, an average global warming of 0.6-1.7°C by 2030 and 1.0-3.9°C by 2070 are expected (Whetton et al. 1995). Taking into account the regional patterns of warming based on GCM results, this global warming estimate translates to a 0.5-2.0°C warming by 2030 and a 1.0-5.0°C warming by 2070 for the southern coastal regions of Australia (Whetton et al. 1995).

3.2 Mean Sea Level Rise

Global mean sea level change for 1990-2100 has been calculated by Wigley and Raper (1992) based on global warmings associated with a range of CO_2 emission scenarios as well as a range of climate sensitivities. Based on their calculations, global average sea level rises are expected to be of the order of 5-35 cm by 2030 and 10-80 cm by 2070 (Whetton et al. 1995).

It should be noted that significant variations in local sea level rise may occur as a result of changes in ocean circulation and local atmospheric pressure associated with global warming and climate change. This was first noted by Mikolajewicz et al. (1990) based on the results of a dynamic ocean model. Gregory (1993) and Cubash et al. (1994) have since quantified this effect using coupled AOGCMs. Both studies find regional differences in mean sea level rise of the order of $\pm$ 50 % of the global average. However there is not agreement between regions experiencing greater or lesser sea level rise.

There is also concern that the current generation of coupled AOGCMs are sequestering too much heat in the southern ocean (England, 1995) and that improved coupled models will be necessary before reliable scenarios of regional changes in mean sea level can be obtained. Changes in coastal boundary currents may also be important for local sea level and so, to gain a more realistic picture of likely local sea level changes, it will be necessary to run finer resolution ocean models which are capable of resolving coastal currents.

In the light of the above uncertainties and caveats, this report will consider a worst case scenario of an 80 cm rise in mean sea level by 2070. It should be clearly understood however, that the actual mean sea level rise by 2070 may be much less than this worst case estimate.

3.3 Changes to Storm Surge Forcing

3.3.1 Methodology

The prevailing meteorological conditions during storm surges along the southern coastline were examined in the previous chapter. Episodes of westerly winds associated with the movement of cold fronts along the southern coastline were found to be responsible for storm surge events in the majority of situations. The colder months, when the subtropical ridge and the polar trough are located further north, were the favoured times of the year for storm surge occurrence. During this time the southern coast is in a more persistent westerly air stream.

The question of how the enhanced greenhouse effect is likely to affect storm surges needs to be addressed in terms of changes to the meteorological forcing and in particular, to changes in the strength and frequency of westerly winds along the south coast under a doubling of CO_2. The seasonally averaged, near surface wind conditions from three sets of GCM experiments are analyzed in this chapter. The use of more than one set of GCM experiments provides an indication of the generality of the findings. The first two GCM experiments examined are the CSIRO Mark I and Mark II slab ocean experiments under $1\times CO_2$ and $2\times CO_2$ conditions.

The CSIRO Mark II GCM contained various improvements over the one used to perform the Mark I experiment. A new soil/canopy scheme including soil type, albedo, roughness length, vegetation type, canopy resistance and interception of moisture, run-off, and deep soil percolation was implemented. A more realistic horizontal and vertical moisture transport scheme, and a new dynamical sea-ice scheme were used. Modifications were made to the cloud schemes - including evaporation of rainfall below cloud base and the computational scheme was modified to allow longer time steps. Despite the advances in the CSIRO Mark II simulation, the Mark I results are still included in this study. This is to enable interpretation of the results in the light of existing studies which have also been based on the Mark I set of experiments.

The third pair of GCM experiments analyzed is from the CSIRO coupled AOGCM under present ($1\times CO_2$) and transient CO_2 conditions. In the transient experiment, atmospheric CO_2 levels are increased at a rate of 1% per year and the output is stored over a time interval, coinciding approximately with a doubling of present day CO_2 levels. The transient experiment will also be referred to as a $2\times CO_2$ experiment.

In addition to examining the seasonally averaged low level wind conditions over the Australian region, daily average wind conditions over a defined region of interest are also examined. Daily variables are only available for the two slab ocean GCM experiments under $1\times CO_2$ and $2\times CO_2$ conditions. The region chosen for detailed analysis is outlined in Figure 3.1a and consists of eight model grid points located to the south of the continent in the Great Australian Bight and extending eastwards into Bass Strait. Model output was saved three times during a model simulated day. The analysis of daily data from these models is based on an average of the data at the three output times. The number of years of daily data varied between experiment and

simulation. In the Mark I experiment, 24 years and 29 years of daily data were stored from the $1\times CO_2$ and $2\times CO_2$ simulations respectively. In the Mark II experiment, 30 years of daily data were available from each of the $1\times CO_2$ and $2\times CO_2$ simulations.

3.3.2 CSIRO-9 Mark I GCM results

Figure 3.1 shows the seasonally averaged winds from six years of analyzed observations from the European Centre for Medium-range Weather Forecasting (ECMWF). During the summer months, when the subtropical ridge is located just to the south of the continent, the westerlies tend to have less influence on the southern coastline. This situation continues into the autumn months. In winter, the subtropical ridge has moved further north and the westerlies have become a more prevalent feature along the southern coast. In spring, the southeastern part of the coastline is most commonly under the influence of a westerly airstream.

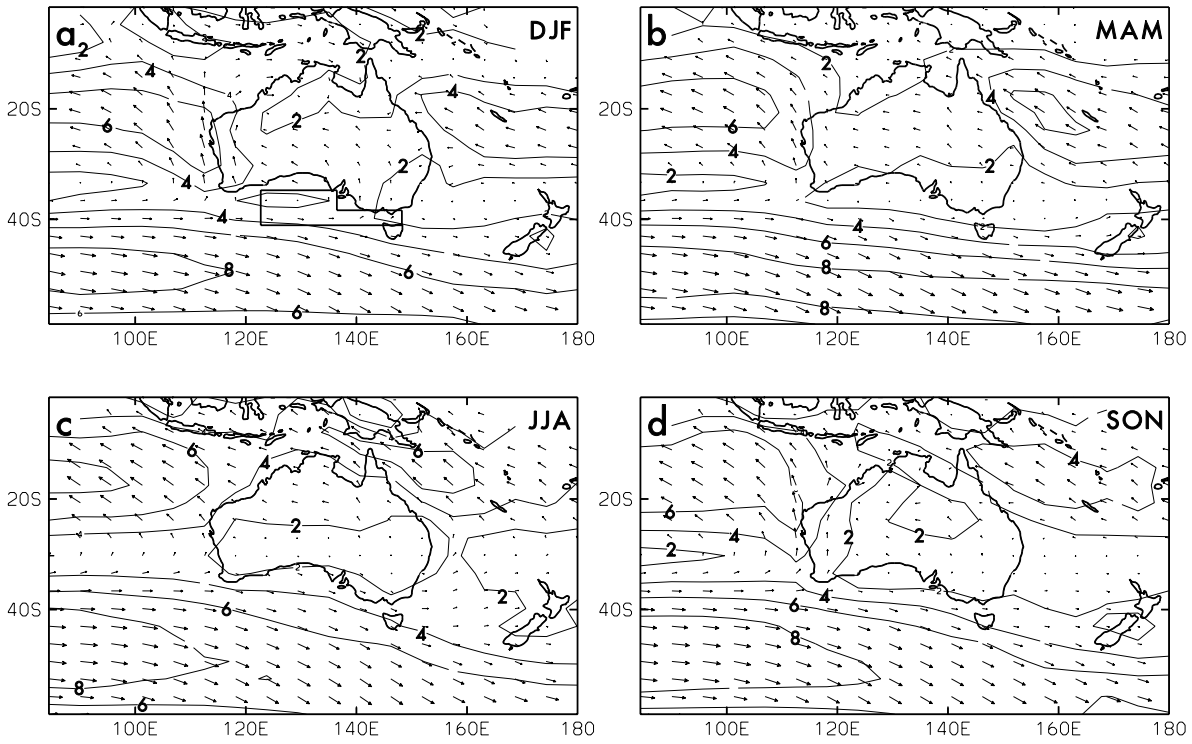

Figure 3.1: Seasonally averaged near-surface winds based on six years of ECMWF analyses for the seasons indicated. The contour interval is 2 m s^{-1}.

The seasonally averaged near-surface winds from 24 years of daily output from the CSIRO-9 Mark I model are shown in Figure 3.2. In general, wind directions in all seasons show close qualitative agreement with the equivalent ECMWF winds (Figure 3.1). The main difference is the wind strength, which is greater in all seasons in the $1\times CO_2$ simulation - particularly around 50°S where the westerly wind maximum in the $1\times CO_2$ simulation is stronger by up to 4 m s^{-1}. In the vicinity of the southern Australian coastline and Bass Strait however, the GCM seasonally averaged winds show reasonably close agreement.

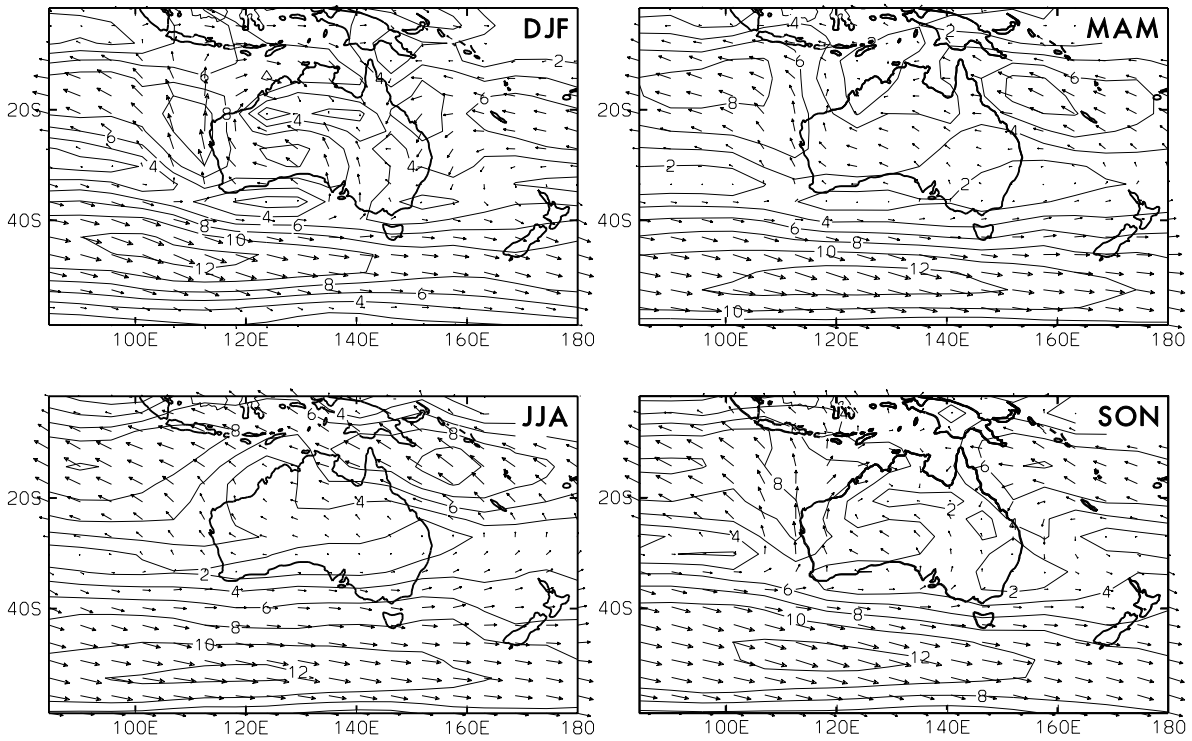

Figure 3.2: Seasonally averaged near-surface winds from the CSIRO R21 Mark I model $1\times CO_2$ simulation for the months indicated.

Figure 3.3 represents the difference between the seasonally averaged winds in the $1\times CO_2$ and $2\times CO_2$ simulations. The shaded areas indicate a reduction in the strength of the winds in the $2\times CO_2$ simulation. In all seasons there is a reduction in the westerly wind maximum located at approximately 50°S in the $2\times CO_2$ simulation. This reduction is attributed to the spatial distribution of heating which occurs under a doubling of CO_2 - whereby more of the heating takes place in the higher latitudes than in the equatorial regions. The reduction in equator to pole temperature gradient causes less intense storms to develop in the mid-latitudes. This result has been found in other studies (eg. Bates and Meehl, 1985; Katzfey and McInnes, 1995).

In addition to the reduction in mean westerly wind maxima in the $2\times CO_2$ experiment, there is a slight broadening of the band of westerlies, resulting in a net increase in the mean westerlies in regions to the north and south of westerly maxima. This is particularly evident in the winter, when a net increase in westerlies is located in a band centred on 40°S. In autumn and spring there is some longitudinal variation present, such that the Australian southern coastal region shows a net reduction in mean westerlies under doubled CO_2.

The relationship between the seasonally averaged winds and the distribution of daily wind speeds and directions over the region of interest is now investigated. Figures 3.4-3.7 represent the percentage of days that the wind is from the direction indicated in each season. The total wind magnitude is broken down into wind speed categories to enable assessment of severe wind events.

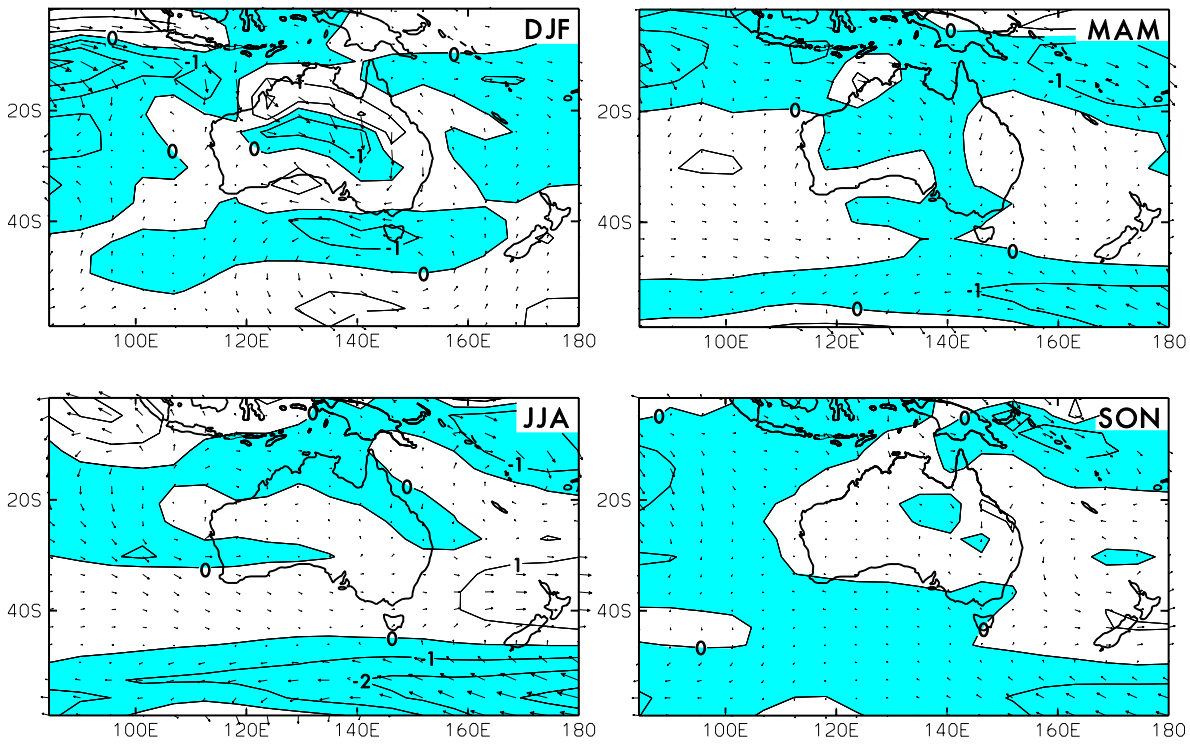

Figure 3.3: Difference between the seasonal averages of the wind field in the CSIRO GCM Mark I $1\times CO_2$ and $2\times CO_2$ simulations. Shaded areas indicate regions where the wind magnitude in the $2\times CO_2$ simulation is less than the $1\times CO_2$ simulation.

Wind frequency histograms for summer are shown in Figure 3.4. Over the total range of wind speeds, the control GCM tends to underestimate the northeasterly through southeasterly wind days and overestimate the south westerly through northwesterly wind days. The $2\times CO_2$ GCM simulation shows an increase in easterly and a reduction in westerly wind days. Lighter wind days in the range of 0-8 m s^{-1} tend to be underestimated in both GCM simulations compared with observations whereas strong wind days in the range of 12-99 m s^{-1} are overestimated. In all wind speed categories, the $2\times CO_2$ simulation shows a reduction in the number of days where the wind is blowing from a southwesterly to a northwesterly direction compared with the $1\times CO_2$ simulation.

In the autumn months (Figure 3.5), the GCMs again produce more westerly wind days than easterly wind days over the region of interest. Lighter wind days in the GCM are mainly underestimated for the easterly and northerly quadrants. As with the summer months, strong wind days in the range of 12-99 m s^{-1} are overestimated in the GCM. In the $2\times CO_2$ simulations there is a net increase in the frequency of westerly wind in the 0-12 m s^{-1} range but a decrease in the 12-99 m s^{-1} range.

Figure 3.6 shows the wind frequency histograms for winter. Over the entire range of wind speeds there is better overall agreement between the $1\times CO_2$ simulation and the observations than for summer and autumn. Again however, there is a bias in the GCM simulation towards more frequent stronger wind days. In the $2\times CO_2$ GCM simulation an increase in frequency of westerly wind days can be seen in the three

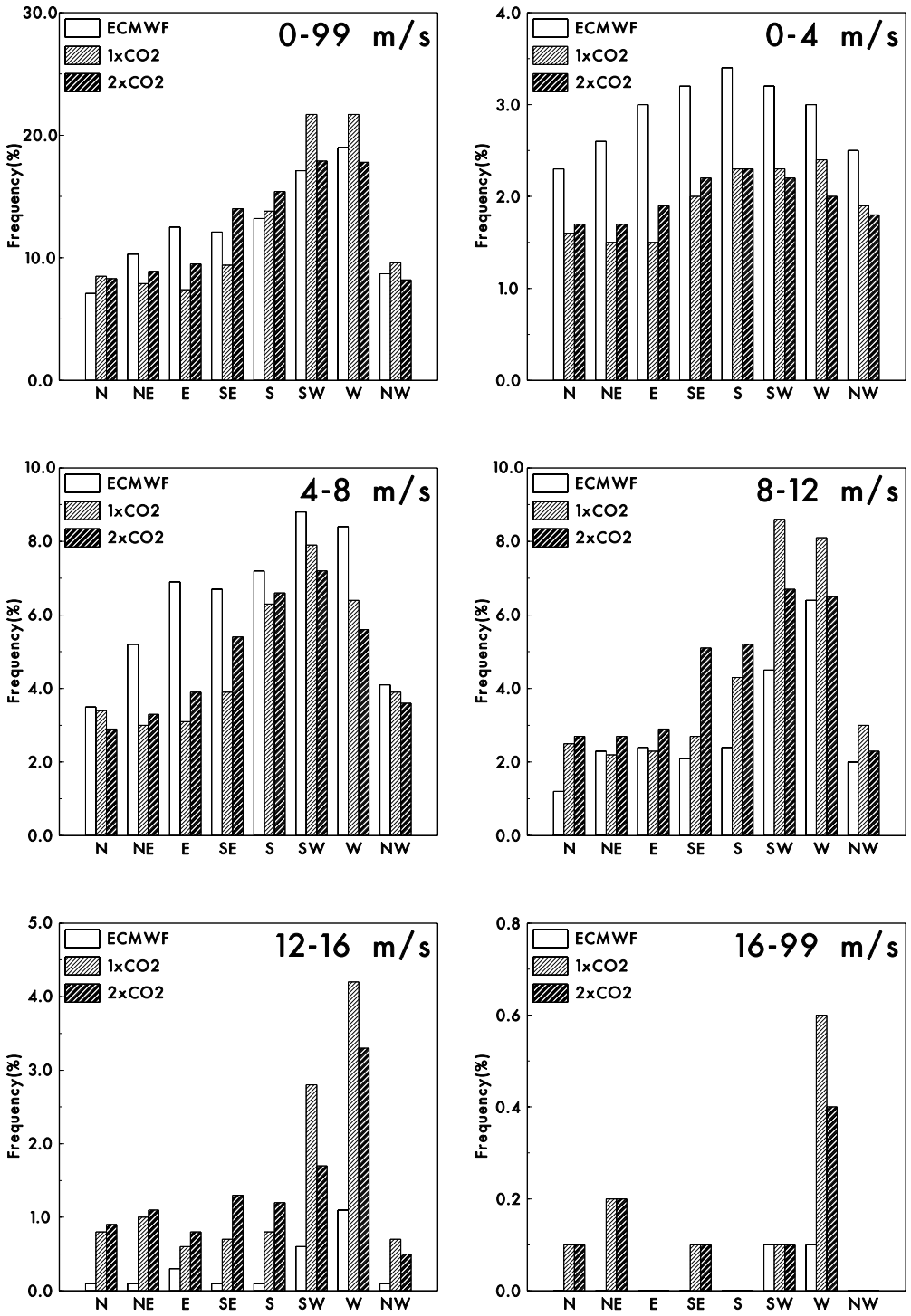

Figure 3.4: Histogram representing the distribution of wind direction averaged over eight GCM gridpoints located to the south of Australia for the summer months (DJF) over the wind speed categories indicated for the CSIRO 9 Mark I model. The vertical axis represents the number of days per 100 days that the wind is blowing from the direction indicated.

wind speed categories from 8-99 m s^{-1}. In each of the three categories the increase is about 1% over the frequencies shown for the $1\times CO_2$ simulation. This is also the case in the southwesterly and northwesterly directions, although the increase is smaller.

Spring shows a similar overall pattern of wind distribution to winter (Figure 3.7) with good agreement between the control simulation and the observations. When the wind direction histograms are broken down into wind speed categories, there is once again a tendency for the control GCM simulation to produce winds of in excess of 12 m s^{-1} more frequently than observed. In the $2\times CO_2$ simulation there is generally a slight reduction in the frequency of stronger wind days from a westerly direction.

It is evident that in all seasons the wind in the $1\times CO_2$ simulation tends to be more frequently from a westerly direction and less frequently from an easterly direction compared with observations. This result is consistent with Katzfey and McInnes (1995) who found that the occurrence of cut-off lows on the east coast of Australia was underestimated in the CSIRO-9 R21 GCM, particularly in the winter months. Low pressure centres located in this region would place the southeast coast in an easterly wind regime.

We now examine the observed and modelled winds with a westerly component in more detail. Figure 3.8 shows frequency distribution curves for all winds ranging from southwesterly to northwesterly in the observations and the $1\times CO_2$ and $2\times CO_2$ simulations. These curves again illustrate the tendency of the models in both the $1\times CO_2$ and $2\times CO_2$ simulations to produce light westerlies (less than 8 m s^{-1}) less frequently than observations indicated. This is most noticeable in summer and winter. The $1\times CO_2$ simulation clearly produces a greater incidence of winds of 10 m s^{-1} compared with observations. The $2\times CO_2$ simulation indicates a reduction in the frequency of wind days greater than 10 m s^{-1} in spring, summer and autumn and a slight increase in winter.

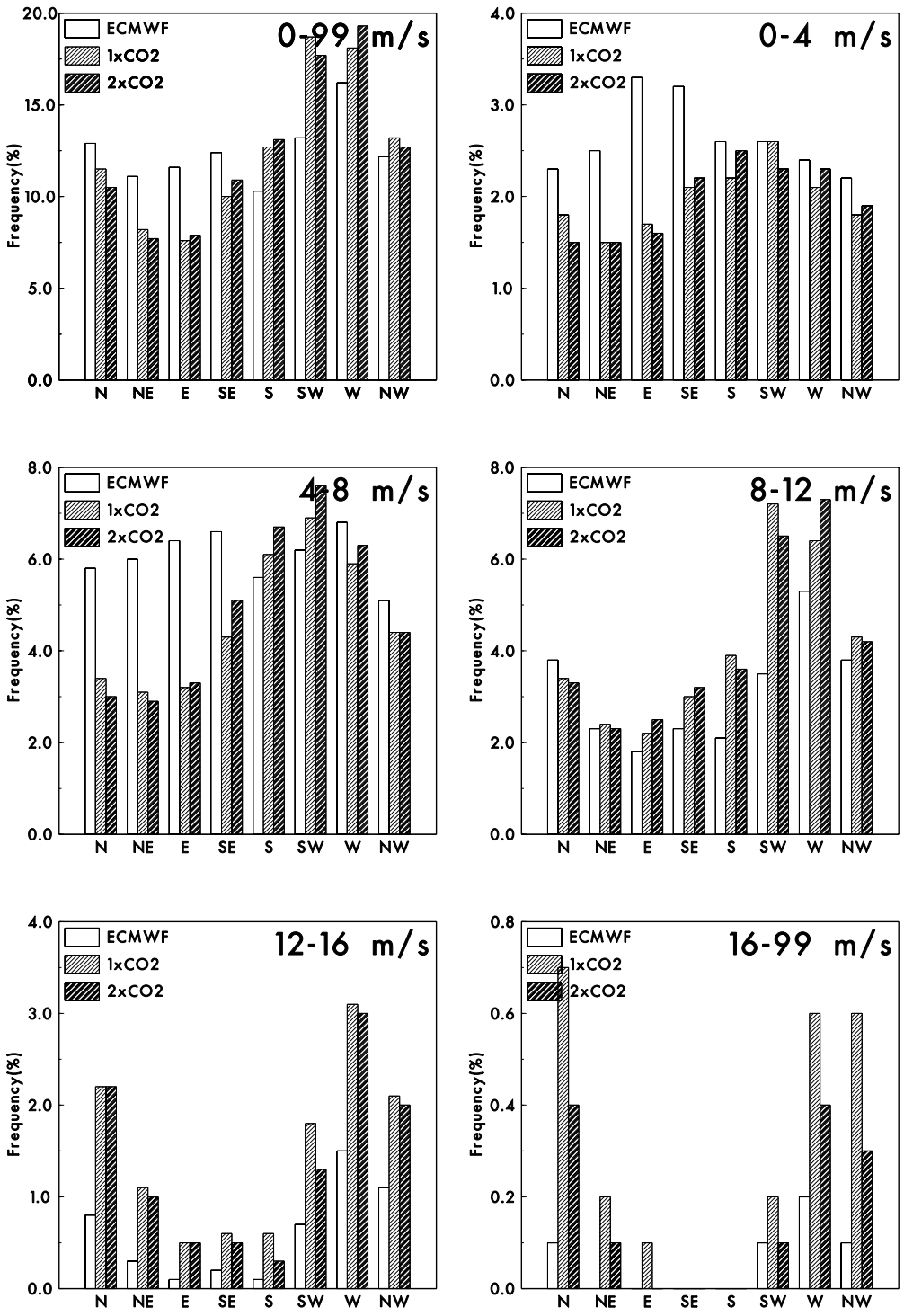

Figure 3.5: Histogram representing the distribution of wind direction averaged over eight GCM gridpoints located to the south of Australia for the autumn months (MAM) over the wind speed categories indicated for the CSIRO 9 Mark I model. The vertical axis represents the number of days per 100 days that the wind is blowing from the direction indicated.

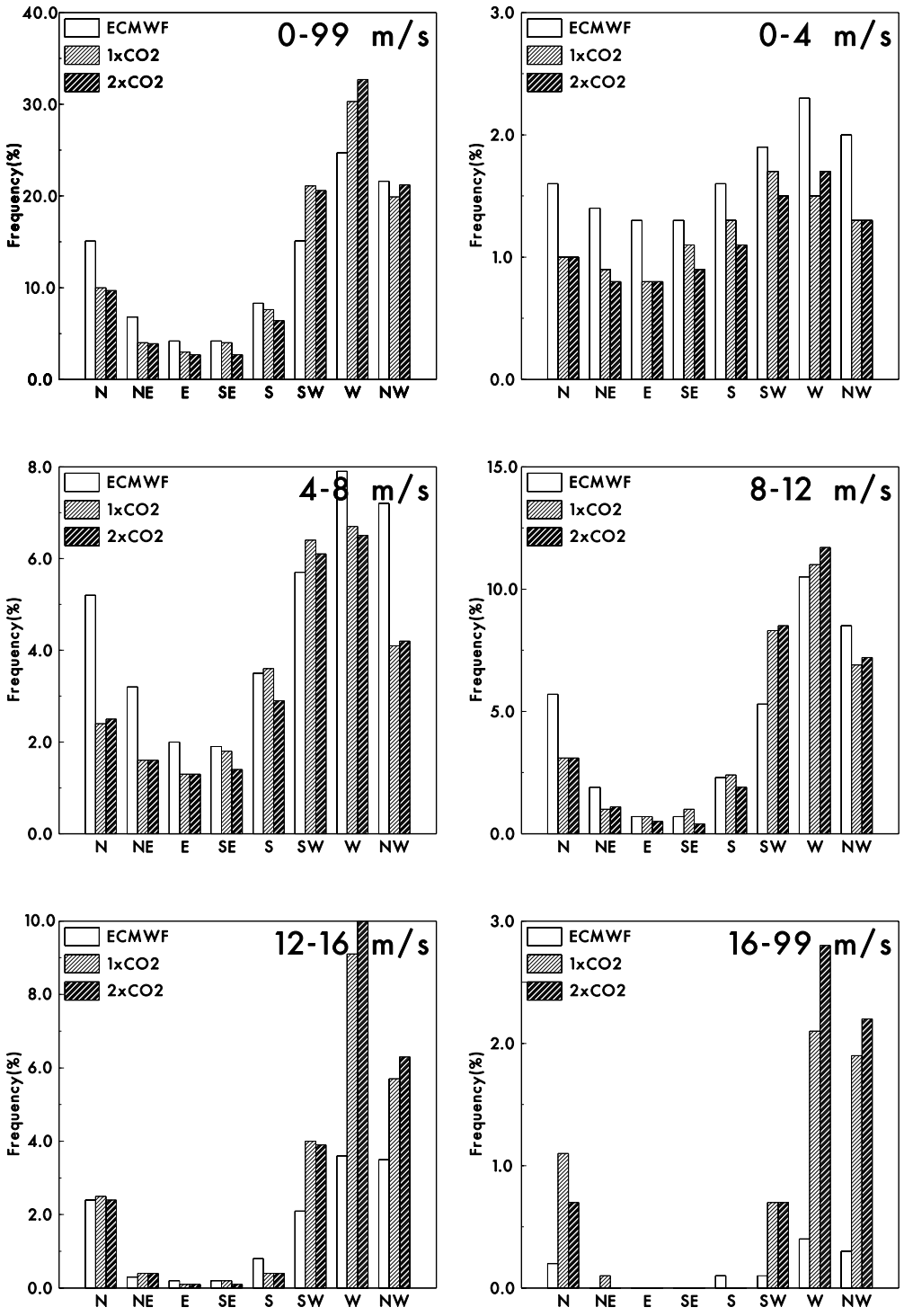

Figure 3.6: Histogram representing the distribution of wind direction averaged over eight GCM gridpoints located to the south of Australia for the winter months (JJA) over the wind speed categories indicated for the CSIRO 9 Mark I model. The vertical axis represents the number of days per 100 days that the wind is blowing from the direction indicated.

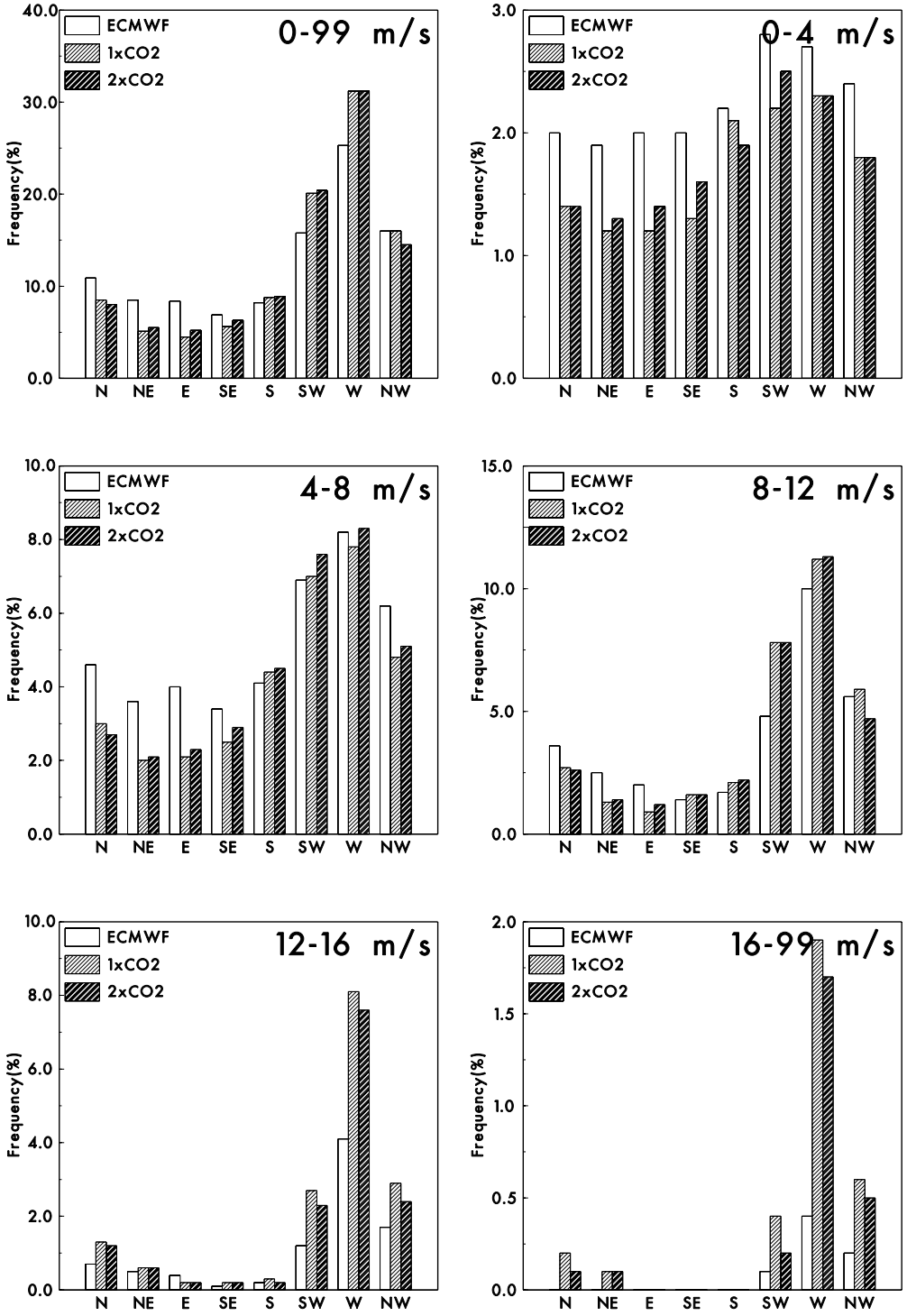

Figure 3.7: Histogram representing the distribution of wind direction averaged over eight GCM gridpoints located to the south of Australia for the spring months (SON) over the wind speed categories indicated for the CSIRO 9 Mark I model. The vertical axis represents the number of days per 100 days that the wind is blowing from the direction indicated.

3.3.3 CSIRO Mark II GCM Results

Figure 3.9 shows the seasonally averaged near surface winds from the $1\times CO_2$ Mark II simulation. Comparing these with Figure 3.2 indicates that the average wind speeds in this simulation are weaker overall than in the Mark I simulation, bringing them into closer agreement with the observations (Figure 3.1). This is most noticable at around 50°S, where the westerly wind maxima has dropped from in excess of 12 m s^{-1} in the Mark I simulation to only 8 or 10 m s^{-1} in the Mark II simulation. Along the southern coastline however, average wind strengths are still slightly stronger than observed. The average wind direction generally shows close agreement with observations.

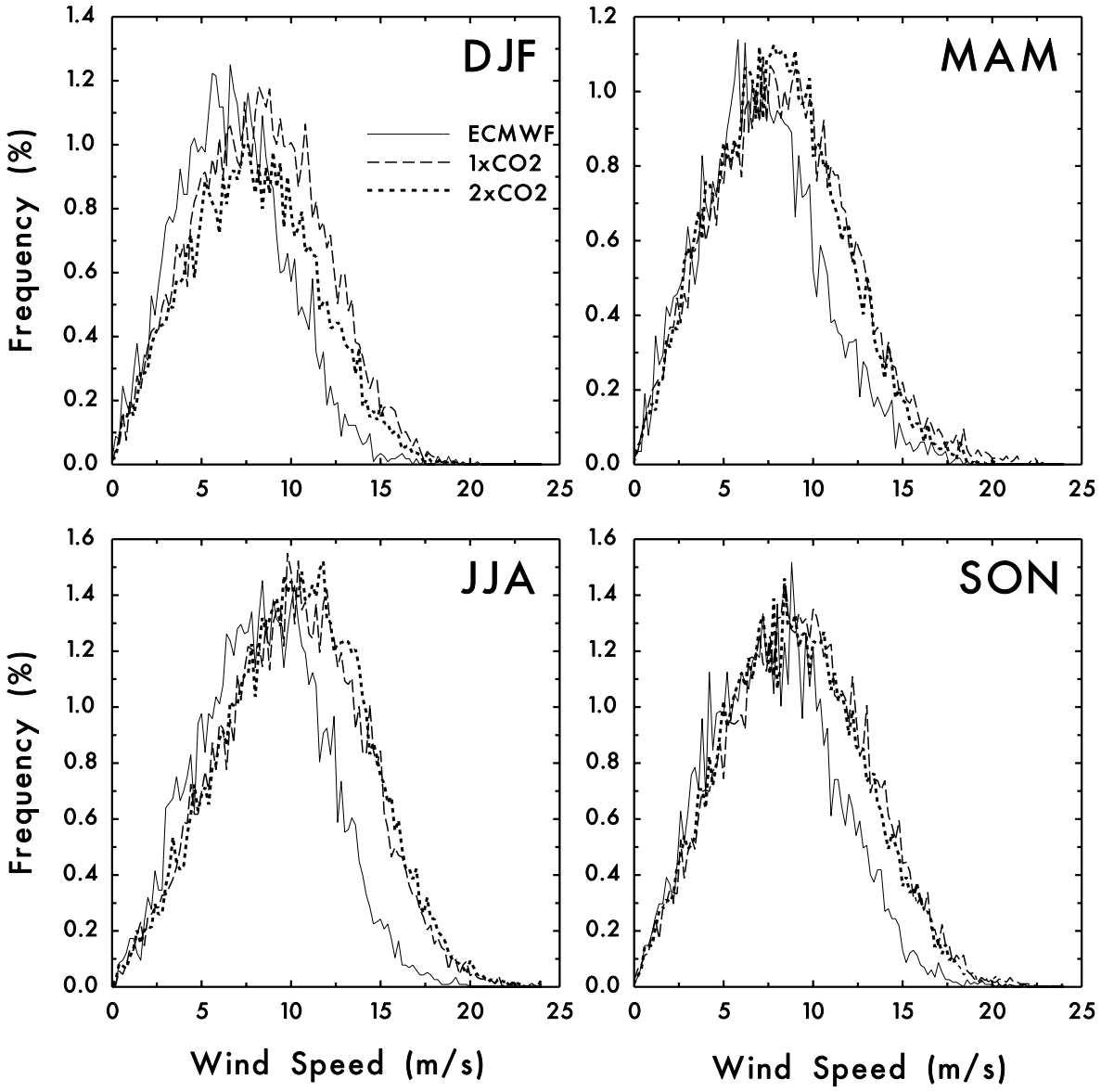

Figure 3.8: Frequency distribution curves for all incidence of winds from southwesterly to northwesterly directions for each season based on CSIRO-9 Mark I daily winds averaged over eight GCM gridpoints located to the south of Australia.

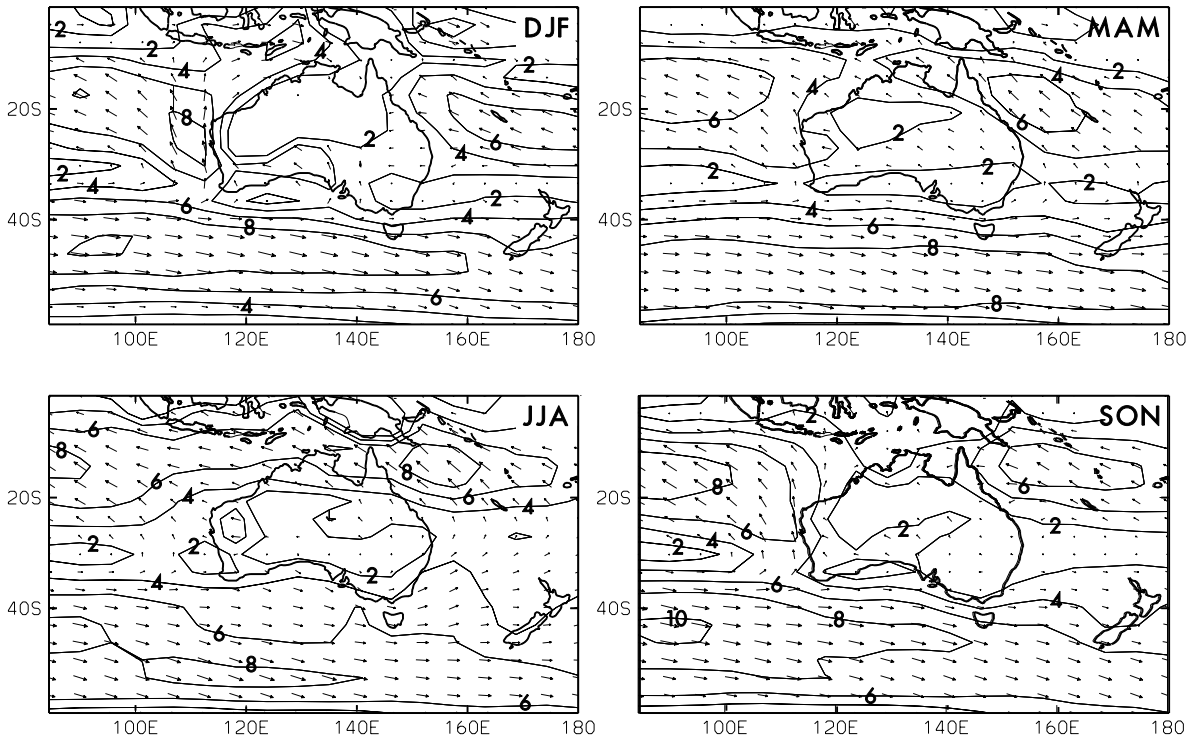

Figure 3.9: Seasonally averaged near-surface winds from the CSIRO R21 Mark II model $1\times CO_2$ simulation for the months indicated.

Figure 3.10 shows the difference between the seasonally averaged winds in the $2\times CO_2$ and the $1\times CO_2$ simulation. Shaded areas, which indicate a reduction in wind strength in the $2\times CO_2$, simulation can be seen in the southern parts of the domain at around 50°S in all seasons and indicate a weakening of the westerlies at that latitudes consistent with that found in the Mark I simulation and other slab ocean GCMs. The shaded area south of the Australian continent during summer indicates a slight weakening of westerly winds, while in the autumn, a weakening has occurred in the Bight but there is a strengthening over areas further south. In winter and spring, areas to the south-west of the continent have experienced an average strengthening in westerlies, whereas the region to the south east of Australia has experienced a reduction in strength in the $2\times CO_2$ simulation. The models do not show consistent agreement in the sign of the change between the $1\times CO_2$ and $2\times CO_2$ average winds over the region south of Australia.

Frequency distribution curves constructed from daily averaged winds ranging from northwesterly to southwesterly in the Mark II model are shown in Figure 3.11. The frequency of light wind days ($\leq$ 5 m s^{-1}) in this experiment shows close agreement with observations and represents an improvement over the Mark I model. In spring, summer and autumn, the frequencies of westerly wind days in the GCM simulations, particularly in the 5 to 10 m s^{-1} range, are considerably greater than observations indicate and are also greater than those produced by the Mark I model simulations. For wind speeds greater than 10 m s^{-1}, the frequencies are higher than observed but by a similar amount to the Mark I model.

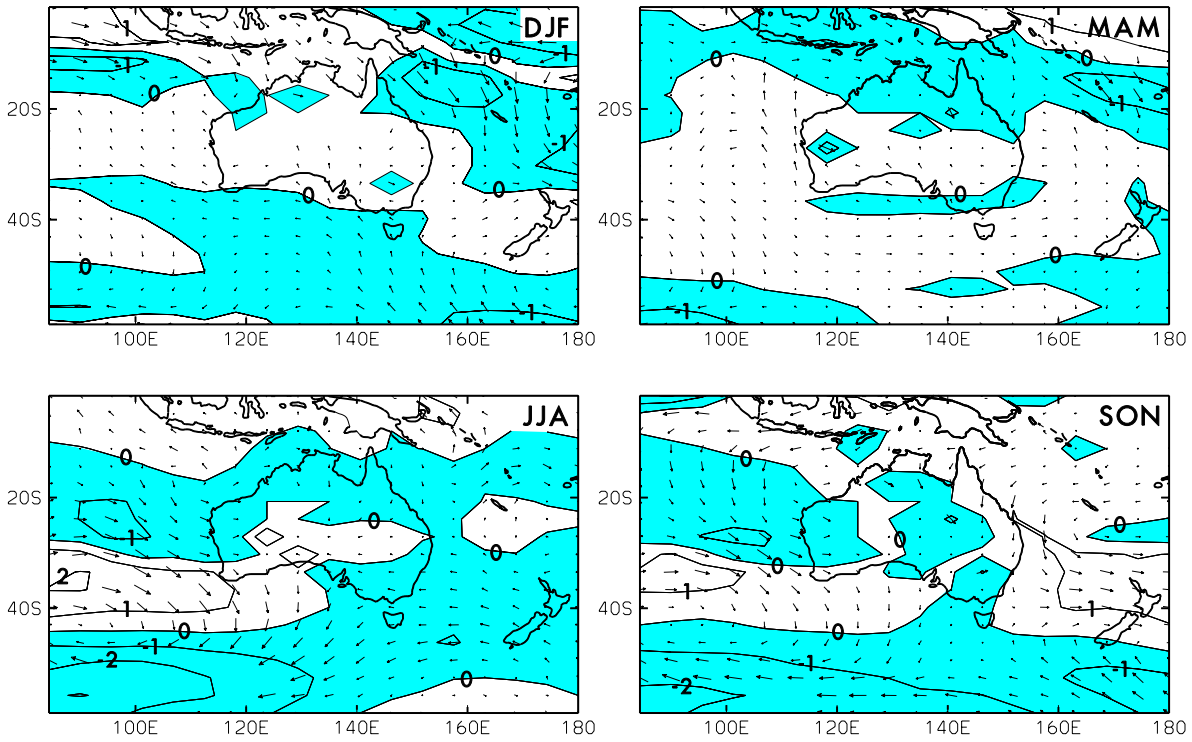

Figure 3.10: Difference between the seasonal averages of the wind field in the CSIRO GCM Mark II $1\times CO_2$ and $2\times CO_2$ simulations. Shaded areas indicate regions where the wind magnitude in the $2\times CO_2$ simulation is less than the $1\times CO_2$ simulation.

Comparing the curves for wind speeds greater than 10 m s^{-1}, there is little overall difference in any of the seasons. In summer, autumn and winter, there are marginal decreases in the frequency of strong wind days in the $2\times CO_2$ simulation, whereas in spring there is a slight increase. This is different to the Mark I experiment which showed a more dramatic reduction in the $2\times CO_2$ experiment in summer, slight reductions in autumn and spring and a slight increase in winter.

3.3.4 Transient Model Results

In the seasonally averaged wind fields from the CSIRO coupled AOGCM $1\times CO_2$ simulation (Figure 3.12), Average wind directions in the control simulation show close agreement with observations (Figure 3.1). Again, wind strengths are generally higher, particularly between 40-60°S. In the transient experiment, the effective doubling of CO_2 clearly has less impact on the wind fields compared with the slab ocean simulations (Figure 3.13). This is attributed to the fact that the dynamic ocean model takes a great amount of heat out of the atmosphere into the southern ocean around 50-60°S, leading to reduced warming at these latitudes and a smaller reduction in the north-south temperature gradient in the southern hemisphere. This feature of the coupled model is subject to considerable uncertainty at this time (England, 1995).

There is no consistency in the sign of the wind speed change between either of the slab ocean GCM experiments (Figures 3.3 and 3.10) and the transient experiment (Figure 3.13). The mean wind has increased marginally in summer and autumn and

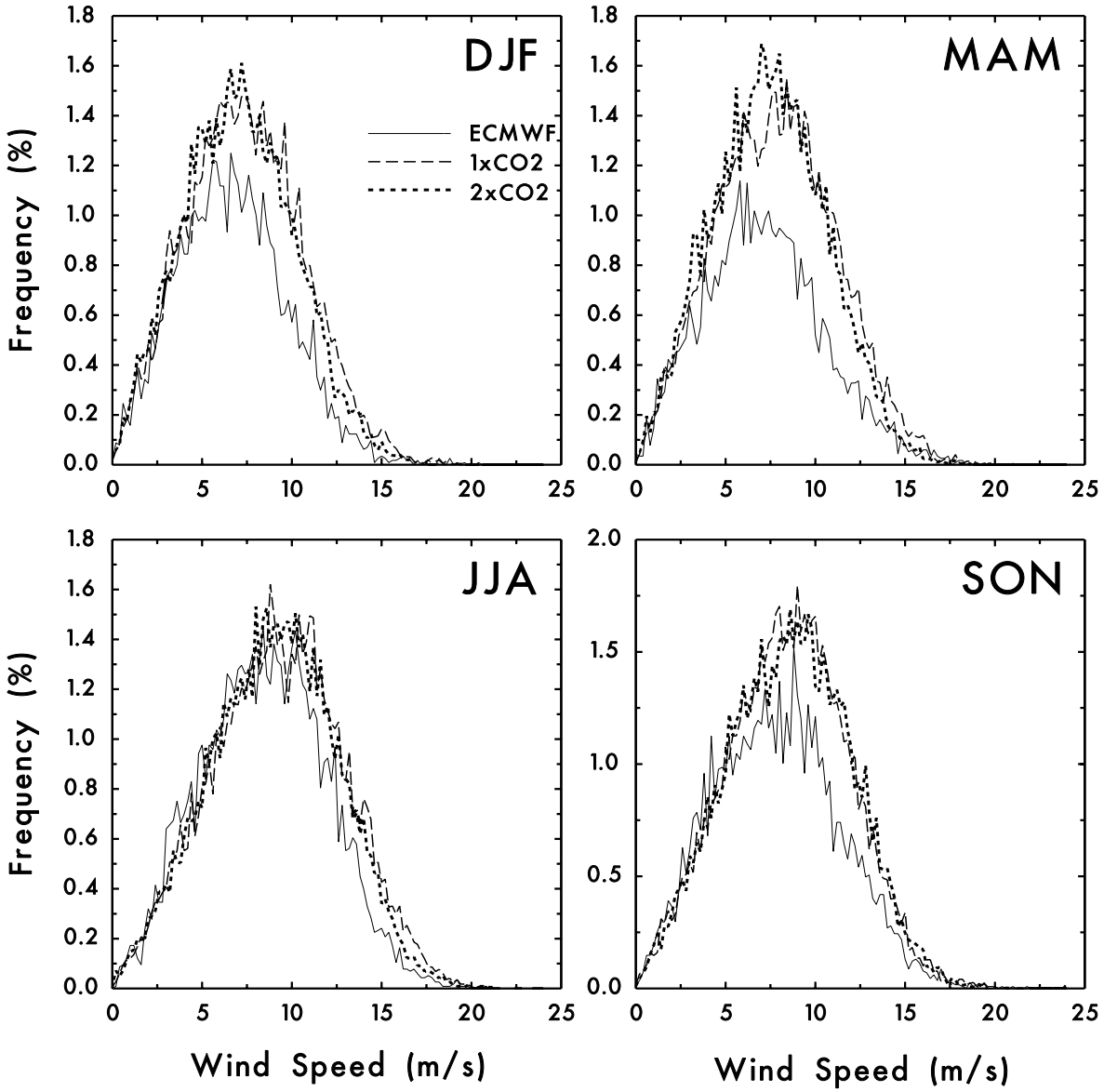

Figure 3.11: Frequency distribution curves for all incidents of winds from southwesterly to northwesterly directions for each of the seasons, based on CSIRO-9 Mark II daily winds averaged over eight GCM gridpoints located to the south of Australia.

decreased in winter and spring in the coupled model results over much of the southern Australian coastline.

3.3.5 Discussion and Scenario Development

A detailed analysis was carried out on the seasonally averaged, near-surface wind fields in two versions of the CSIRO slab ocean model GCM simulations and the CSIRO AOGCM, to determine whether there was a consistent change in the averaged wind patterns between different GCM experiments over the southern coastal regions.

The differences between the $1\times CO_2$ and $2\times CO_2$ wind fields for each of the three

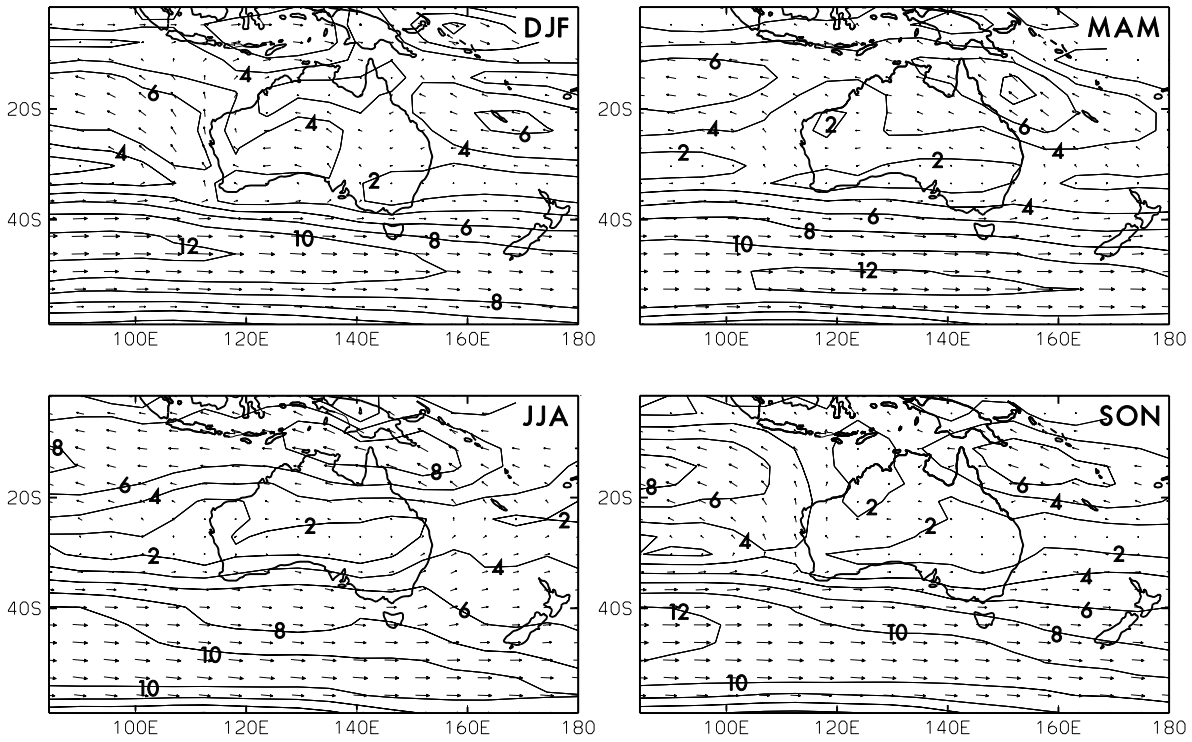

Figure 3.12: Seasonally averaged, near-surface winds for each season from the CSIRO coupled AOGCM $1\times CO_2$ simulation.

experiments indicated that there was no consistent change between the models over southern Australia. This highlights the difficulty in assessing the implications of climate change in this region, which occurs because slight seasonal changes in the strength or the meridional movement of the subtropical ridge and subpolar trough can have major implications for the westerly wind regime along Australia's south coast.

Considerable meridional variation was also evident in the difference fields of the three experiments, which introduces an added complexity in the determination of average wind changes over southern Australia. For example, at 40°S in the winter time case, the Mark I model shows a mean increase in winds in the $2\times CO_2$ experiment from 85°E to 180°E. The Mark II model shows a mean increase from 85°E to 140°E and then a decrease from 140°E to 180°E. In the coupled experiment, a decrease is evident from about 90°E to 170°E but there is an increase to the east and west of this region.

The daily winds over eight gridpoints to the south of Australia were analyzed in the two slab ocean GCM experiments. In general, when considering both the directional distribution of winds as well as magnitudes, the differences between the $1\times CO_2$ and $2\times CO_2$ simulations were considerably smaller than the differences between the $1\times CO_2$ and the observed winds. This is probably partly due to the resolution of the GCM. For example, there was a tendency for the GCMs to underestimate easterly wind days and overestimate westerly wind days. The synoptic situations, which lead to easterlies over southern Australia include depressions such as cut-off lows with

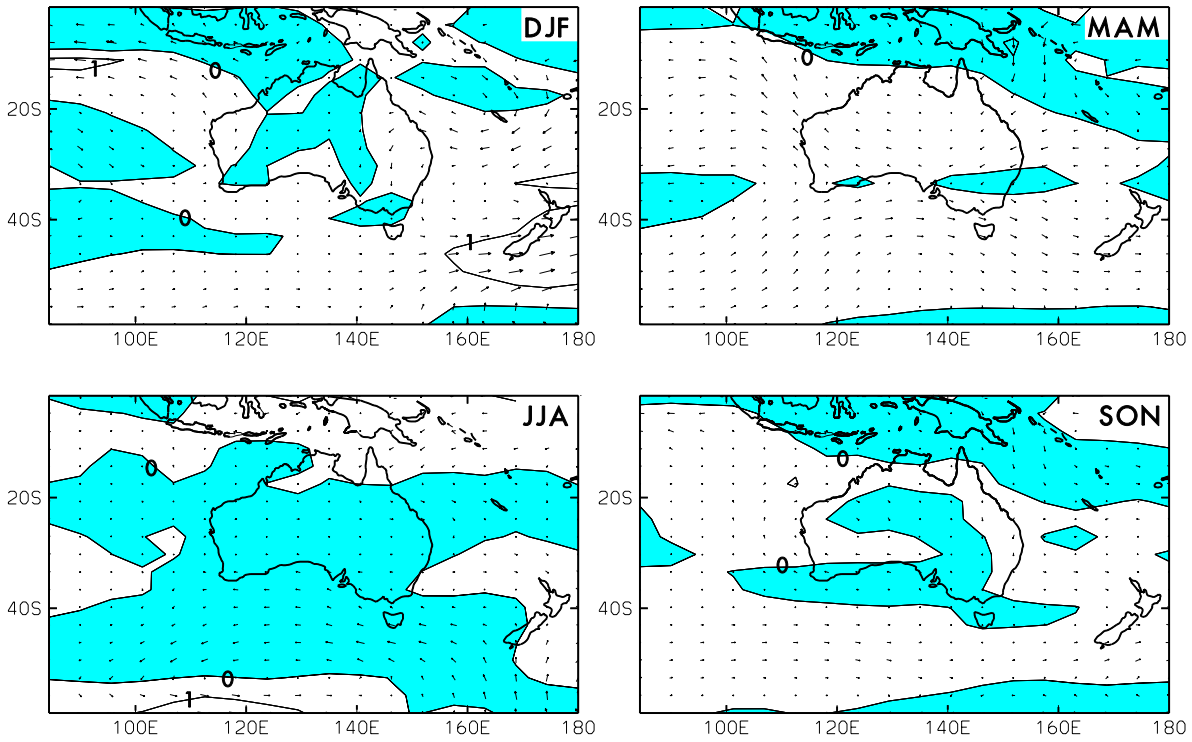

Figure 3.13: Difference between the seasonal averages of the wind field in the CSIRO coupled AOGCM $1\times CO_2$ and $2\times CO_2$ simulations. Shaded areas indicate regions where the wind magnitude in the $2\times CO_2$ simulation is less than the $1\times CO_2$ simulation.

an associated blocking high further south in the Tasman Sea. These situations are generally not well captured by GCMs (Katzfey and McInnes, 1995). On the other hand, westerlies over the south coast of Australia are generally caused by planetary scale phenomena, which are better captured by GCMs of current resolution.

Frequency distribution curves for the winds ranging from northwesterly to southwesterly were produced for the two slab ocean simulations over the same eight gridpoints. Considering autumn, winter and spring (when surges are most common), and wind speeds greater than 12.5 m s^{-1}, there was once again no consistent change between the $1\times CO_2$ and $2\times CO_2$ simulations. In autumn there was a marginal shift to lower wind speed values in both slab ocean experiments, a shift in spring in the Mark I simulation and winter in the Mark II simulation. Winter in the Mark I model and spring in the Mark II model showed a marginal shift towards more frequent and stronger wind days. This shift ranged between 0% and 10% for a given frequency. In spring of the Mark II experiment, the shift to stronger, more frequent westerly wind days is more marginal. In the other seasons the reduction in the $2\times CO_2$ westerlies for a given frequency is also of the order of 10% at most.

While it is not possible to deduce any conclusive changes in magnitude or frequency of westerly wind days due to the enhanced greenhouse effect, this analysis provides justification for selecting a range of possible changes which can be explored at the regional scale using high resolution LAMs. The analysis presented here suggests

that a change of around $\pm 10\%$ in wind strength during extreme events is a reasonable scenario for enhanced greenhouse change.

3.4 The Impact of Climate Change on East Coast Lows

Two previous studies have examined how east coast lows may be affected by climate change. McInnes et al. (1992) studied the impact of warmer sea surface temperatures on east coast lows. In that study, a high resolution atmospheric model was used to simulate four known cases of cut-off lows under control and elevated SST conditions. It was found that warmer SSTs caused intensification of the storms. Central pressures attained lower values and there was an associated increase in the strength of the near surface winds. Rainfall increased both in peak values and areal extent.

Katzfey and McInnes (1995) examined the representation of cut-off lows in the CSIRO 9 Mark I GCM. Detailed analysis indicated that a GCM cut-off low exhibited similar characteristics of formation and evolution to observed cut-off lows, giving confidence in the model's ability to represent these phenomena at the current resolution. It was found that the control GCM simulation tended to underestimate the frequency of occurrence of these systems, particularly in autumn and winter, indicating resolution limitations or possible deficiencies in aspects of the model's representation of physical processes. The $2\times CO_2$ simulation produced even fewer occurrences of cut-off lows in all seasons. This is because the warming which occurs in the enhanced greenhouse simulation with a slab-ocean GCM is greater at high latitudes than the equator. The temperature gradient between these locations is therefore reduced and consequently fewer mid-latitude storms are produced. It is possible that a different result may be found using coupled AOGCMs, but this has not yet been studied and the result may depend on the parameterisations in the AOGCM (England, 1995).

East coast lows or cut-off lows can produce flooding over Victoria due to extreme precipitation. Storm surges can also be generated, although this depends on the location and subsequent movement of the low relative to the coast. For example, east coast lows can generate storm surges if they are located in the Tasman Sea, so that the east coast is under the influence of a southerly wind regime (McInnes and Hubbert, 1994). The storm surges, however, tend to affect the NSW coastline further to the north.

CHAPTER 4: Modelling Storm Surges in Bass Strait

4.1 Model Description and Methodology

4.1.1 Atmospheric Model

The atmospheric model used in this study is a limited area hydrostatic, primitive equation, grid point model which can be run at varying horizontal and vertical resolutions. The model derives its initial and boundary conditions from analyses either from the Australian Bureau of Meteorology or the ECMWF. The boundary conditions are applied via a one- way nesting procedure and are updated every 12 hours throughout the model simulations.

Two atmospheric model simulations are performed on the boxed area in Figure 4.1 to provide surface pressure and winds at a higher spatial resolution than available from analyses. The horizontal resolution of the model is 45 km. The first simulation (Case 1) was run over the time interval 1100 UTC 21 May 1994 to 1100 UTC 29 May 1994. The second simulation (Case 2) was performed over the time interval 2300 UTC 3 November 1994 to 2300 UTC 7 November 1994.

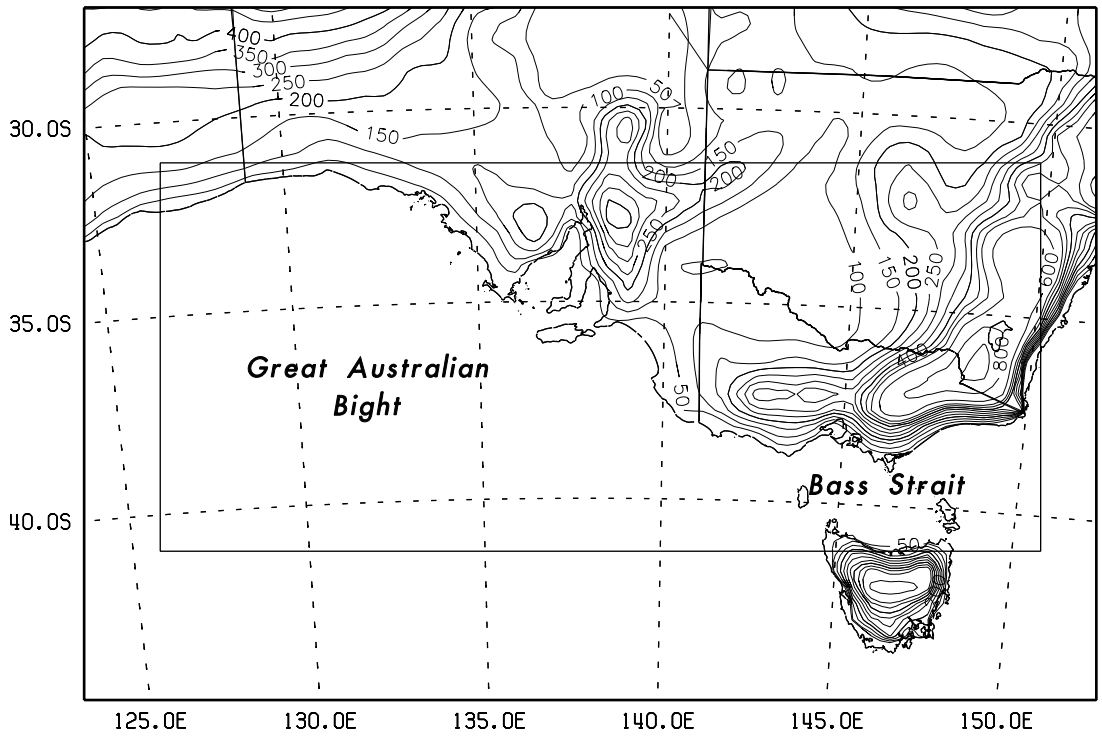

Figure 4.1: The domain used by the atmospheric model. The inner box denotes the domain used by the storm surge model.

4.1.2 Ocean Model

The storm surge model used is a depth integrated ocean-current model, developed specifically to simulate currents and sea surface elevations on continental shelves. The model is driven by wind stresses, atmospheric pressure gradients and bottom friction. An earlier fixed coastline version of the storm surge model is described in Hubbert et al. (1990) and Hubbert et al. (1991). The major development in the version used in the present study is its ability to model inundation of low lying coastal areas. This means that the coastal boundary is capable of moving in response to the occurrence of coastal flooding or drying. The model equations and the major features of the model are described in Appendix 1.

Model simulations have been conducted on the inner grid shown in Figure 4.1. Figure 4.2 shows the entire grid and the bathymetry used in the storm surge model as well as the locations of four Seaframe gauges which are used for model verification. The horizontal resolution of the storm surge simulations is 12 km.

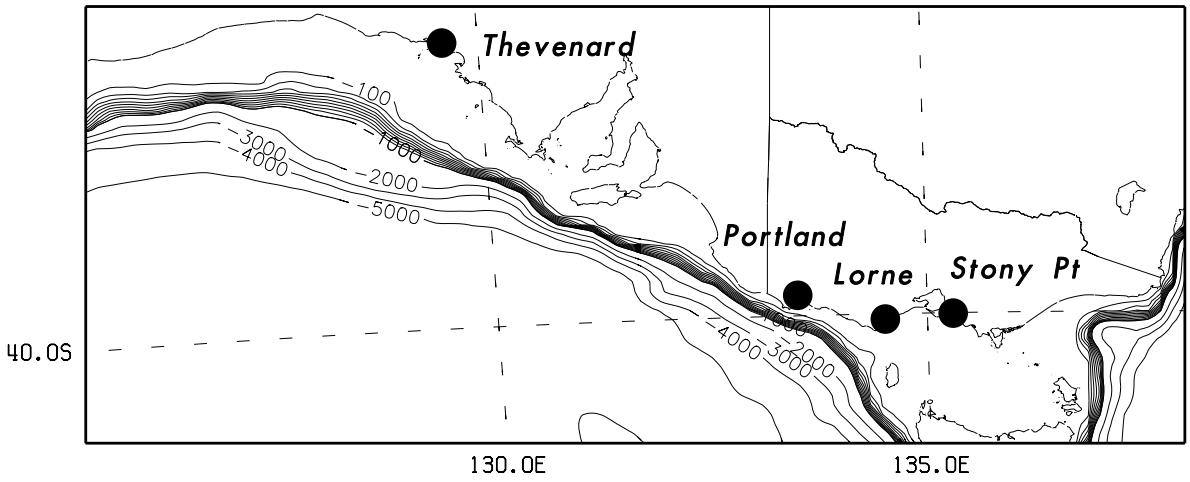

Figure 4.2: The grid over which storm surge model simulations are carried out.

4.2 Case 1 - May 1994

4.2.1 Synoptic Description

The first surge event modelled occurred in May 1994. Figure 2.3 indicates that elevated sea levels were recorded as far west as Hillarys and propagated eastward over the subsequent eight days. MSLP analyses from the Australian Bureau of Meteorology RASP model at 24 hourly intervals are shown in Figure 4.3 for six days during the event. At 1100 UTC 22 May 1994 (Figure 4.3 a), a trough was located to the south of Western Australia and the southwest region of the coast is under the influence of westerlies. The Victorian coastline was under the influence of westerlies following the passage of a front. Sea levels were elevated in Bass Strait in response to this system.

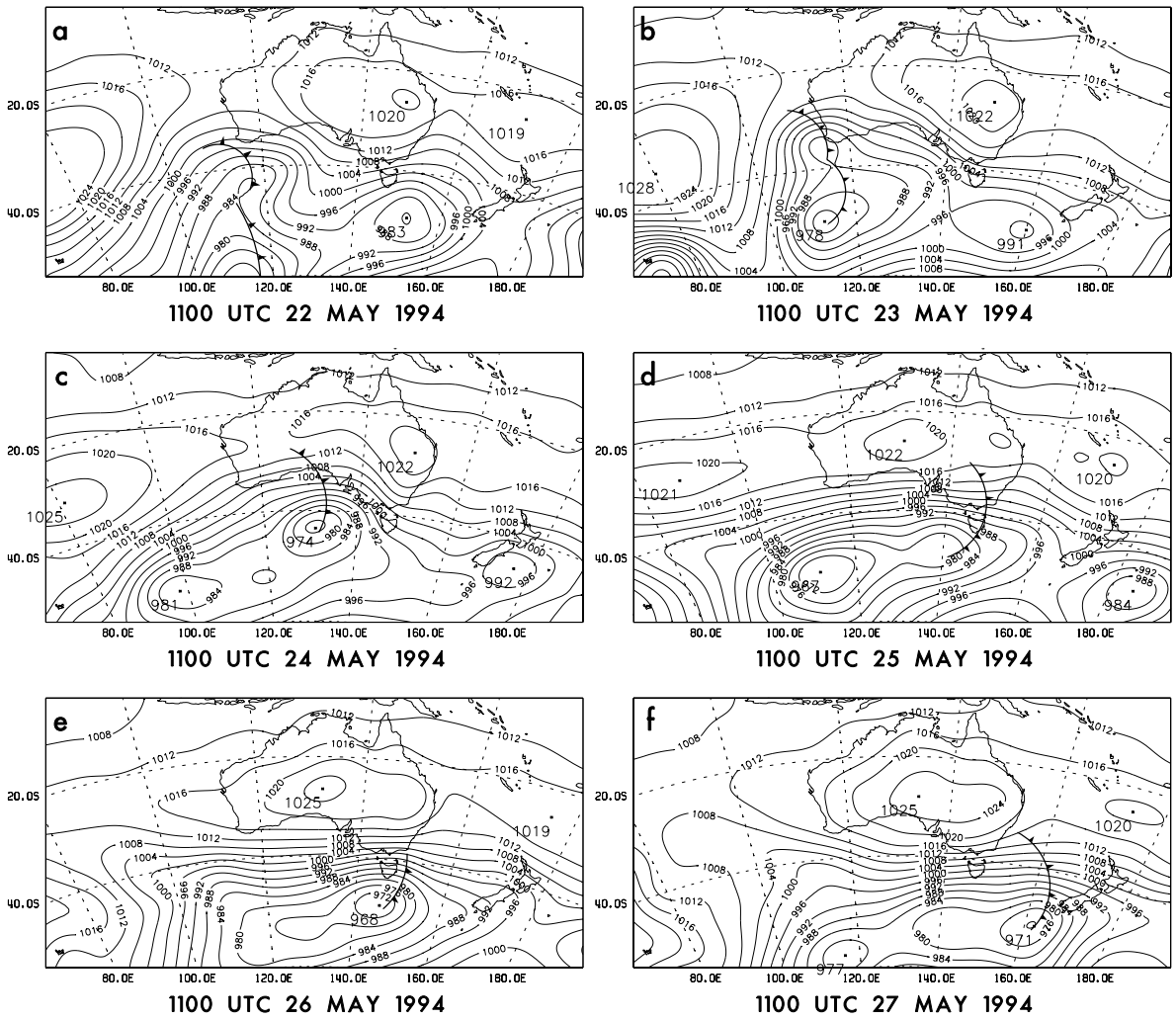

Figure 4.3: Bureau of Meteorology analyses of mean sea level pressure for Case 1.

During the following day (Figure 4.3b), the westerly flow on the west coast intensified as a second low moved into the region from the south. The remainder of the south coast was under a northwesterly wind regime.

In the 24 hours to 1100 UTC 24 May 1994 (Figure 4.3 c) the low intensified and moved into the Bight, placing the southern coastline to Adelaide under strong coast parallel flow. A surge in excess of 1.1 m was recorded at Thevenard at this time and at Port Stanvac some 12 hours later. Over the next two days the low in the Bight moved to the south of Tasmania (Figures 4.3 d and e) and westerlies in excess of 20 m s^{-1} affected the coastline from Adelaide to eastern Bass Strait. Sea levels at Portland and the Bass Strait gauges increase on 25 May and reach peak values on 26 May. By 1100 UTC 27 May (Figure 4.3 f) the low moved well to the southeast of Australia and pressure gradients over the southeastern coastline began to weaken.

This storm surge event was initiated by the sustained and predominantly westerly winds associated with the eastward passage of a low pressure system well to the south of the continent. Atmospheric pressures in the vicinity of the south coast were typically

around 1000 hPa - which would produce sea level increases of around 13 cm. This suggests that changes in atmospheric pressure do not play a major role in the initiation or maintenance of the elevated sea levels in this region.

Rainfall during the event was confined mainly to coastal regions. For example, Wilson's Promontory received 117 mm of rain over the eight day interval, with the largest daily rainfall total of 39 mm occurring in the 24 hours to 2300 UTC 26 May 1994. Melbourne, however, received less than 10 mm over the eight days.

4.2.2 Atmospheric Model Results

An atmospheric model simulation of Case 1 was performed over an eight day interval commencing at 1100 UTC 21 May 1994. A comparison of observed and modelled wind speed and direction at St Kilda for seven days commencing on 0000 UTC 22 May 1994 is shown in Figure 4.4. The winds during the first three days were predominantly northerly, with average speeds of between 15 and 20 m s^{-1}. Modelled wind speeds showed close agreement, although directions showed more of a westerly component during this time. On 26 May, when sea levels reached their peak at St Kilda, wind speeds increased to between 20 and 25 m s^{-1} and shifted to westerly. The modelled wind speed and direction during this time showed very close agreement. The westerlies weakened to around 10 m s^{-1} over the following two days and again, this is well captured by the model.

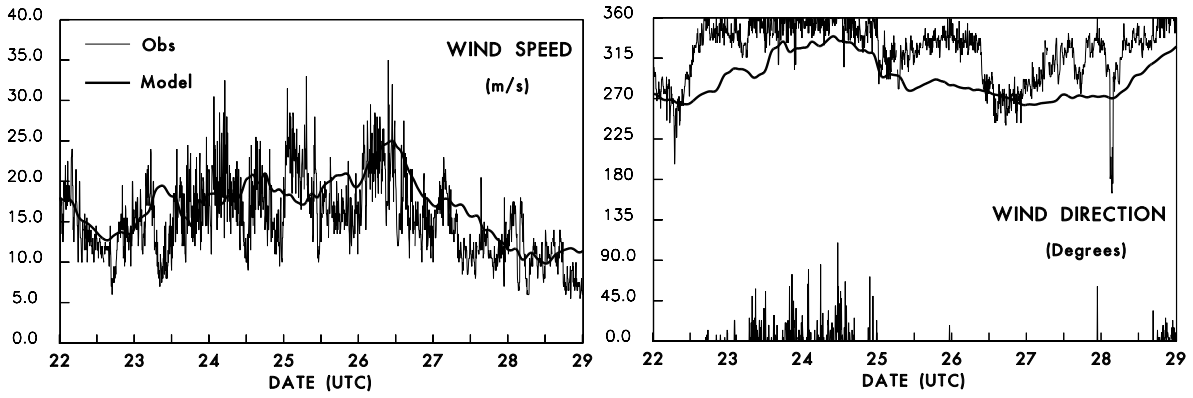

Figure 4.4: Observed and modelled wind speed and direction at St Kilda during part of May 1994.

Figure 4.5 shows the spatial variation in the model generated windfield at three and five days into the simulation. At three days (Figure 4.5a), a low pressure system was located in the southwest of the domain which was evident in the clockwise rotation of the windfield. Westerlies of up to 20 m s^{-1}, shifting to north-northwesterlies further eastward, were affecting the coastline from Thevenard to Bass Strait. At this time, Thevenard was approaching a storm surge peak, while water levels at the Bass Strait gauges were not yet increasing. Five days into the simulation (Figure 4.5b), a post-frontal westerly air stream of in excess of 20 m s^{-1} became established in a band to the south of 35°S. At Thevenard winds decreased to less than 10 m s^{-1} and sea levels

were abating. The Bass Strait gauges were recording maximum storm surges at this time.

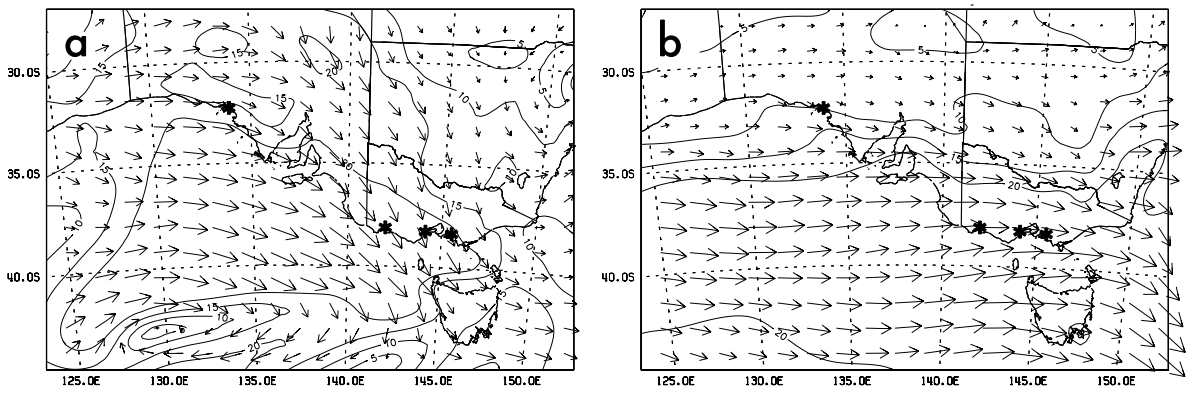

Figure 4.5: Modelled wind field at (a) 72 hours and (b) 120 hours into the model simulation corresponding to 1100 UTC 24 May 1994 and 1100 UTC 26 May 1994 respectively.

4.2.3 Storm Surge Model Results

Time series of observed and modelled sea level heights at the four locations identified in Figure 4.2 are shown in Figure 4.6. At Thevenard, the observed sea levels reached peak heights of around 1.1 m just over three days into the simulation. The modelled surge shows remarkably close agreement with the observed surge in terms of time, although the peak surge is slightly underestimated.

Observations at Portland indicated a lower peak surge of around 0.5 m. Again, the model captures the timing of the peak very closely, although it slightly underestimates the magnitude.

The time series of observed sea levels at Lorne and Stony Point both exhibit an oscillatory signal with a 12 hour period superimposed on the background residual heights. These oscillations are not seen in the model simulation. The cause of the oscillations and the inability of the model to capture them is to be investigated further.

The modelled surge heights at Lorne and Stony Point both show a build-up to the peak surge earlier than observed, particularly on the third and fourth days of the simulation. This is most likely due to the modelled winds, which show more of a westerly component during this time than the observed, more northerly winds. The timing of the peak surge and subsequent decay in elevations shows good agreement with observations.

Figure 4.7 shows the modelled wind generated current and sea surface elevation over the entire modelled region. At 72 hours, an eastward flowing current confined to the shallow continental shelf became established, with the current speed exceeding one knot in places. The model simulated sea surface elevations are shown in Figure 4.7b

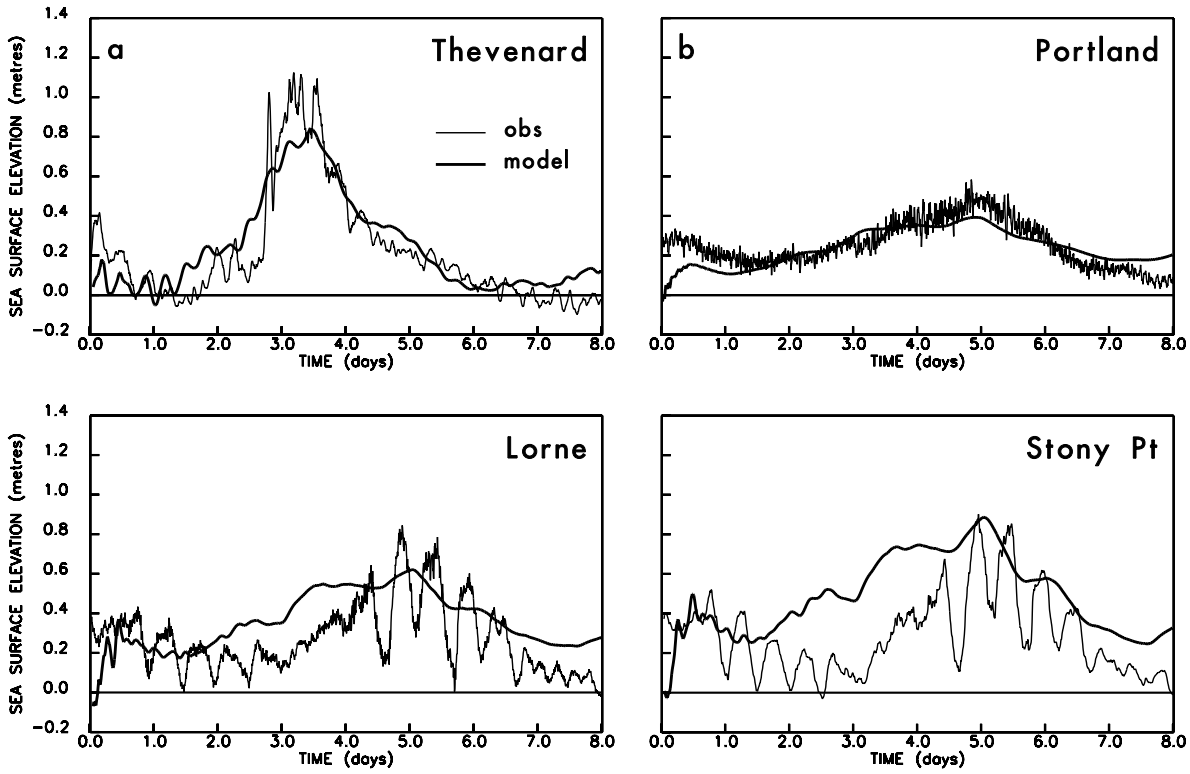

Figure 4.6: Observed and modelled residual sea level height for Case 1. Time series commences at 1100 UTC 21 May 1994.

and indicate a clear build-up of water against the coast in the vicinity of Thevenard, with some build up also evident in Bass Strait. By 120 hours (Figure 4.7c), sea levels diminished at Thevenard, showing further amplification along the coastline to the east, particularly in Bass Strait.

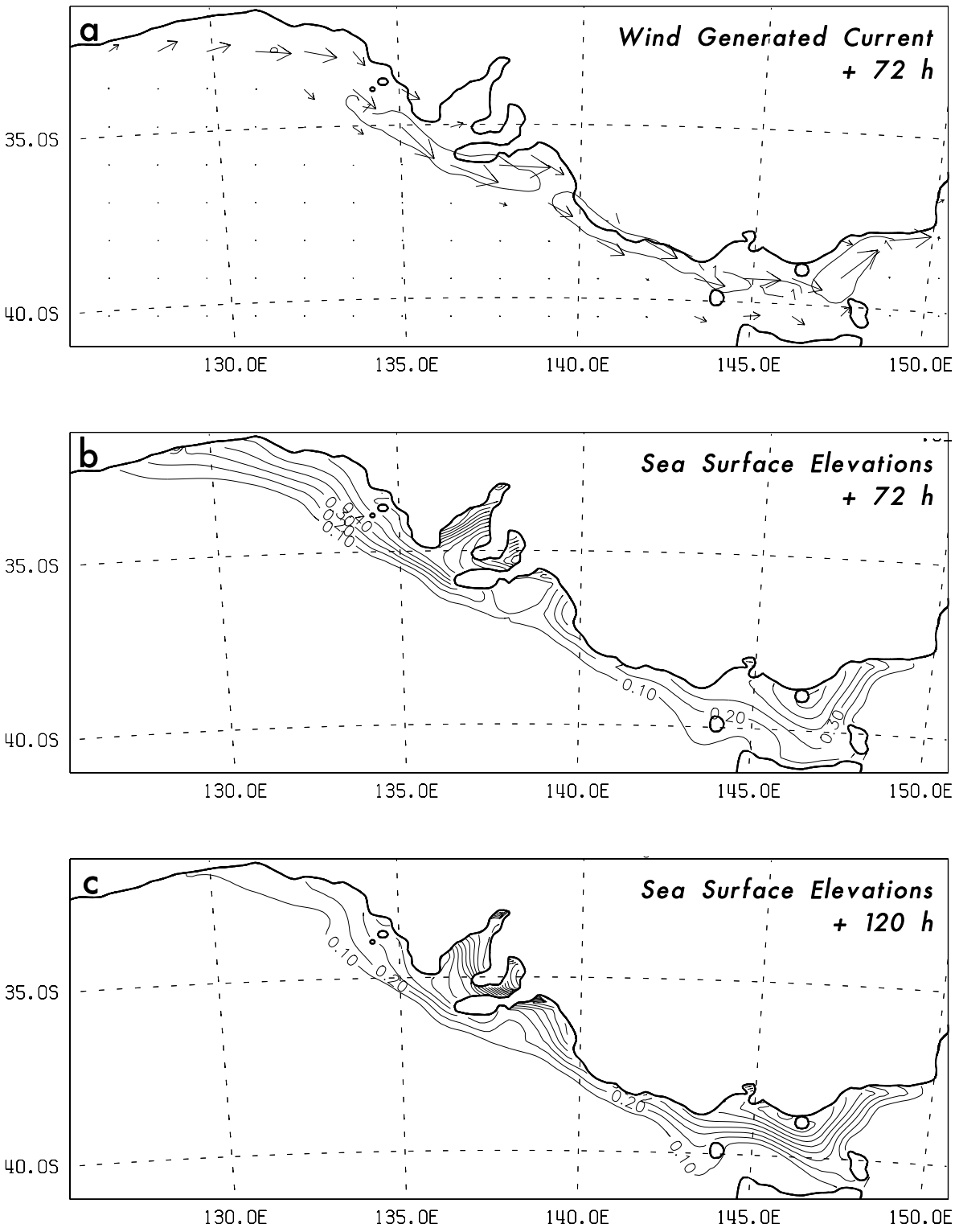

Figure 4.7: (a) Wind generated surface current. (b) Sea surface elevations at 72 hours into the model simulation. (c) Sea surface elevations at 120 hours.

4.3 Case 2 - November 1994

4.3.1 Synoptic Description

The storm surge which occurred in early November 1994 was restricted mainly to the eastern half of the southern coastline. Thevenard recorded only a 0.2 m residual sea level on 6 November 1994 (Figure 2.2), while Port Stanvac, Portland and the Bass Strait gauges recorded more than 0.4 m. MSLP analyses from the Australian Bureau of Meteorology from 4 November 1994 to 7 November 1994 are shown in Figure 4.8 and indicate that a ridge of high pressure was located over the western half of the continent (Figures 4.8 a, b, c). Meanwhile, a low pressure system and associated cold front were approaching southeastern Australia from the southwest, placing this part of the continent in a strong southwesterly airstream. The low intensified as it moved to the northeast on 5 and 6 November (Figures 4.8 b and c). On 7 November, the ridge of high pressure moved eastwards, the low slipped further to the south and pressure gradients over southeastern Australia weakened.

Rainfall amounts were moderate for this event. Over the four day interval, about 60 mm of rain was recorded at Colac and Wonthaggi, 45 mm at Wilson's Promontory and about 14 mm in Melbourne.

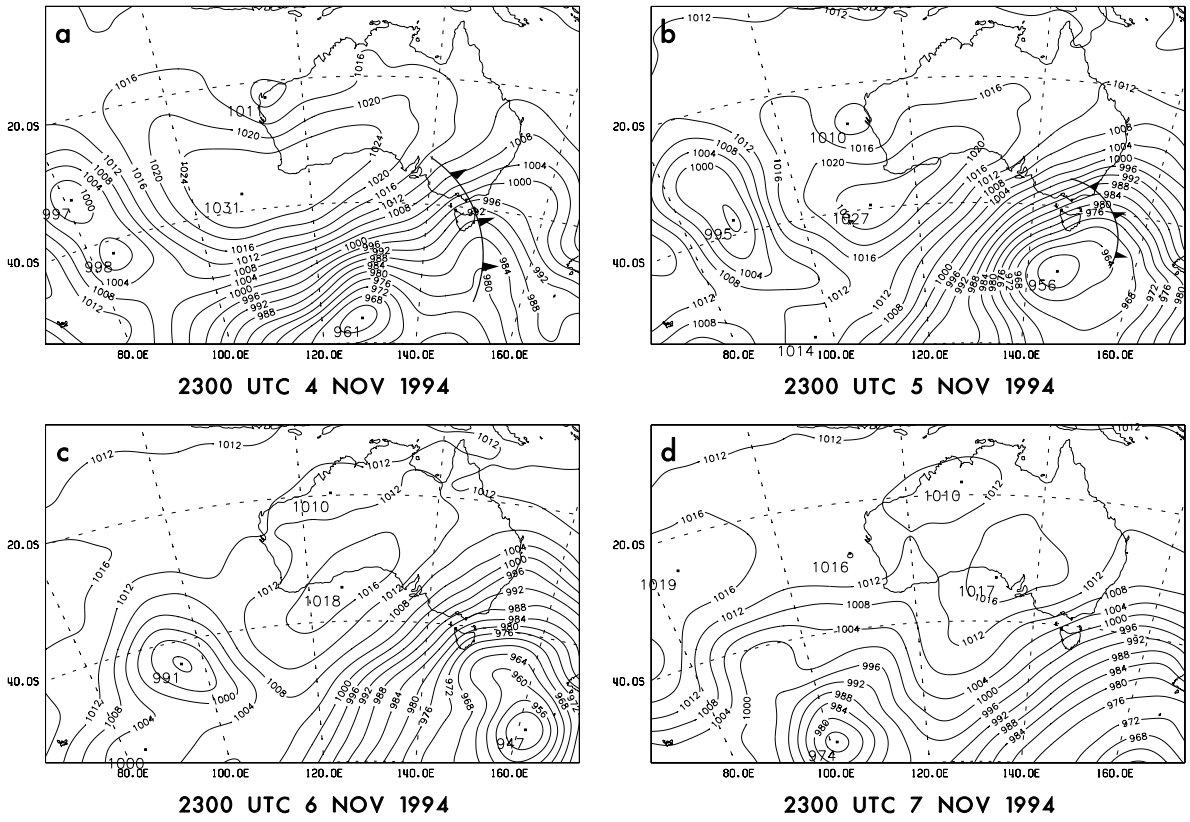

Figure 4.8: Bureau of Meteorology analyses of mean sea level pressure for Case 2.

4.3.2 Atmospheric Model Results

A four day atmospheric model simulation of Case 2 has been performed, commencing at 2300 UTC 3 November 1994. Modelled and observed wind speeds and direction are shown in Figure 4.9. During the first day, winds swung from southerlies to north-westerlies and then back to south-westerlies while their strength increased from about 10 to 20 m s^{-1}. The model captures the wind changes well, although their magnitudes are slightly underestimated. From midway through 5 November, a westerly airstream was established and wind strength increased to about 25 m s^{-1}. The strongest winds were experienced on 6 November at which time sea levels in Bass Strait and Port Phillip Bay peaked. Modelled winds during this time show good agreement, although peak winds are again slightly underestimated.

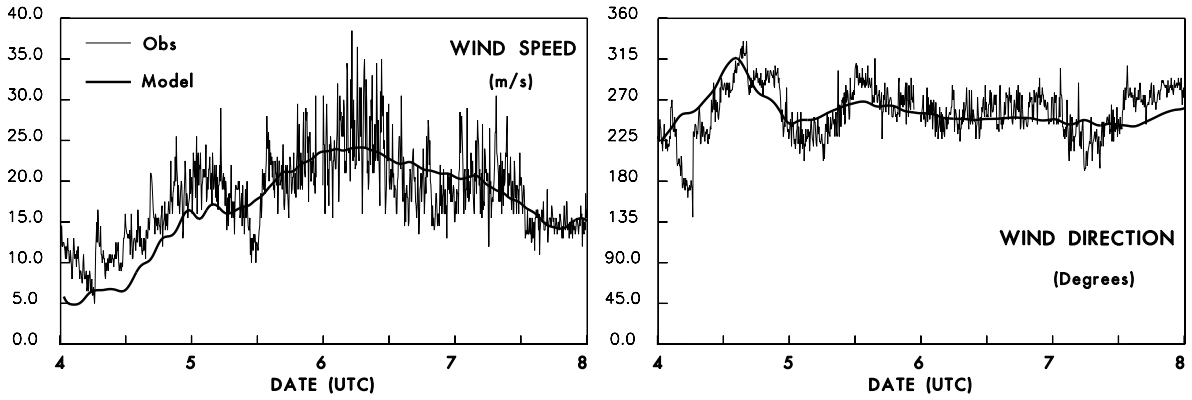

Figure 4.9: Observed and modelled wind speed and direction at St Kilda for Case 2 (November 1994).

The wind field over the entire model domain is shown in Figure 4.10 at 24 and 48 hours into the model simulation. A major difference between this simulation and the May case is the occurrence of a more southwesterly airstream rather than the westerlies that occurred in Case 1 and the strongest winds were confined to the region east of Thevenard. This explains why sea level residuals at Thevenard remained low in this event. In Bass Strait the strongest winds became established 48 hours into the simulation, which coincided with the time of maximum sea level residuals in this region.

4.3.3 Storm Surge Model Results

The observed and modelled storm surges are compared in Figure 4.11. In this case, Thevenard is further west of the most intense atmospheric forcing and this is reflected in both the observed and modelled residual sea levels which reached peak values of only 0.2 m. The model also produced only slight increases in residual sea level. At Portland the modelled sea levels were slightly underestimated. The modelled sea levels at Lorne and Stony Point were reasonably well captured, although once again, the 12 hour oscillation present in the observed time series was not present in the model.

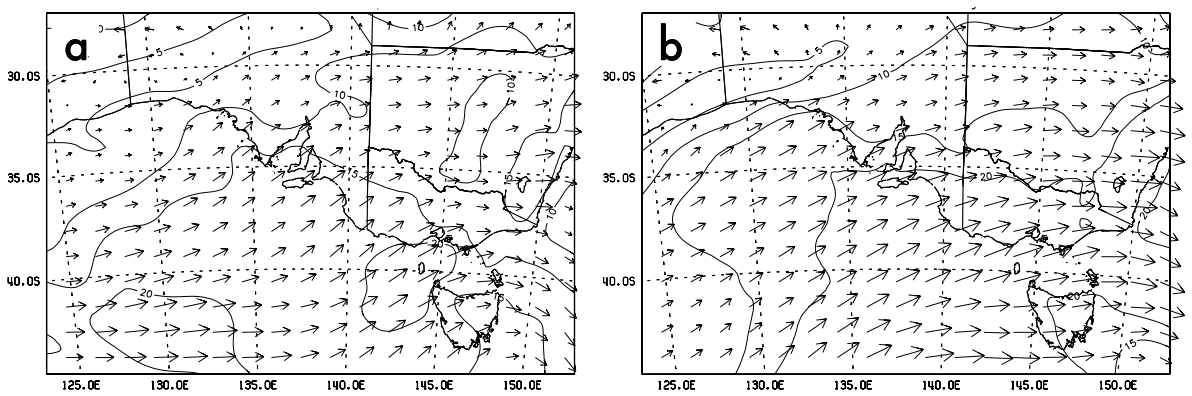

Figure 4.10: Modelled wind field at (a) 24 hours and (b) 48 hours into the model simulation (corresponding to 2300 UTC 4 Nov 1994 and 2300 UTC 5 Nov 1994 respectively).

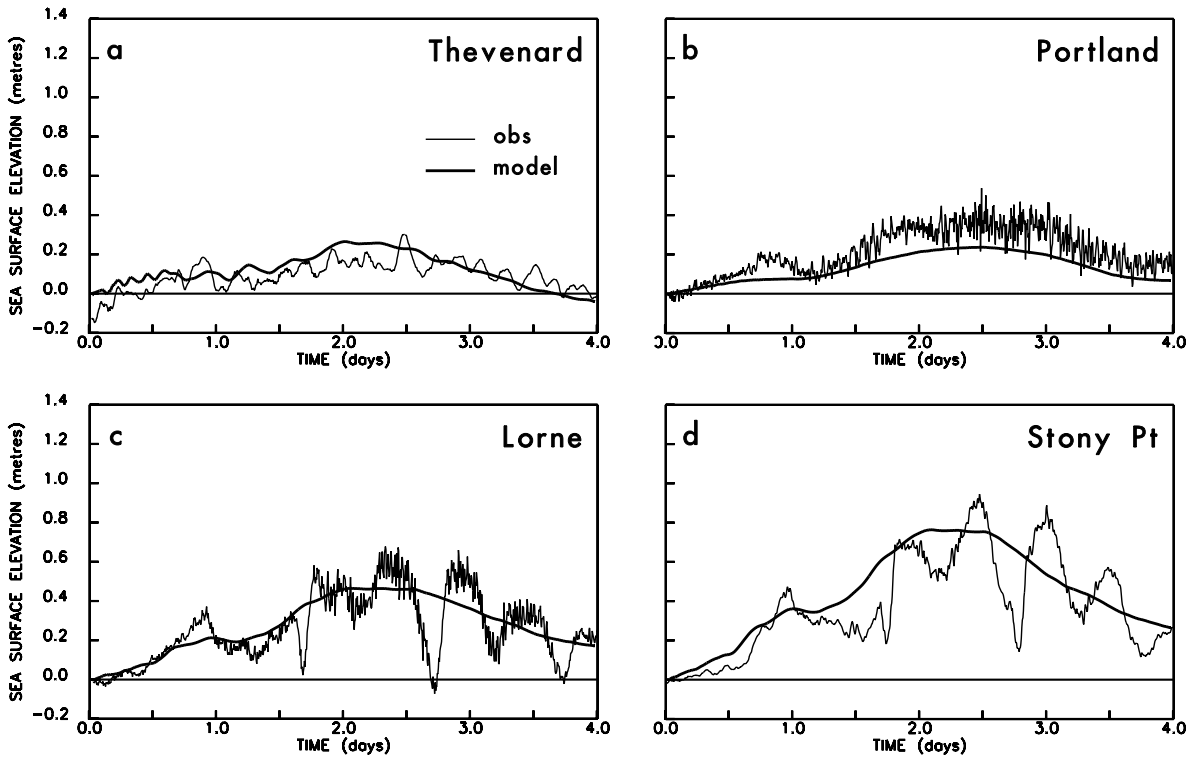

Figure 4.11: Observed and modelled residual sea level height for Case 2. Time series commences at 2300 UTC 3 November 1994.

The modelled sea levels over the entire domain are shown in Figure 4.12 at 24 and 48 hours into the model simulation respectively. Unlike the May case (Figure 4.7), the surge remains concentrated along the southern coastline further to the east and, again, this reflects the spatial differences in wind forcing between the two cases.

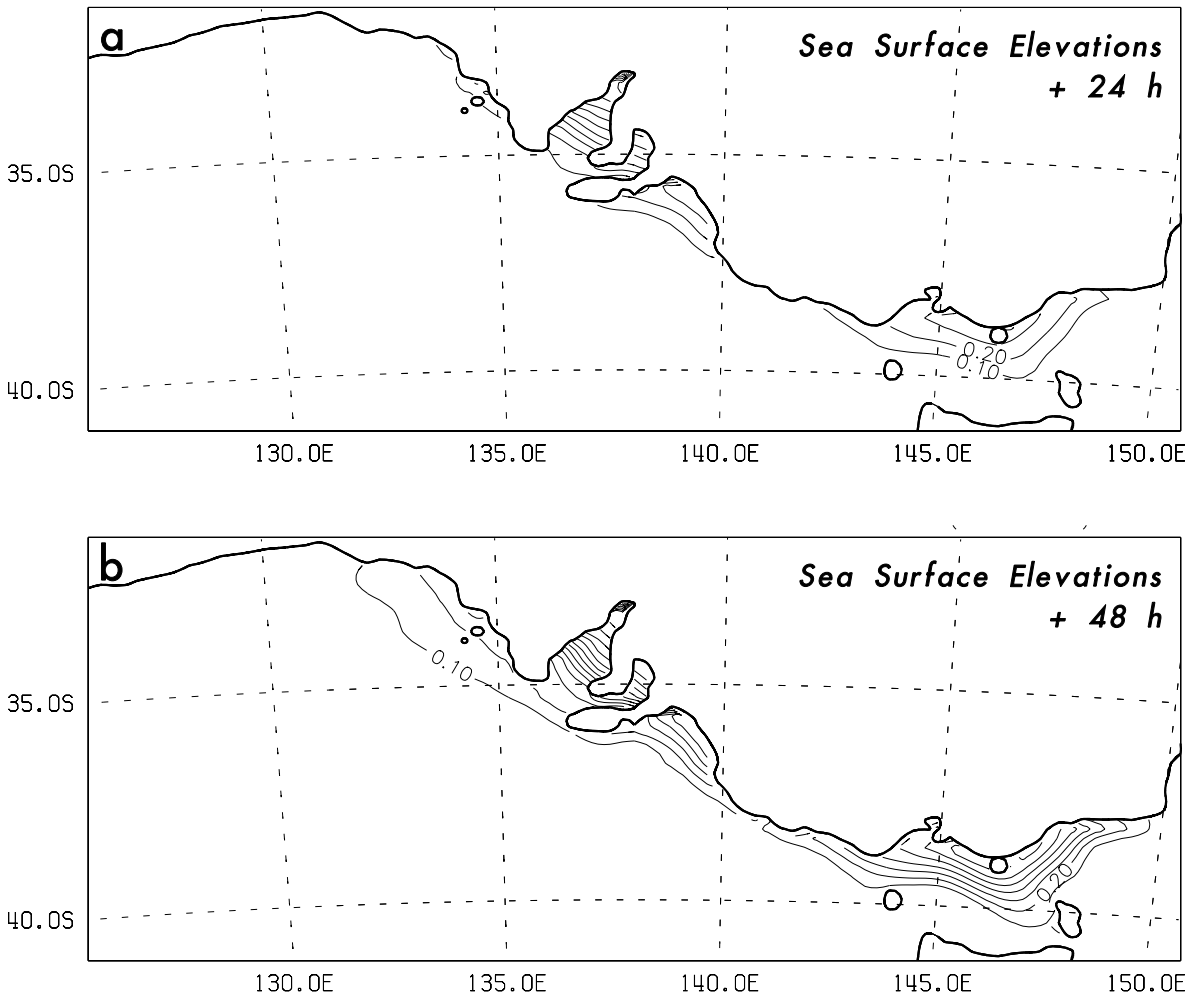

Figure 4.12: Sea-levels at 24 and 48 hours into the model simulation.

4.4 Sensitivity Experiments

4.4.1 Atmospheric Model Results

Limited area models have been used in previous studies to determine the possible effect of SST increases on specific weather systems. For example, McInnes et al. (1992) examined SST increases on mid-latitude cyclones affecting Australia's east coast and Evans et al. (1994) modelled cases of tropical cyclones under varied SSTs. In these studies increased SSTs resulted in a deepening of the central pressure of the cyclone and an increase in precipitation. McInnes et al. (1992) showed that the deepening of the low pressure centre produces stronger pressure gradients, and hence the winds surrounding the centre of the low. This has implications for storm surge generation along the east coast of Australia, as discussed in McInnes and Hubbert, (1994).

The mean annual sea surface temperature increase predicted by the CSIRO 9 Mark I GCM model under doubled CO_2 conditions is of the order of 4°C over the ocean immediately to the south of Australia. Sensitivity experiments were performed on the May and November cases studied in this report to determine if a temperature

increase of this magnitude could have a local impact on frontal systems travelling along the south coast. It was found that since the low pressure systems associated with the fronts were located well to the south of the continent in both cases, any intensification of the low which occurred as a result of higher SSTs did not produce significant increases in the winds experienced near the south coast. The only impact of the higher SSTs was an increase of approximately 20% in the precipitation associated with the frontal passage, although neither of these events produced significant rainfall. Based on the findings of McInnes et al. (1992) it is likely that a Bass Strait depression, such as the one which caused the 1934 floods, would demonstrate a greater sensitivity to local SST changes, possibly causing even higher rainfall and a stronger storm surge.

4.4.2 Storm Surge Model Results

Analysis of extreme winds in two GCM simulations in chapter 3 under $1\times CO_2$ and $2\times CO_2$ conditions indicated that there was no consensus among the model results as to whether westerly wind events would become more or less frequent and intense. Disagreement was particulary marked over the latitude band between 35°S and 45°S, which is the region most relevant to storm surge generation on the Victorian coast. The results gave a range of wind strength changes of $\pm 10\%$ under a doubling of CO_2.

The impact of a range of wind speed changes is explored using the storm surge model in this section. For each of the cases studied the surface winds which drive the storm surge model are varied for the duration of the event by an amount ranging from -10% to +20% and the results are summarized in Figure 4.13.

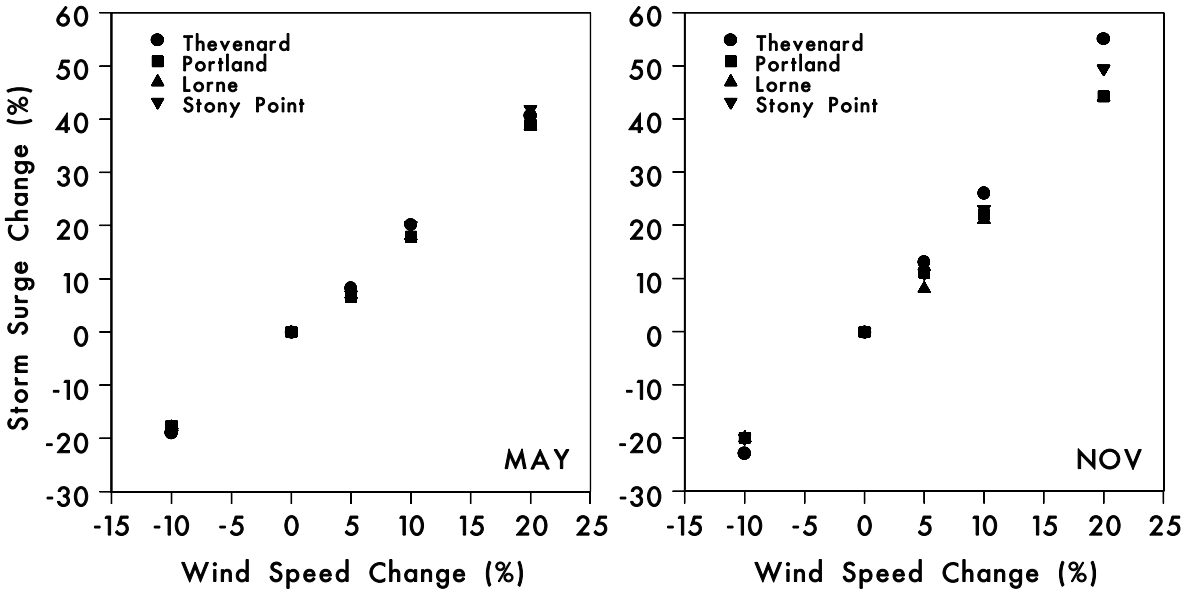

Figure 4.13: The percentage storm surge change plotted as a function of percentage wind speed change at each of the four stations for the two case studies, based on sensitivity experiments.

The percentage change in peak storm surge height at a given location varies lin-

early with percentage change in wind speed, with a constant of proportionality of approximately two. For example, for Case 1 the percentage storm surge height variation is approximately twice that of the percentage wind speed variation at Thevenard, Stony Point and Lorne, and between one and 1.5 times greater than the percentage wind speed change at Portland. For Case 2 however, the percentage storm surge response at all locations is more than twice that of the wind speed change.

The storm surge response can be understood more fully by considering the governing equations of motion for the storm surge model (see Appendix 1: Equations A1-A3). An increase in surface wind speed will increase the currents through the wind stress term (Equation A4). This term consists of the product of the wind magnitude and wind speed component, as well as the drag coefficient - which is proportional to the wind magnitude. Typically a 10% increase in winds will increase the wind stress by 25-30%. However the effect of the increased wind stress on the currents is partly offset by the bottom friction term (Equation A6) and the diffusion term (last term in Equations A1 and A2), which are both functions of the current speed.

CHAPTER 5: Modelling Inundation in Port Phillip Bay

5.1 Experimental Design

In this chapter the impact of storm surges on Port Phillip Bay is studied using the storm surge inundation model described in chapter 4. The simulations are carried out on higher resolution model grids and sensitivity experiments are performed to determine the possible effects of worst case scenarios of climate change at the regional scale.

5.1.1 Inundation Model and Model Grids

The inundation model used in this part of the study, is an extension of the storm surge model described in chapter 4. When the model is run with sufficiently high resolution and accurately specified coastal topography, increasing water levels at coastal boundaries can be translated inland over adjacent lower lying land grid points. Dry grid cells become wet if the gradient of sea level to land height exceeds a given value. In order to maintain realistic flooding rates, and prevent instantaneous flooding of low lying flat land, a grid cell is filled at a rate calculated from the shallow water equations at each subsequent model time step. This means that a dry cell adjacent to a flooding wet cell cannot itself begin filling until the adjacent cell fills to at least the height of the cell flooding into it. The sea level in the new wet cell is calculated from the shallow water equations and depending on the wind stress, this height may in fact be greater than the sea level in the cell which originally flooded into it.

Similar logic is applied to the draining procedure. A wet grid cell drains if the gradient of the sea level is greater than a given value and the depth of water is less than a given value. As with the flooding, in order to maintain realistic drainage rates and prevent instantaneous drying of large areas of flat land, a cell is drained at a rate calculated from the shallow water equations at each subsequent model time step. This means that a wet cell adjacent to the draining cell cannot commence draining until the first cell has fully drained.

When coastal flooding occurs a range of terrain types is encountered which affects the flow rate of the flood water differently. These are taken into account in the model by assigning an appropriate 'bottom' friction coefficient to each grid point, which is dependent on the terrain type. A limited number of terrain types has been used and includes muddy ocean floors, sandy beaches and grass. Other features such as roads, railway lines, sea walls, levees and major buildings also affect the inland flow of water. It was beyond the scope of this study, to include many such features, since their representation requires highly detailed and accurate digitized topographic maps and correspondingly high model resolution. However, considerable effort was made to represent the Mordialloc Creek and Patterson River on the Mordialloc domain. The

rivers were widened to provide sufficient grid points on the grid to ensure numerical stability and levee banks were also included in some simulations. It should be noted however, that the relatively low resolution of the model for this type of application means that the results should be used only to provide qualitative guidance to the areas most vulnerable to storm surge inundation.

Two levels of model simulation are conducted for each case study. Initially the entire Port Phillip Bay region is modelled on a 500 m grid shown in Figure 5.1. These runs provide boundary conditions for higher resolution storm surge and inundation simulations over the three smaller regions indicated in Figure 5.1.

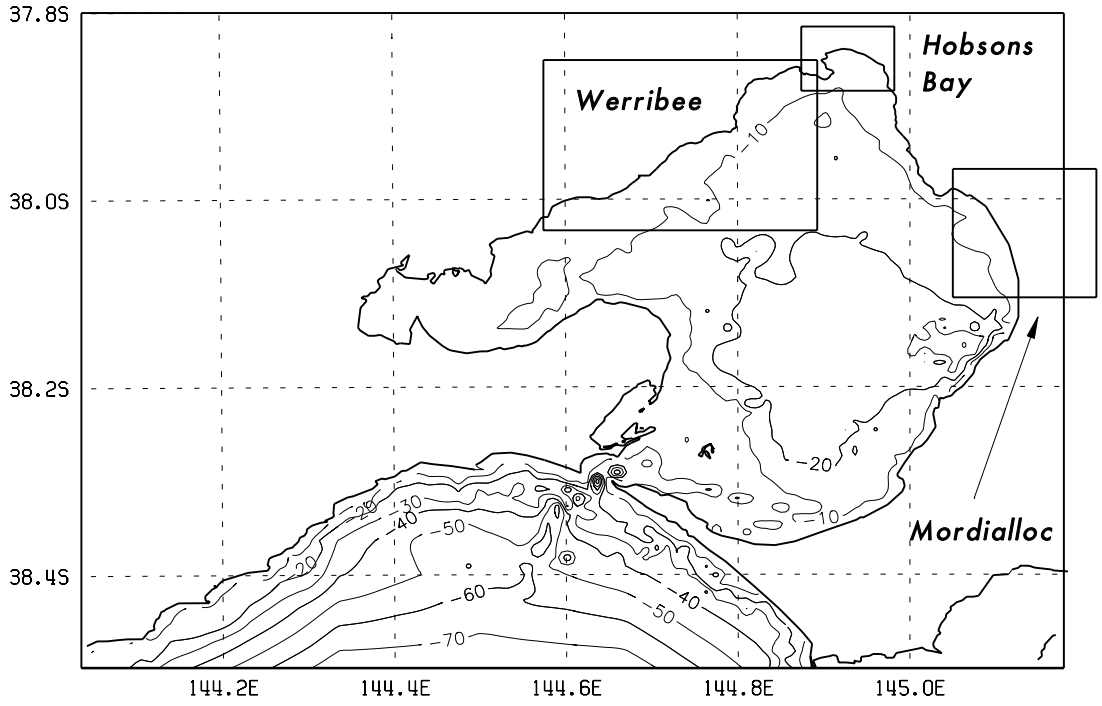

Figure 5.1: The Port Phillip Bay domain showing the three sub-domains of Hobsons Bay, Werribee and Mordialloc.

On the Port Phillip Bay model grid, there is an open boundary in Bass Strait, extending approximately from Lorne to Stony Point, which enables tidal and storm surge information from Bass Strait to be imposed. These boundary elevations are applied using a nesting procedure whereby a cosine function weights the elevations at one on the boundary and diminishes their influence to zero over ten gridpoints into the interior domain. This ensures a smooth transition of boundary information to the model grid.

Three methods for providing boundary conditions were tested. In the first, the modelled surges from the 12 km grid were used to provide elevations along the open boundary. An advantage of this method is that elevations are known at all points along the boundary and there is greater flexibility in defining the position of the open boundary. The disadvantage is that errors on the outer grid are transferred

to the inner grid. In the second method, the National Tidal Facility tidal residuals for Lorne and Stony Point were used to obtain a linearly varying signal across the open domain. Tidal forcing was applied separately for both methods and the tidal amplitudes and phases for seven constituents (M2, S2, N2, K2, O1, K1, P1) were imposed. In the third method the raw sea level measurements at Lorne and Stony Point were linearly interpolated along the boundary, thereby avoiding the need to impose tidal forcing separately. This method was found to produce the most accurate results. The atmospheric forcing was applied to the Port Phillip Bay model by interpolating the surface winds and pressure from the atmospheric model grid to the 500 m grid.

The open boundaries of the three smaller grids are nested within the sea levels produced on the Port Phillip Bay simulation. Each domain differs in resolution and horizontal extent. The Hobsons Bay domain (Figure 5.2) has a grid resolution of 30 m, Werribee (Figure 5.3) has a resolution of 100 m and Mordialloc (Figure 5.4) operates on a 50 m grid. Major inflow tributaries have been incorporated into the Hobsons Bay and Mordialloc grids and flow rate data has been used to input the appropriate mass flux at these locations. The flow rates used for the Yarra River on the Hobsons Bay region for the May and November events were 12 and 21 m^3s^{-1} respectively. This compares with mean flow rates for those months of 8 and 17 m^3s^{-1} respectively. The flow rate for the Mordialloc Creek during both storms was approximately 3 m^3s^{-1} which is virtually unchanged from the base flow rate of 2 m^3s^{-1}. It is worth noting that the estimated flow rate for the 100 year flooding event in this creek is 112 m^3s^{-1}.

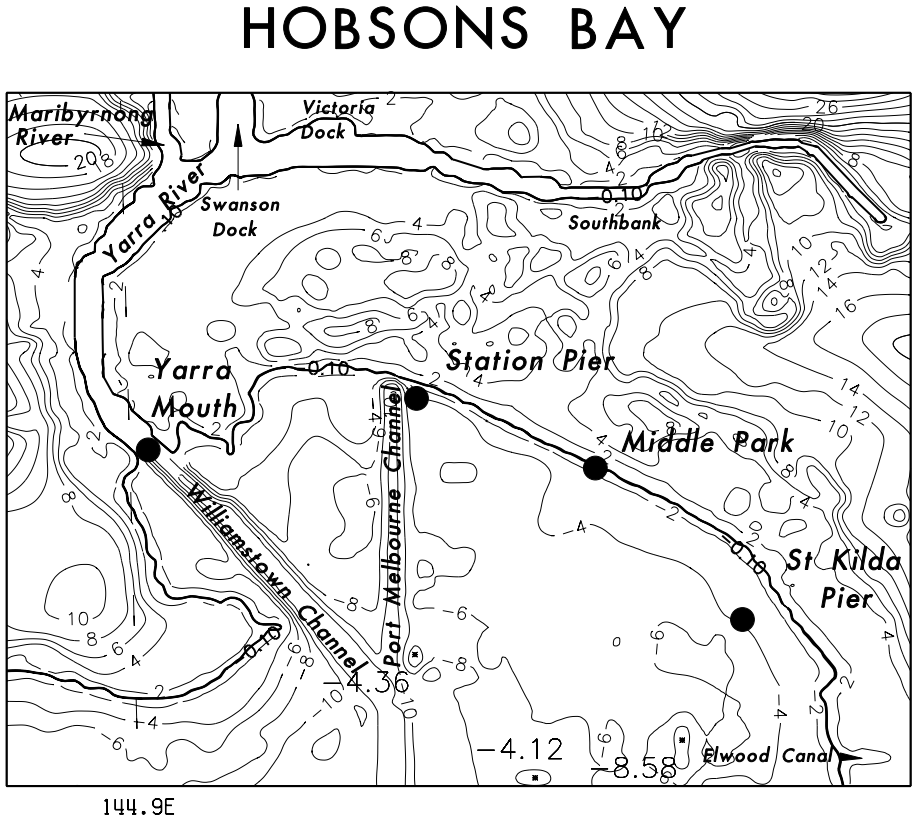

Figure 5.2: The Hobsons Bay domain. The model grid resolution is 30 m and topographic and bathymetric contours are 2 m apart.

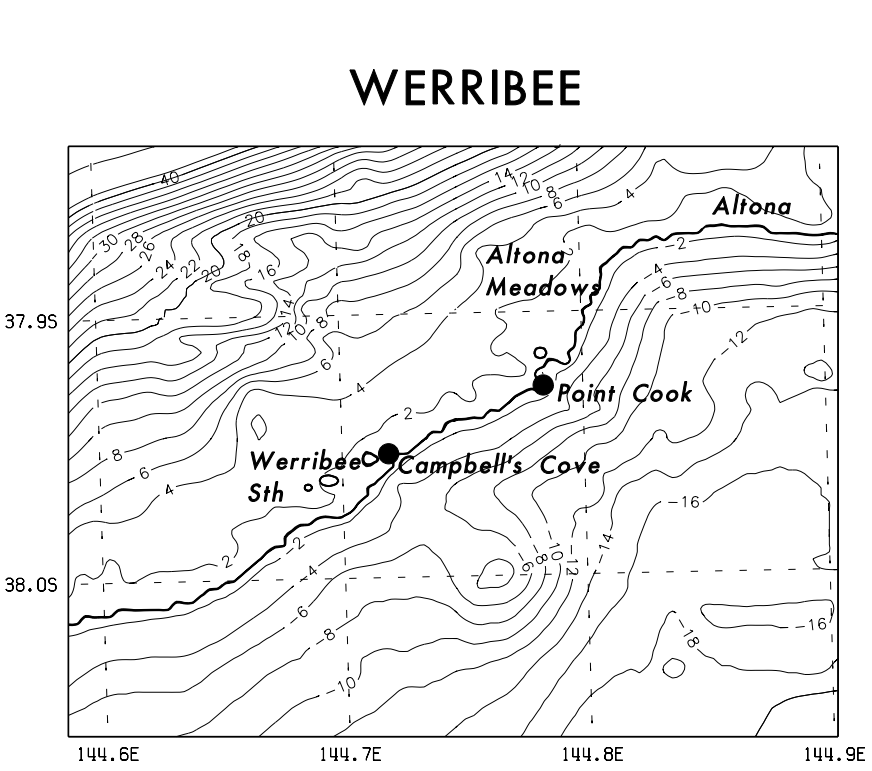

Figure 5.3: The Werribee domain. The model grid resolution is 100 m and topographic and bathymetric contours are 2 m apart.

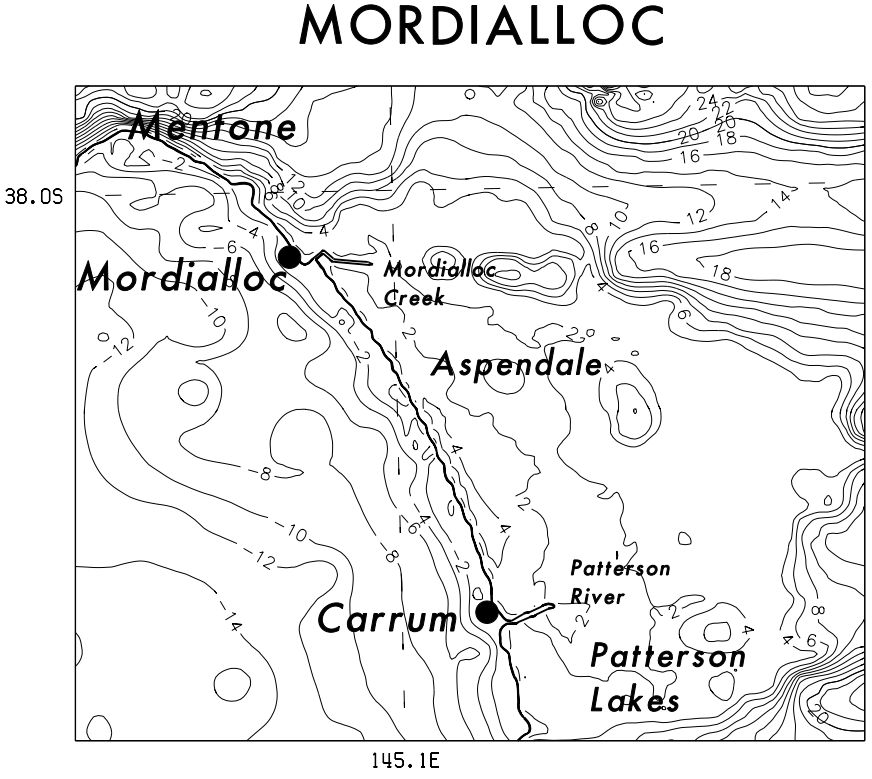

Figure 5.4: The Mordialloc domain. The model grid resolution is 50 m and topographic and bathymetric contours are 2 m apart.

All heights, depths and tide data were referenced to the Australian Height Datum (AHD). Bathymetry values for the grids were obtained from admiralty charts and Melbourne Water. Areas such as the shipping channels were manually coded from Port of Melbourne Authority charts. High resolution representation of the zero, one, two and three metre topographical contours were used, as well as other spot height information. The topographical and bathymetric data were interpolated to the study grids using statistical interpolation techniques.

5.1.2 Sensitivity Experiments

A set of three sensitivity experiments were conducted on each model domain for the May and November cases. The first experiment was a control simulation (EXP. 1) in which actual sea levels were simulated. In the second experiment (EXP. 2), the effect of the same storm occurring in combination with a mean sea level rise was investigated. The background sea levels were increased by 80 cm, which is the worst case scenario for mean sea level rise by 2070. In the third experiment (EXP. 3), the wind speeds were also increased by 10%, in an attempt to simulate the impact of a more severe storm on the increased mean sea level. For this experiment the storm surge component of the imposed sea levels on the open boundary was elevated by a further 20% - to ensure consistency with the sensitivity experiments from the previous chapter, in which a 10% increase in winds produced a 20% increase in surge height.

5.2 Port Phillip Bay Simulations

5.2.1 Case 1 - May 1994

The observed and modelled time series of sea levels at St Kilda are presented in Figure 5.5 and show reasonably close agreement. A slight discrepancy in the model occurs between the two peaks, where sea levels do not recede as the observations indicate. The predicted tidal signal is shown also and indicates that sea levels for this event were, up to 0.8 m higher than normal. Figure 5.6 shows the spatial variation of the surge across Port Phillip Bay at its peak. A pronounced east-west gradient is evident with the highest surge located on the eastern side of the Bay. This is also reflected in Table 5.1 which shows peak sea levels at St Kilda, Werribee and Mordialloc. The peak surge height at Mordialloc is about 0.38 m higher than at Werribee. At St Kilda, the modelled value of 1.20 m is slightly lower than the observed sea level height of 1.24 m.

In the sea-level rise only experiment (EXP. 2), the surges at St Kilda, Werribee and Mordialloc are approximately 0.80 m higher than the control simulation peak heights. The results for EXP. 3 show a further increase in sea level heights of just over 0.20 m which indicates that this rise is largely due to the elevated sea levels at the southern boundary and little redistribution of the sea level due to local wind effects has occurred in this event.

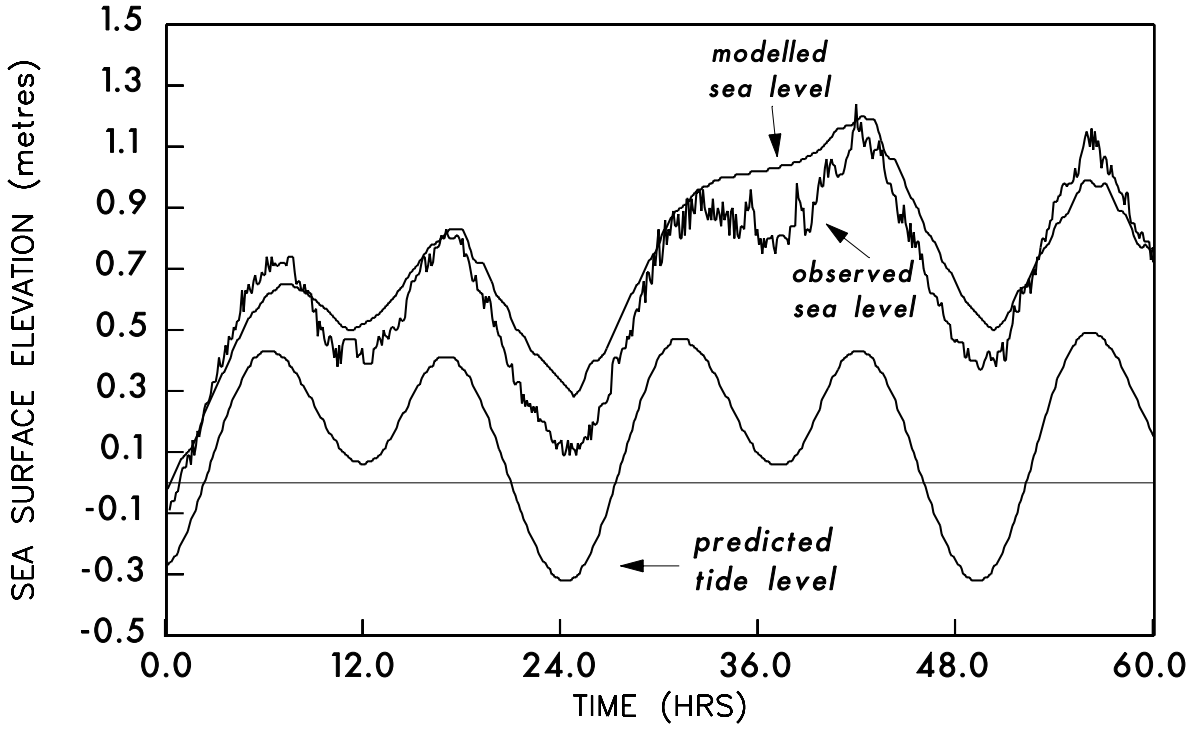

Figure 5.5: Curves showing the observed and modelled sea levels at St Kilda over a 60 hour interval, commencing at 2300 UTC 24 May 1994. The predicted tide at Williamstown is also shown. All sea levels are referenced to AHD.

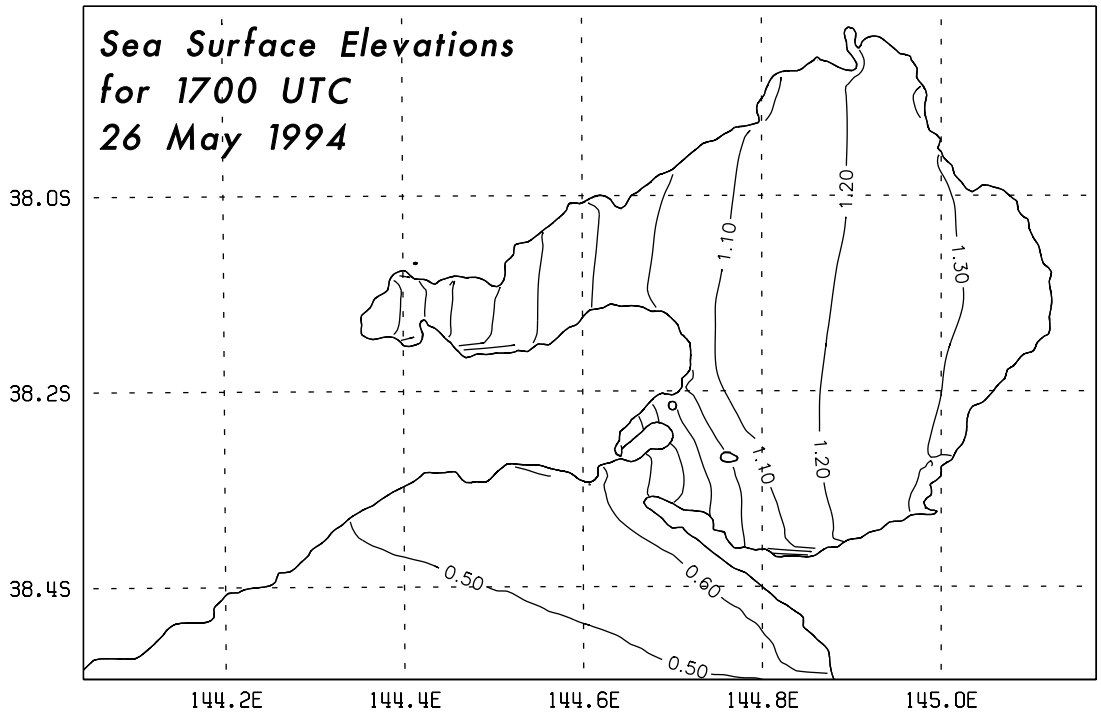

Figure 5.6: Model simulated sea surface elevations for 1700 UTC 26 May 1994. Units are in metres and sea levels are referenced to AHD.

Experiment	St Kilda	Werribee	Mordialloc
EXP. 1	1.20	0.92	1.30
EXP. 2	2.01	1.72	2.11
EXP. 3	2.22	1.95	2.35

Table 5.1 Summary of storm surge heights for Case 1 (May 1994) for the three sensitivity experiments.

5.2.2 Case 2 - November 1994

Figure 5.7 shows the modelled and observed time series at St Kilda for the latter 60 hours of model simulation. This event produced a slightly larger peak storm surge at St Kilda (1.30 m) than the May event. The predicted tide levels indicate that about 0.9 m of the maximum sea level was due to storm surge.

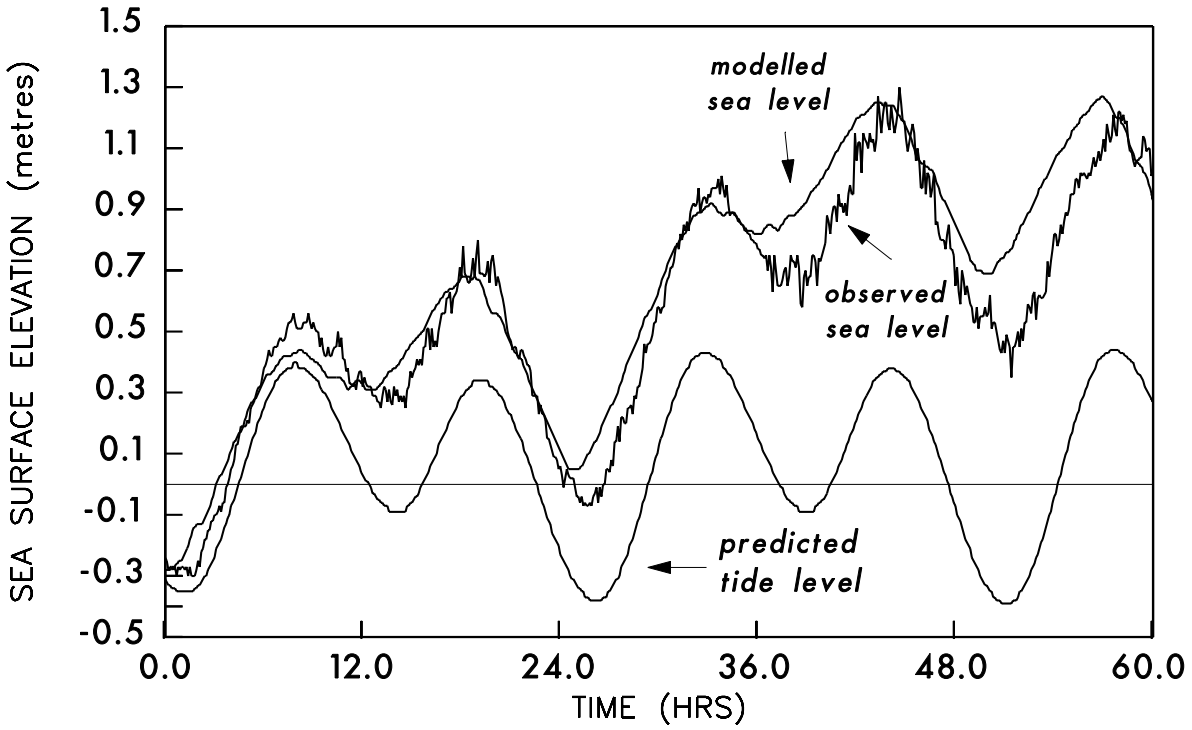

Figure 5.7: Curves showing the observed and modelled sea levels at St Kilda over a 60 hour interval, commencing at 2300 UTC 4 November 1994. The predicted tide at Williamstown is also shown. All sea levels are referenced to AHD.

Figure 5.8 shows the structure of the surge event across Port Phillip Bay at 0700 UTC on 6 November which is when the peak surge at St Kilda occurred. Unlike

the May event, the sea level contours are aligned in more of a northwest-southeast orientation. The winds for this event were slightly southwesterly (Figure 4.9), whereas the May case winds had a more northwesterly component (Figure 4.4).

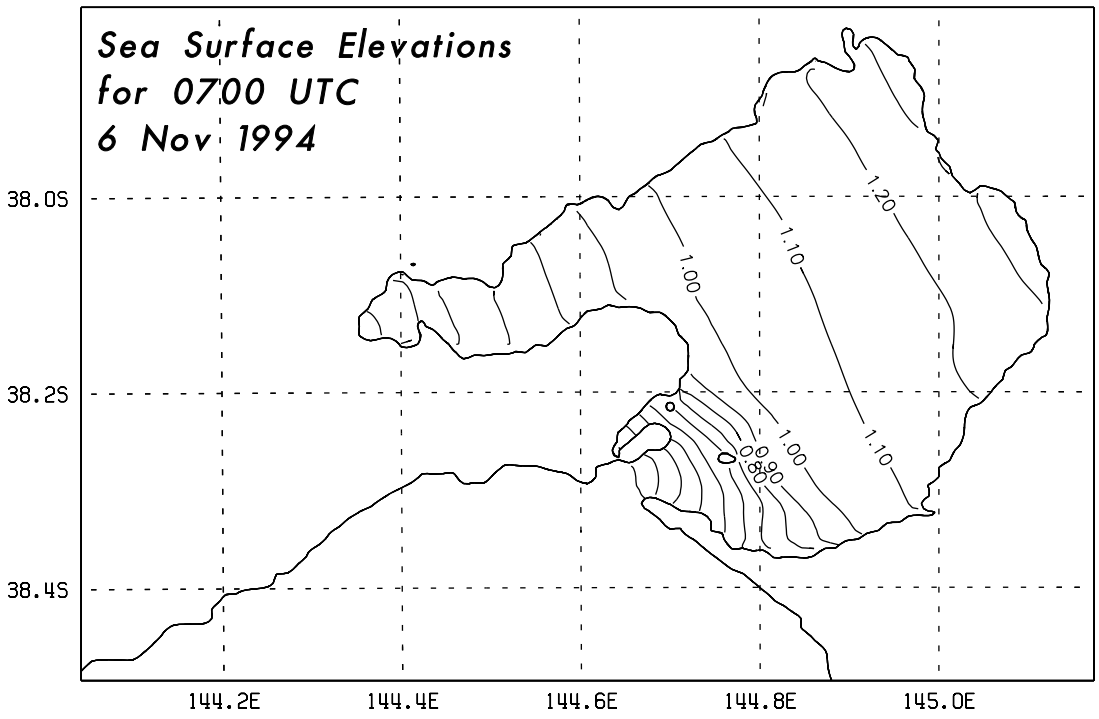

Figure 5.8: Model simulated sea surface elevations for 0700 UTC 6 November 1994. Units are in metres and sea levels are referenced to AHD.

Table 5.2 summarizes the peak sea level heights around the Bay and, once again, the modelled peak at St Kilda of 1.25 m was slightly lower than the observed peak of 1.30 m. The peak at Werribee was slightly higher than the May case and at Mordialloc, it was slightly lower, due to the different orientation of the sea level contours. As with the May case, the results of EXP. 2 show peak values which are approximately 80 cm higher than the control simulation.

In the third sensitivity experiment the sea level increase again is largely due to the imposed increase at the southern boundary. However, the differences between the EXP. 3 and EXP. 2 heights for St Kilda, Werribee and Mordialloc were 0.25, 0.22 and 0.27 m respectively indicating a some redistribution of water towards the eastern side of the bay due to local wind effects.

5.3 Inundation Modelling Results

A set of three sensitivity experiments have been run for both the May and November storms. The results were compared by calculating the model grid squares which were inundated and converting these to an areal coverage. As stated earlier, it was

Experiment	St Kilda	Werribee	Mordialloc
EXP. 1	1.25	0.94	1.28
EXP. 2	2.06	1.75	2.08
EXP. 3	2.31	1.97	2.35

Table 5.2 Summary of storm surge heights for Case 2 (November 1994) for the three sensitivity experiments.

beyond the scope of this study to carry out the modelling at sufficiently high resolution to capture many terrain features and their effects on the inundation. Therefore, the modelling results should be seen as indicative of the areas most vulnerable to inundation under worst case scenario conditions and the results for the different regions, cases and sensitivity experiments should be viewed in a comparative sense.

5.3.1 Hobsons Bay Region

The inundation results for both the May and November storms are summarized in Table 5.3. For both control simulations, the total area inundated was 0.9 km^2 with only 0.1 km^2 under more than a metre of water. Figure 5.9a shows the inundation at the time of the peak surge for the November control simulation. The beach front extending from Port Melbourne to Elwood was most dramatically affected by the inundation, as were low lying areas along the Yarra River.

	May 1994			Nov. 1994		
	Area < 1 m	Area > 1 m	Total Area	Area < 1 m	Area > 1 m	Total Area
EXP. 1	0.8	0.1	0.9	0.8	0.1	0.9
EXP. 2	0.9	0.8	1.7	0.9	0.9	1.8
EXP. 3	1.3	1.0	2.3	1.8	1.1	2.9

Table 5.3 Summary of the area (km^2) inundated over the Hobsons Bay region for both Case 1 and Case 2 for the three sensitivity experiments. All areas are relative to the control experiment coastline.

In EXP. 2 the total area inundated was just over twice that of the control simulation, with slightly more inundation occurring in the November case. Approximately half of the area was under more than a metre of water in both cases. In EXP. 3 for the May case, the area of inundation increased to 2.3 km^2 compared with 2.9 km^2 for the November case. This difference is probably related to the fact that the November storm surge was slightly higher than the May surge and so it was able to penetrate to more inland gridpoints. The different pattern in wind forcing may have also contributed to the result. Figure 5.9b shows the inundated areas of the November storm for EXP. 3. A much broader region along the coastline and the banks of the Yarra was affected in this experiment.

5.3.2 Werribee Region

The inundation results for the May and November cases are shown in Table 5.4. As with the Hobsons Bay domain, more inundation occurred in the November case than the May case. The mean sea level increase imposed in EXP. 2 produced more than a doubling of area inundated for each of the cases than the respective control cases. This compares to approximately a doubling of area inundated in the two cases on the Hobsons Bay domain and suggests that the Werribee region contains more low lying land which is vulnerable to the effects of a mean sea level rise. Compared to EXP. 2, the impact of increased winds in EXP. 3 produced a 13% and 19% increase in the area inundated for the two cases respectively. These are smaller relative differences compared to those which occurred on the Hobsons Bay region and are most likely related to the geographical location. The Werribee region is on the western side of the Bay and would be less affected by an increase in westerly or southwesterly winds than a location on the north or east of the Bay.

	May 1994			Nov. 1994		
	Area < 1 m	Area > 1 m	Total Area	Area < 1 m	Area > 1 m	Total Area
EXP. 1	11.2	0	11.2	15.1	0.7	15.8
EXP. 2	21.4	9.0	30.4	22.4	12.0	34.4
EXP. 3	21.8	12.5	34.3	25.8	15.2	41.0

Table 5.4 Summary of the area (km^2) inundated over the Werribee region for both Case 1 and Case 2 for the three sensitivity experiments. All areas are relative to the control experiment coastline.

Figure 5.10a shows the regions of inundation along the foreshore, particularly in the vicinity of Campbell's Cove, Point Cook and Altona for the November case. The spatial distribution of the inundation for EXP. 3 is illustrated in Figure 5.10b.

5.3.3 Mordialloc Region

Table 5.5 summarizes the inundation results for the May and November cases over the Mordialloc grid. Under control conditions inundation in both cases totals only 0.5 km^2 (note that these values exclude the area within the Pattersons River which appears inundated because it lies above mean sea level) and the inundated area is confined to the beach front, as illustrated in Figure 5.11a for the November case.

The 80 cm sea level rise increases the area of inundation slightly more in the November case to 1.6 km^2 (Figure 5.11b) than the May case (1.4 km^2). The affected regions differ also with less inundation occurring on the north side of the Mordialloc Creek in the May case, due to the slight northerly component in the winds in the May case compared with the slight southerly component in the November case.

The additional increase of winds in EXP. 3 produces more inundation in the May case (2.7 km^2) than the November case (1.7 km^2). The impact of the stronger winds in the November case can be seen in the shift in inundation further eastward (Figure 5.11c) even though the total area of inundation has increased only slightly.

The final two experiments illustrate the importance of the existing levees on the Mordialloc Creek and Patterson River. Without them, the total inundation increases fivefold in EXP. 3 for November (Figure 5.11d). It is interesting to note that the pattern of inundation is consistent with the described pattern of flooding during the 1934 flood (Section 2.2.2).

5.4 Summary and Discussion

Two present day storms have been modelled over the Port Phillip Bay region. Comparison of modelled sea levels with observations at St Kilda indicate that the storm surge model captured the structure of the storm surge and tidal signal reasonably accurately. However there is a tendency for the storm surge model to slightly over estimate the peak surge.

The model is then used to conduct sensitivity experiments for the two cases. In the first, the impact of the two storms - with an imposed mean sea level rise of 80 cm - was investigated. The peak storm surge height at the three locations was found to be approximately 80 cm higher also. A 10% increase in wind speed on top of the sea level rise produced a further increase in storm surge peaks of around 20 cm in both cases.

Inundation simulations on three regions within the Bay at high spatial resolution were then conducted to identify the areas most vulnerable to the impact of a mean

	May 1994			Nov. 1994		
	Area < 1 m	Area > 1 m	Total Area	Area < 1 m	Area > 1 m	Total Area
EXP. 1 levees	0.4	0.1	0.5	0.4	0.1	0.5
EXP. 2 levees	0.9	0.5	1.4	1.1	0.5	1.6
EXP. 3 levees	1.9	0.8	2.7	1.1	0.6	1.7
EXP. 2 no levees	5.8	0.7	6.5	5.6	0.6	6.2
EXP. 3 no levees	6.5	1.2	7.7	7.5	1.3	8.8

Table 5.5 Summary of the area (km^2) inundated over the Mordialloc region for both Case 1 and Case 2 for the three sensitivity experiments. All areas are relative to the control experiment coastline.

sea level rise and a more severe storm surge. The three regions - Hobsons Bay at the northern end of the Bay, Werribee to the northwest and Mordialloc to the east - all showed minor inundation restricted mainly to the beaches and river banks under control conditions. Considerably greater inundation occurred under the storm conditions when a background mean sea level rise was imposed. The additional 10% increase in wind speeds had varied impact, depending on the events and the regions. For example, the May event had a greater impact on the Mordialloc domain while Hobsons Bay was affected more adversely by the November event. These results are related to the slight directional differences in wind forcing between the two events. Werribee experienced a smaller relative increase overall due to its location on the eastern side of the bay. The removal of levees in simulations over the Mordialloc region produced considerably greater inundation on the eastern side of the railway line from the Mordialloc Creek to the Patterson River.

The results presented here have several important implications. The first of these is the importance of adequately designed and maintained flood protection measures such as levee banks in low lying coastal regions. Studies such as this can provide guidance as to the design levels of such structures. Secondly, while the sea level rise scenario used in this study was at the extreme end of the range of uncertainty for the latter half of the next century, the two present day storm surge events modelled are not particularly rare, having return periods of several years. A more severe storm surge could produce more damage under a less dramatic background sea level rise. Finally, the two events studied here did not produce extreme precipitation so that river flow rates were unaffected. The impact of a storm surge coinciding with increased run-off and hence higher river flow rates could be far more severe.

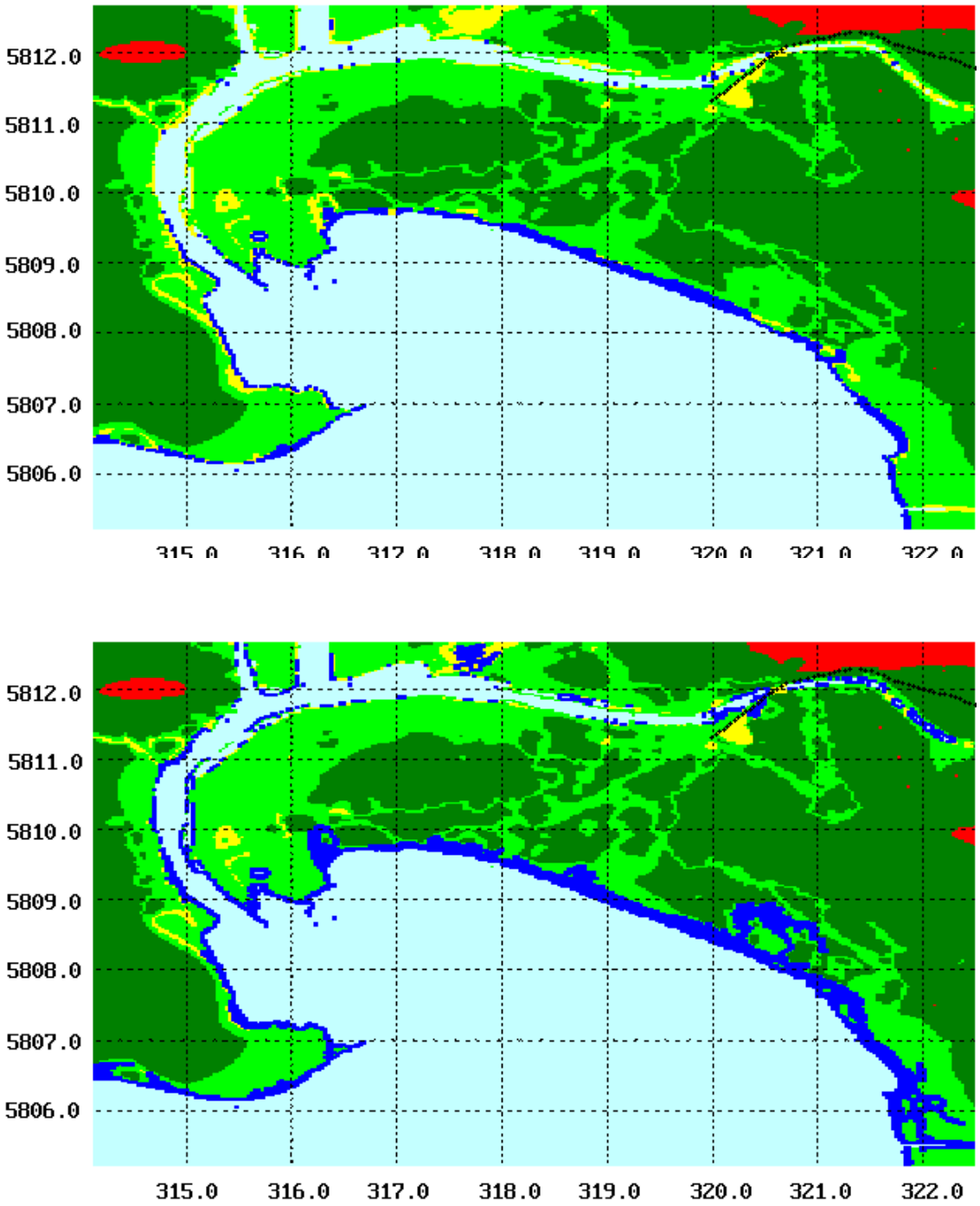

Figure 5.9: Diagram showing the modelled inundation on the Hobsons Bay region for the November case for (a) EXP. 1 (control) and (b) EXP. 3 (see p. 50). Light blue denotes areas of water relative to present day conditions. Dark blue denotes areas of land which have become inundated. Yellow indiates land points lying between 0 m and 2 m in elevation, light green: 2-4 m, dark green: 4-20 m and red: greater than 20 m.

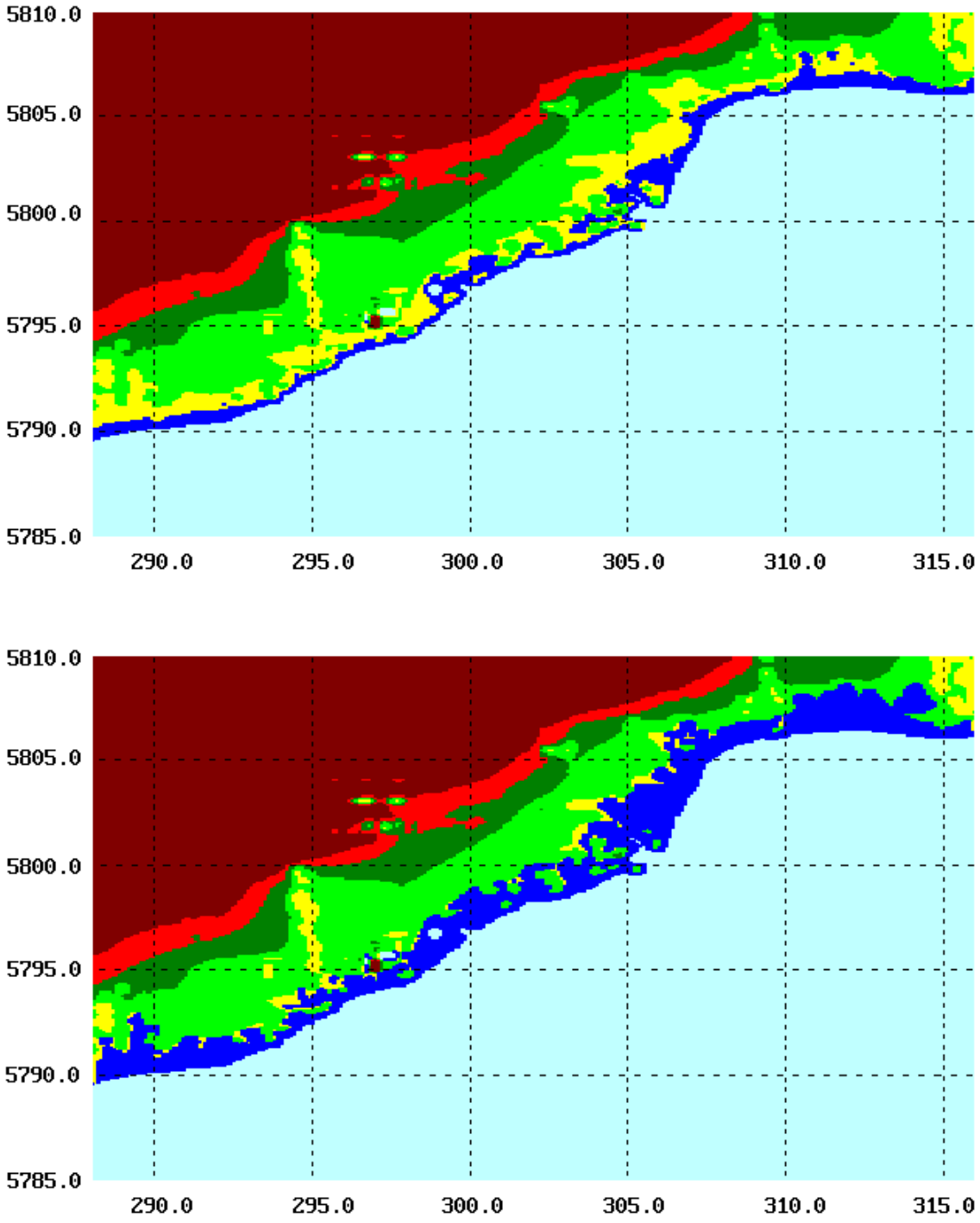

Figure 5.10: Diagram showing the modelled inundation on the Werribee domain for the November case for (a) EXP. 1 (control) and (b) EXP. 3 (see p.50). Light blue denotes areas of water relative to present day conditions. Dark blue denotes areas of land which have become inundated. Yellow indicates land points lying between 0 m and 2 m in elevation, light green: 2-4 m, dark green: 4-6 m, red: 6-10 m, and brown: greater than 10 m.

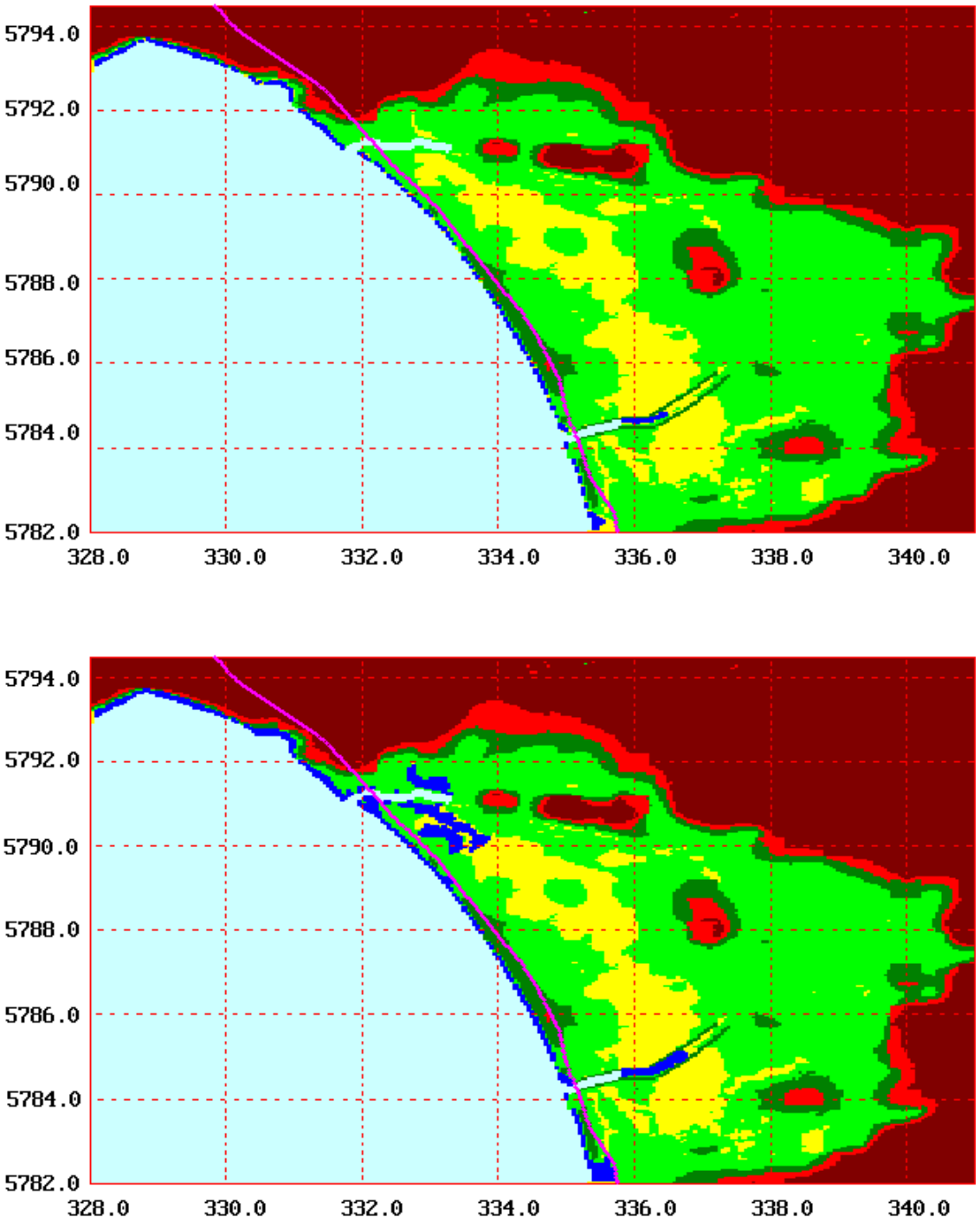

Figure 5.11: Diagram showing the modelled inundation on the Mordialloc domain for the November case for (a) EXP. 1 (control) and (b) EXP. 2 (see p. 50), with levee banks included. Light blue denotes areas of water relative to present day conditions. Dark blue denotes areas of inundated land. Yellow indicates land oints lying between 0 m and 2 m in elevation, light green: 2-4 m, dark green: 4-6 m, red: 6-10 m, and brown: greater than 10 m.

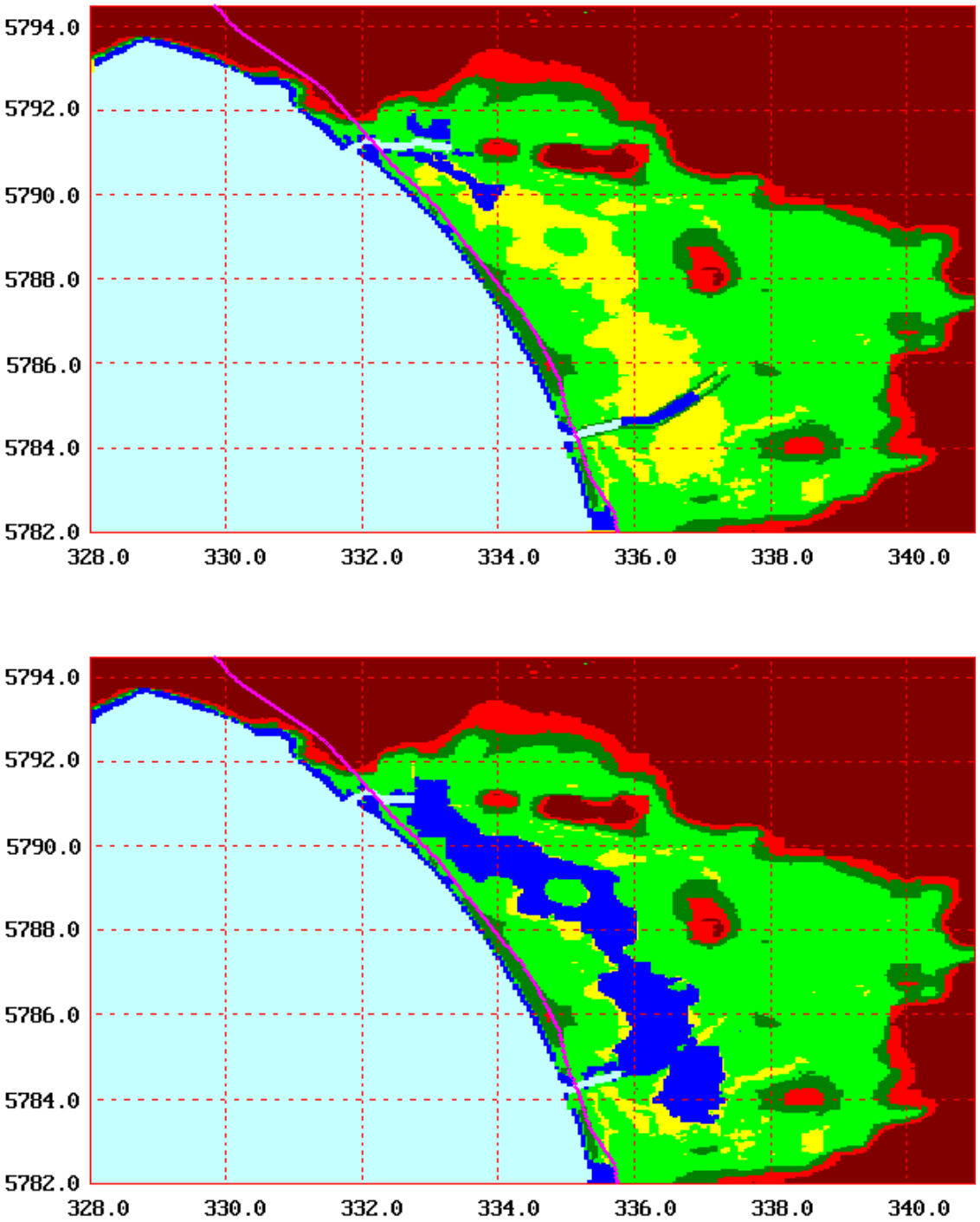

Figure 5.11: Diagram showing the modelled inundation on the Mordialloc domain for the November case for EXP. 3 (see p. 50), (c) with levee banks and (d) without levee banks. Light blue denotes areas of water relative to present day conditions. Dark blue denotes areas of inundated land. Yellow indicates land oints lying between 0 m and 2 m in elevation, light green: 2-4 m, dark green: 4-6 m, red: 6-10 m, and brown: greater than 10 m.

CHAPTER 6: Conclusions

6.1 Summary

An investigation has been conducted into extreme events which affect Victoria's coastline and Port Phillip Bay in particular. Storm surges generated by severe atmospheric storms were the main focus of this study.

Three types of weather situations were identified as being potential contributors to coastal inundation along Victoria's coast - storm surges, flooding from extreme rainfall or a combination of both.

The most commonly occurring situation is the westerly airflow associated with the passage of cold fronts. Storm surges generated in this way are most likely to occur during the colder months of the year when the sub-tropical ridge has moved further north, placing the south coast on average in a more persistent westerly flow regime. The main mechanism for storm surge generation is surface wind drag rather than changes in atmospheric pressure. This is because the low pressure systems associated with the fronts are usually too far south to have a direct influence on the size of the surge. The rainfall produced by cold fronts is usually not extreme enough to produce flooding.

The second type of situation identified is when a low pressure system intensifies in Bass Strait, producing both extreme rainfall and a storm surge. A classic example is the 1934 flood. In this case the storm surge was most likely caused by a combination of inverse barometer effects, as well as wind setup on Bass Strait and Port Phillip Bay from the southerly to southwesterly winds which occurred as the low moved eastwards. The third situation consists of a combination of an extreme rainfall event such as a depression over Victoria or the east coast which causes flooding in catchment areas, followed by a situation such as a cold front which produces a storm surge along the southern coast. Two examples of the first type of situation were modelled in the present study.

Examination of sea level data from the tide gauges of Lorne and Stony Point in Bass Strait and Williamstown in Port Phillip Bay, indicated that storm surges which affect the open coastline are also experienced inside the Bay. However, usually the peak response at Williamstown is attenuated slightly compared to the signals recorded in Bass Strait.

The identification of westerly airflow as the primary cause of storm surges along Victoria's coastline enabled a study of several GCM simulations to be undertaken. Both control and doubled CO_2 simulations were analyzed to determine what changes to the frequency and severity of westerly wind days occurred. Daily data and seasonally averaged winds from the CSIRO GCM Mark I and II experiments were analyzed, as

was the seasonally averaged winds from the coupled AOGCM.

Results over the region of interest were inconclusive. There was no consensus between the different model simulations as to whether westerly wind days would become more or less frequent or severe under a doubling of CO_2. Examination of the seasonally averaged differences between the $1\times CO_2$ and $2\times CO_2$ daily data over southern Australia showed that changes ranging from a 10% increase to a 10% decrease in the frequency and intensity of severe westerly wind days (winds greater than 12.5 m s^{-1}) were possible. Taking into consideration all seasons, a reduction in the frequency and intensity of strong westerlies was more often suggested in the $2\times CO_2$ simulation.

The coupled AOGCM results indicated less impact caused by a doubling of CO_2 compared to the two slab ocean simulations. This is because the large heat capacity of the ocean delays the warming signal. There is concern however, that the coupled model may be sequestering too much heat in the southern ocean, thereby reducing the warming at high southern latitudes and giving a misleading picture of possible changes along the Victorian coast.

For the purpose of investigating the possible impact of climate change on storm surges, it was decided to devise a worst case scenario to incorporate into sensitivity experiments conducted using a high resolution storm surge model. The most extreme event was taken to be a 10% increase in the strength of the winds in a present day extreme event. The worst case scenario for sea level rise for the year 2070 was chosen also to incorporate into sensitivity experiments. This amounted to an 80 cm mean sea level rise. In addition to this, sensitivity experiments were performed using the atmospheric model in which a 4°C SST increase was imposed to determine if this had any local impact on the strength of the winds which generate storm surges.

Two storm surge events, which occurred in May 1994 and November 1994, were chosen for high resolution modelling on a region encompassing most of the southern coastline with a grid resolution of 12 km. Detailed comparison of the modelled winds and surges with available observations indicated that the models were able to capture the main features of the two events with a high degree of accuracy. There was a tendency however, for the storm surge model to slightly overestimate the height of the surge at some locations. Sensitivity experiments involving SST increases in the atmospheric model revealed that there was negligible impact on the pressure or surface winds near the coast in the two events. This was largely due to the fact that cold fronts are part of large scale synoptic systems, which are less affected by changes on the regional scale. The only impact of increasing SSTs in the atmospheric model was to increase the rainfall. Rainfall amounts, particularly in coastal areas, were low to begin with and so the increased rainfall was not considered to be of major significance.

Sensitivity experiments using the storm surge model on the larger grid involved varying the wind speeds by differing amounts and establishing a relationship between wind speed changes and storm surge heights. It was found that the storm surge response was approximately twice that of the wind speed change on the open coastline for wind speeds ranging from a 10% reduction to a 20% increase. The relationship

between wind speed and storm surge changes could be explained in terms of the wind stress term in the governing model equations.

A set of storm surge simulations was also conducted over Port Phillip Bay at 500 m grid resolution. Tidal forcing was also applied so that areas of inundation could be studied. A set of three experiments was conducted for the two cases - a control simulation, a simulation in which mean sea level was increased by 80 cm, and a simulation which incorporated the sea level rise and a 10% increase in the surface wind speed.

In the control simulations of the two cases, the total sea level heights at St Kilda verified well against observations, although the modelled minima tended to be slightly overestimated. The second sensitivity experiment produced sea level increases of around 80 cm at the three locations. In the third sensitivity experiment, a further increase in sea levels of over 20 cm occurred with a slightly greater increase occurring on the eastern side of the Bay.

Three sections of the coastline were then modelled on even higher resolution grids so that areas most vulnerable to inundation could be identified. Sensitivity experiments were performed to provide an estimation of the worst possible inundation which could occur under maximum mean sea level increases and storm intensities. It should be stressed that the occurrence of such a set of circumstances is extremely unlikely.

The results highlighted the sensitivity of the three regions to the different prevailing wind directions which occurred in the two modelled cases. In general, the western side of the bay was less sensitive to wind strength changes than the eastern side since the storm surge events tend to be caused by westerly winds. However, Hobsons Bay was more vulnerable to southwesterlies than westerly or northwesterly events. Considerable sensitivity was also apparent within the Mordialloc domain where the amount of overtopping of levees on the north and south of the Mordialloc Creek appeared to be dependent on the wind strength and direction. Simulations over this region without levee banks on the Mordialloc Creek and Patterson River highlighted the importance of such flood control measures in minimizing the amount of inundation which would occur in this region due to storm surges under the worst case scenarios examined here. It is important to note, however, that the combined effect of a storm surge with heavy rainfall run-off has not been modelled in the present study. An event such as the 1934 floods, which produced both extreme rainfall and storm surge, could cause failure of the existing flood protection system under less extreme scenarios of sea level rise and leading to far greater flooding.

6.2 Implications and Future Work

The sensitivity of storm surges to changes in wind strength highlights the importance of evaluating the changes which occur to the meteorology due to the enhanced greenhouse change, as well as the effect of mean sea level rise. However, as was illustrated in chapter 3, current GCMs do not produce a consensus with regard to the

changes in wind strength and frequency along the southern coastline which may occur as a result of doubling current levels of CO_2. Therefore, there is a clear need to improve the estimates of changed meteorology for future coastal impact studies.

There are several steps needed to achieve this outcome. Firstly, improvements are needed to coupled AOGCMs which address the uptake of heat by the oceans and produce more realistic large-scale climate change scenarios. Such models should also be used to identify regional variations in the mean sea level rise due to changes in ocean circulations. Secondly, limited area models nested within improved GCMs are needed to produce higher resolution climate simulations over a region of interest. Thirdly, a better understanding of synoptic climatologies at the regional scale in the current and enhanced greenhouse climate would enable better estimates of the coastal impacts of climate change. As we have seen from our analyses of the synoptic forcing mechanisms for extreme events on the Victorian and New South Wales coasts, different coastal areas experience different types of forcing. More generally, this implies a need for detailed analyses of the synoptic forcing mechanisms and how they may change, for each particular coastal region of interest.

In short, there is no simple way of estimating likely changes in extreme coastal events and resulting inundation for particular locations. More reliable AOGCM simulations are needed, along with finer resolution nested models, and proper attention to the relevant meteorological forcing mechanisms and how these may change. Each of these steps can be achieved within the next few years and this should be the objective of a comprehensive research program.

APPENDIX 1: The Storm Surge Model

The major features of the model are detailed below.

- The shallow water equations are solved on an Arakawa C-grid.
- The non-linear advection terms are included.
- An efficient time-splitting finite difference scheme is used, which yields a more accurate and stable solution than standard explicit techiques (three different time steps are used to solve the gravity wave, advective and the physics components of the equations of motion).
- A radiation condition, which solves for the group velocity, is used on the open lateral boundaries.
- The resolution and map projection are variable and a generalised grid generator has been developed, which sets the model up in any specified location using high resolution global and regional bathymetry files.
- The model can be one-way nested within itself to allow multiple high resolution simulations to be carried out over specific regions of interest.
- Inundation and drying of coastal points as a function of tides or storm surges is computed from the basic momentum and continuity equations, thus incorporating realistic flow rates.
- A large range of terrain types can be specified and associated bottom friction factors calculated.

The non-linear, depth integrated momentum equations and continuity equation solved by the model are:

$$\frac{\partial U}{\partial t} = fV - mg\frac{\partial \zeta}{\partial x} - \frac{m}{\rho_w}\frac{\partial P}{\partial x} - m\left(U\frac{\partial U}{\partial x} + V\frac{\partial U}{\partial y}\right) + \frac{1}{\rho_w H}(\tau_{sx} - \tau_{bx}) - \nu\nabla^2 U \quad (A1)$$

$$\frac{\partial V}{\partial t} = -fU - mg\frac{\partial \zeta}{\partial y} - \frac{m}{\rho_w}\frac{\partial P}{\partial y} - m\left(U\frac{\partial V}{\partial x} + V\frac{\partial V}{\partial y}\right) + \frac{1}{\rho_w H}(\tau_{sy} - \tau_{by}) - \nu\nabla^2 V \quad (A2)$$

$$\frac{\partial \zeta}{\partial t} = -m^2\left[\frac{\partial}{\partial x}\left(\frac{UH}{m}\right) + \frac{\partial}{\partial y}\left(\frac{VH}{m}\right)\right] \quad (A3)$$

where U and V are the depth averaged currents in the x and y directions respectively, H is the total water depth, ζ is the sea surface elevation, f is the Coriolis parameter, g is the acceleration due to gravity, m is the map factor, P is the atmospheric surface pressure, ρ_w is the water density, ν is the coefficient of viscoscity and τ_{sx} and τ_{sy}

represent the surface wind stress and τ_{bx} and τ_{by}, the bottom frictional stress in the x and y directions respectively.

The surface wind stresses are computed using the quadratic relationship:

$$\begin{aligned} \tau_{sx} &= C_D \rho_a |\mathbf{u_a}| u_a \\ \tau_{sy} &= C_D \rho_a |\mathbf{u_a}| v_a \end{aligned} \tag{A4}$$

where $|\mathbf{u_a}| = (u_a^2 + v_a^2)^{1/2}$, u_a and v_a are the horizontal components of wind velocity near the ocean surface, ρ_a is the density of air and C_D is the drag coefficient expressed as follows:

$$C_D = \begin{cases} [0.7 + 0.065|\mathbf{u_a}|] \times 10^{-3}, & |\mathbf{u_a}| < 20 \text{ m s}^{-1} \\ [2.28 + 0.033(|\mathbf{u_a}| - 20.0)] \times 10^{-3}, & |\mathbf{u_a}| > 20 \text{ m s}^{-1} \end{cases} \tag{A5}$$

The bottom stress is represented by a Manning's n depth-dependent friction relation, (Signell and Butman, 1992):

$$\begin{aligned} \tau_{bx} &= \rho_w \frac{gn^2}{(H+\zeta)^{1/3}} (U^2 + V^2)^{1/2} U \\ \tau_{by} &= \rho_w \frac{gn^2}{(H+\zeta)^{1/3}} (U^2 + V^2)^{1/2} V \end{aligned} \tag{A6}$$

where n has the value 0.0264. The drag coefficient in this formulation increases with decreasing depth.

REFERENCES

Adams, J.R., 1987: *Tide levels during November - December 1934. Flood and high tide frequency analysis for Williamstown*, Board of Works Internal Report, 64 pp.

Bates, G.T. and Meehl, G.A., 1986: 'The effect of CO_2 concentration on the frequency of blocking in a General Circulation Model coupled to a simple mixed layer ocean model'. *Mon. Weath. Rev.*, **114**, 687-701.

Black, K.P., Hatton, D.N. and Colman, R., 1990: *Prediction of extreme sea levels in northern Port Phillip Bay and the possible effect of a rise in mean sea level*, Report to the Board of Works Melbourne by the Victorian Institute of Marine Sciences, VIMS, Melbourne, 141 pp.

Coastal Investigations Unit 1992: *Victorian Coastal Vulnerability Study*, Port of Melbourne Authority and Office of the Environment, Melbourne Australia 60 pp plus maps and appendices.

Cubash, U., Santer, B.D., Hellbach, A., Hegerl, G., Höck, H., Maier-Reimer, E., Mikolajewicz, U., Stössel, A. and Voss, R., 1994: 'Monte Carlo climate change forecasts with a global coupled ocean-atmosphere model'. *Climate Dynamics*, **10**, 1-19.

England, M.H., 1995: 'Using chlorofluorocarbons to assess ocean climate models'. *Geophysical Research Letters, in press.*

Evans, J.L., Ryan, B.F. and McGregor, J.L., 1994: 'A numerical exploration of the sensitivity of tropical cyclone rainfall intensity to sea surface temperature'. *J. Climate*, **7**, 616-623.

Gregory, J.M., 1993: 'Sea level changes under increasing atmospheric CO_2 in a transient coupled ocean-atmosphere GCM experiment'. *J. Climate*, **6**, 2247-2262.

Holland, G.J., Lynch, A.H. and Leslie, L.M., 1987: 'Australian east- coast cyclones. Part I: Synoptic overview and case study'. *Mon. Weath. Rev.*, **115**, 3024-3036.

Hubbert, G.D., Holland. G.J., Leslie, L.M. and Manton, M.J., 1991: 'A real-time system for forecasting tropical cyclone storm surges'. *Weath. and Forecast.*, **6**, 86-97.

Hubbert, G.D., Leslie, L.M. and Manton, M.J., 1990: 'A storm surge model for the Australian region'. *Q. J. R. Meteorol. Soc.*, **116**, 1005-1020.

Katzfey, J.J. and McInnes, K.L., 1995: 'GCM simulations of eastern Australian cut-off lows'. *submitted to J. Climate, Nov. 1994.*

McInnes, K.L. and Hess, G.D., 1992: 'Modifications to the Australian region limited area model and their impact on an east coast low event'. *Aust. Met. Mag.*, **40**, 21-31.

McInnes, K.L. and Hubbert, G.D., 1994: 'The impact of east coast lows on storm surges: Implications for climate change'. *Climate Impact Assessment Methods for Asia and the Pacific.* Australian International Development Assistance Bureau, Canberra, 97-103.

McInnes, K.L., Leslie, L.M. and McBride, J.L., 1992: 'Numerical simulation of cut-off lows on the Australian east coast: sensitivity to sea surface temperature'. *Int. J. Climatol.*, **12**, 783-795.

McInnes, K.L., McBride, J.L. and Leslie, L.M., 1994: 'Cold fronts over southeastern Australia: Their representation in an operational numerical weather prediction model'. *Weath. Forc.*, **9**, 384-409.

Mikolajewicz, U. and Maier-Reimer, E., 1990: Internal secular variability in an ocean circulation model. *Climate Dynamics*, **4**, 145-156.

Reeder, M.J., Keyser, D. and Schmidt, B.D., 1991: 'Three-dimensional baroclinic instability and summertime frontogenesis in the Australian region'. *Q. J. Roy. Met. Soc.*, **117**, 1-28.

Vecchio, G. 1980: *A study of storm surges along the Adelaide foreshore*, Bureau of Meteorology, Meteorological Note 107, 13pp.

Whetton, P.H., Mullan, A.B. and Pittock, A.B., 1995: 'Climate Change Scenarios for Australia and New Zealand', *Greenhouse 94*, Wellington, 9-14 October 1994, ed. Pearman, G.I. and Manning, M. *(in press).*

Wigley, T.M.L. and Raper, S.C.B., 1992: 'Implications of revised IPCC scenarios'. *Nature*, **357**, 293-300.